VOLUME 12 (1959) No. 5

NUCLEAR PHYSICS

JOURNAL DEVOTED TO THE EXPERIMENTAL AND THEORETICAL STUDY OF THE FUNDAMENTAL CONSTITUENTS OF MATTER AND THEIR INTERACTIONS

EDITOR: L. ROSENFELD · COPENHAGEN

S. A. E. JOHANSSON, On spontaneous fission rates 449

E. S. FRADKIN, The Green's function method in quantum statistics 465

J. L. URETSKY and P. J. REDMOND, Calculation of the magnetic moments of nucleons by use of a modified propagator 485

L. J. B. GOLDFARB and J. R. ROOK, The polarization of deuterons and particles of arbitrary spin II 494

H. J. ROSE, W. TROST and F. RIESS, The spin assignments of the 9.16-MeV and 6.44-MeV states in N^{14} 510

L. K. PANDIT and S. N. BISWAS, K^+-meson-nucleon scattering and K^+—Y relative parity 521

J. OLKOWSKY, M. LE PAPE, I. GRATOT et L. COHEN, Un nouvel isotope du gadolinium très déficient en neutrons 527

H. IZBICKI, Note on „double binomial coefficients" 532

NORTH-HOLLAND PUBLISHING COMPANY - AMSTERDAM

August (2) 1959

EDTIORIAL BOARD

AUSTRALIA & NEW ZEALAND:	H. Messel (Sydney), M. L. Oliphant (Canberra)
AUSTRIA:	B. Karlik, (Vienna), H. Thirring (Vienna)
BELGIUM:	M. de Hemptinne (Louvain), J. Verhaeghe (Ghent)
CANADA:	G. Volkoff (Vancouver)
DENMARK:	C. Møller (Copenhagen), S. Rozental (Copenhagen)
FINLAND:	L. Simons (Helsinki)
FRANCE:	A. Berthelot (Saclay), S. Gorodetzky (Strasbourg)
GERMANY (DEM. REP.):	G. Hertz (Leipzig)
GERMANY (FED. REP.):	W. Gentner (Freiburg i. B.), J. H. D. Jensen (Heidelberg)
GREAT BRITAIN:	S. Devons (Manchester), T. H. R. Skyrme (Harwell)
HUNGARY:	L. Janossy (Budapest)
INDIA:	H. Bhabha (Bombay), R. Ramanna (Trombay)
IRISH REPUBLIC:	J. McConnell (Maynooth)
ISRAEL:	G. Racah (Jerusalem)
ITALY:	E. Amaldi (Rome)
JAPAN:	S. Kikuchi (Tokyo), S. Tomonaga (Tokyo)
MEXICO:	M. Moshinsky (Mexico)
NETHERLANDS:	H. Brinkman (Groningen), S. R. de Groot (Leiden)
NORWAY:	E. Hylleraas (Oslo), A. Lundby (Oslo), H. Wergeland (Trondheim)
POLAND:	L. Infeld (Warsaw)
PORTUGAL:	J. M. Araújo (Porto), J. R. de Almeida Santos (Coimbra)
SOUTH AMERICA:	G. Beck (Saõ Paulo), J. Leite Lopes (Rio de Janeiro)
SPAIN:	J. M. Otero (Madrid), C. Sanchez del Rio (Madrid)
SWEDEN:	O. Klein (Stockholm), K. Siegbahn (Uppsala), I. Waller (Uppsala)
SWITZERLAND:	P. Huber (Basel), P. Scherrer (Zürich)
U.A.R. & ARAB COUNTRIES:	F. El Bedewi (Alexandria), M. G. Nooh (Cairo)
U.S.A.	H. H. Barschall (Madison, Wisconsin), V. Weisskopf (Cambridge, Mass.)
U.S.S.R.:	M. A. Markov (Moscow), I. S. Shapiro (Moscow), D. V. Skobeltzyn (Moscow)
YUGOSLAVIA:	I. Supek (Zagreb)

CONTRIBUTIONS may be sent to the Editor, Professor L. Rosenfeld, NORDITA, Blegdamsvej 17, Copenhagen Ø, either directly, or preferably through the intermediary of one of the members of the Editorial Board of the country or region in which the author is working. They may be written in English, French or German.

NUCLEAR PHYSICS is published in fortnightly issues. The subscription price per volume of 700 pages is fl 57.00; 114s; a 15.00. Post-free.

SUBSCRIPTIONS should be sent to the publishers, NORTH-HOLLAND PUBLISHING COMPANY, P.O.Box 103, Amsterdam or to any subscription-agent.

BOOKS FOR REVIEW should be sent to Professor Rosenfeld.

No part of this issue may be reproduced in any form, by print, photoprint, microfilm or any other means without written permission from the publisher. Reprints, photoprints or microfilms are obtainable at cost from the publisher.

Printed in the Netherlands

REPRINTS OF NUCLEAR PHYSICS

Available at the Publishers

NUCLEAR ENERGIES AND THE SHELL MODEL

by

NISSAN ZELDES

Department of Physics, The Hebrew University of Jerusalem, Israël

and

Department of Mathematical Physics, University of Birmingham, England

volume 7 (1958) no. 1,
84 pages, 20s., $ 2.80

PARTICLES AND SYMMETRIES

by

E. CORINALDESI

University College of North Staffordshire, Keele, England

volume 7 (1958) no. 4
68 pages, 17s., $ 2.25

ENERGY LEVELS OF LIGHT NUCLEI. VI

by

E. AJZENBERG-SELOVE

Department of Physics, Haverford College, Haverford, Pennsylvania

and

T. LAURITSEN

Kellog Radiation Laboratory, California Institute of Technology, Pasadena, California

volume 11 (1959) no. 1
320 pages, 40s., $ 5.30

NORTH-HOLLAND PUBLISHING COMPANY

NIEUWE ZIJDS VOORBURGWAL 68-70 AMSTERDAM-C HOLLAND

2.J *Nuclear Physics* **12** (1959) 449—464; © *North-Holland Publishing Co., Amsterdam*
Not to be reproduced by photoprint or microfilm without written permission from the publisher

ON SPONTANEOUS FISSION RATES

SVEN A. E. JOHANSSON
Department of Physics, University of Lund

Received 29 April 1959

Abstract: An attempt is made to explain the irregular behaviour of the spontaneous fission half-lives. The influence of a single nucleon on the barrier height is calculated from the level scheme of Nilsson. It turns out that in many cases the single particle effect changes the barrier height quite considerably compared to the smooth change expected from the liquid drop model. The calculated changes are compared with the experimental data. They account quantitatively for the irregularities in the spontaneous fission rates. Finally, predictions of spontaneous fission half-lives are made for the heavier nuclei and the application of these predictions to some problems is discussed.

1. Introduction

The spontaneous fission of the heavy nuclei has been thoroughly investigated for rather many years. The half-lives for a large number of nuclei have been determined. Some attempts have been made to systematize the spontaneous fission periods. It was first noticed by Seaborg [1]) and by Whitehouse and Galbraith [2]) that the half-life for even-nuclei decreases exponentially with the parameter Z^2/A. The odd-mass nuclei have much longer half-lives and no systematic variation. Ghiorso [3]) and Huizenga [4]) later found that this relationship is only approximately true. It was found that the half-lives of the isotopes of the even-Z elements show a maximum. Furthermore, for nuclei with $N > 152$ the half-lives drop sharply with increasing N. These features are shown in fig. 1, which contains the available experimental material.

The general increase in fission rate with Z^2/A is expected on the basis of the liquid drop model. The deviations from the general trend are more difficult to explain. It is sometimes stated that an increase in fission rate can be due to an increase in the ground state deformation. From the available experimental and theoretical values for the deformations it is clear, however, that there is no correlation between spontaneous fission rate and deformation.

The relation between spontaneous fission and α-decay periods has been discussed by several authors. Some empirical relationships have been found. Even if they indicate a connection between the two processes this is no solution of the problem.

August (2) 1959

Swiatecki [5]) has obtained a correlation between the semi-empirical mass formula and the spontaneous fission rates. He calculates the difference between the actual ground state masses and the values given by the mass formula. Assuming that the energy surface at the saddle point is smooth, the variations in barrier height can be obtained. This assumption is somewhat uncertain, however. As will be shown later the fluctuations in level spacing seem to be as great at the saddle point as in the ground state.

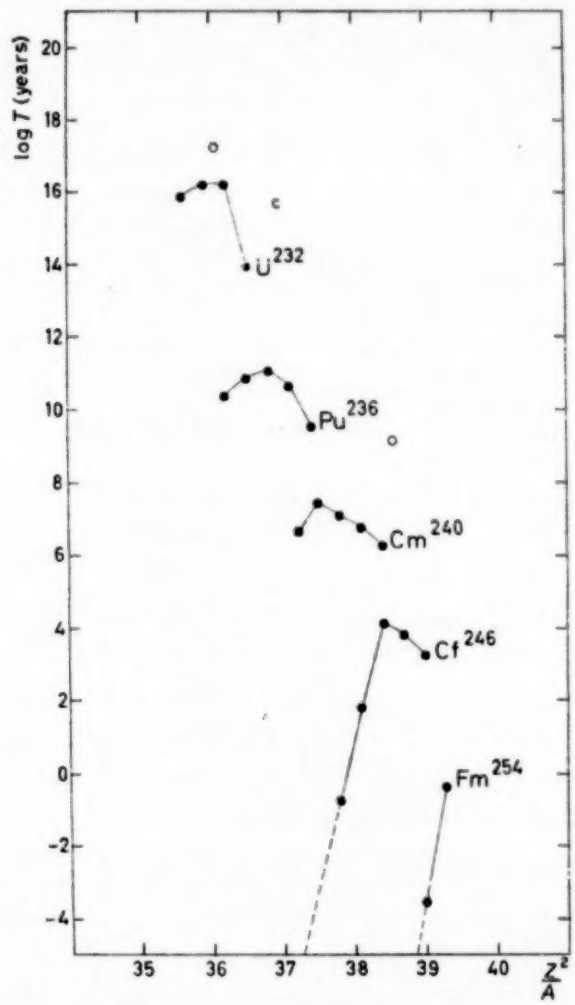

Fig. 1. Experimental values of the spontaneous fission half-lives. Dots: the even nuclei $U^{232-238}$, $Pu^{236-244}$, $Cm^{240-248}$, $Cf^{246-254}$ and $Fm^{254-256}$. Open circles: the odd-neutron nuclei U^{235}, Pu^{239} and Cf^{249}. The dashed line indicates an empirical extrapolation to the heavier Cf and Fm nuclei.

In the present paper an attempt is made to relate the fluctuations in spontaneous fission rate to the properties of the single particle orbits. If, for a certain orbit, the energy as a function of the deformation is known, it can be determined how the nucleons occupying this particular orbit will affect the barrier height.

2. General Plan of the Calculations

As has been shown in fig. 1, the general trend of the spontaneous fission rates is in agreement with the drop model. The half-lives decrease with increasing values of Z^2/A. There are strong deviations, however. The addition of two neutrons in some cases increases the fission rate, contrary to the prediction of the drop model. We will try to explain this by calculating the change in barrier height caused by the addition of a nucleon in a certain single particle orbit. Since the general trend is in agreement with the drop model, it is convenient to calculate the deviations from this model. This means that we take the difference between the changes in barrier height expected in the two models, namely the single particle model and the drop model.

In the drop model it is easy to calculate the change in barrier height caused by the addition of one nucleon. The change in surface energy is in the first approximation two thirds of the total surface energy divided by the number of nucleons. The error introduced by this simplifying assumption is small. This is because the change is small compared to the irregular changes due to the single particle orbits. Moreover, any error in the drop model calculation will be practically the same for all the nuclei studied.

In the case of the single particle model one has to know the level scheme as a function of the deformation. Furthermore, it is necessary to know the configuration of the nuclei studied. The level scheme then gives directly the change in barrier height caused by the addition of one extra nucleon. It turns out that the characters of the orbits are quite different but that most of them cause a considerable increase or decrease of the barrier height.

Calculating the penetrability exactly in spontaneous fission is extremely difficult. The exact penetration formula is too complicated. Furthermore, one does not know the shape and height of the barrier with any certainty. It is much easier to get approximately the change in penetrability for a small change in barrier height. The procedure in the present paper has been to calculate the difference in barrier height between the drop model and the single particle model. The corresponding difference in fission rate is calculated from a simplified penetration formula. The calculated changes in fission rate hence represent the deviations from the smooth curve expected on the basis of the drop model. These calculated deviations are finally compared with the experimental results.

In calculating the barrier penetration it is necessary to know the shape of the barrier. In the drop model it is known fairly well. It can in principle be calculated also from the single particle level scheme. There are so many uncertainties involved, however, that no reliable results can be obtained. Therefore we have used the drop model barrier for the calculation of the

changes in penetrability caused by the single particle levels. The calculation is fortunately rather insensitive to errors in the assumed shape of the barrier.

3. Single Particle Level Scheme

The single particle levels of a deformed potential have been calculated by several authors. The most detailed work is that of Nilsson [6]). He takes into account both the spin-orbit interaction and the deviations in shape from the harmonic oscillator potential. Furthermore, the calculated level scheme has been compared with a very extensive experimental material by Mottelson

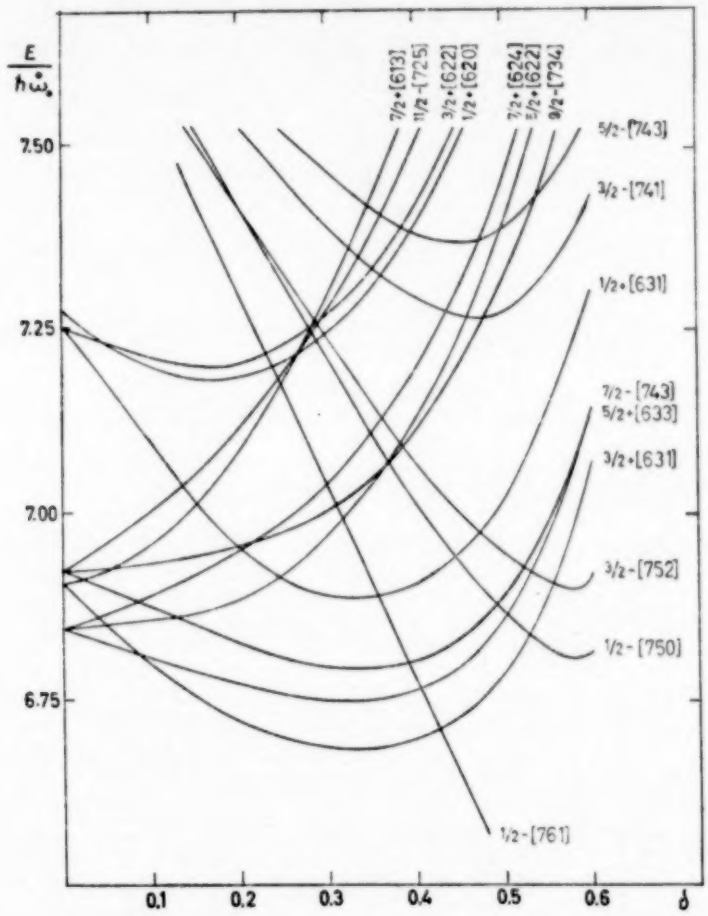

Fig. 2. Neutron levels for neutron numbers from 139 to 160. Spin, parity, and the asymptotic quantum numbers N, n_z and Λ are written beside each level.

and Nilsson [7]). The parameters are slightly adjusted to reproduce the experimental level order as well as possible. Hence this level scheme should fairly well represent the actual situation.

The tables and diagrams of Nilsson in general give values only for deformations up to $\delta = 0.3$. For some orbitals values are given up to $\delta = 0.5$ in the recent work by Mottelson and Nilsson. In the present work it is necessary to

have values up to $\delta = 0.6$. The level scheme is therefore extrapolated to greater deformations. This extrapolation is made using the asymptotic representation discussed by Nilsson. It should be quite good at these great deformations.

Figs. 2 and 3 show the level diagram for the levels of interest in the following discussion, namely for the neutron numbers $138 < N < 161$ and the proton numbers $90 < Z < 107$. The energy is not as usual given in the δ-dependent unit $\hbar\omega_0(\delta)$ but in the δ-independent unit $\hbar\mathring{\omega}_0$. It is then easy to see directly the influence of a certain level on the fission barrier.

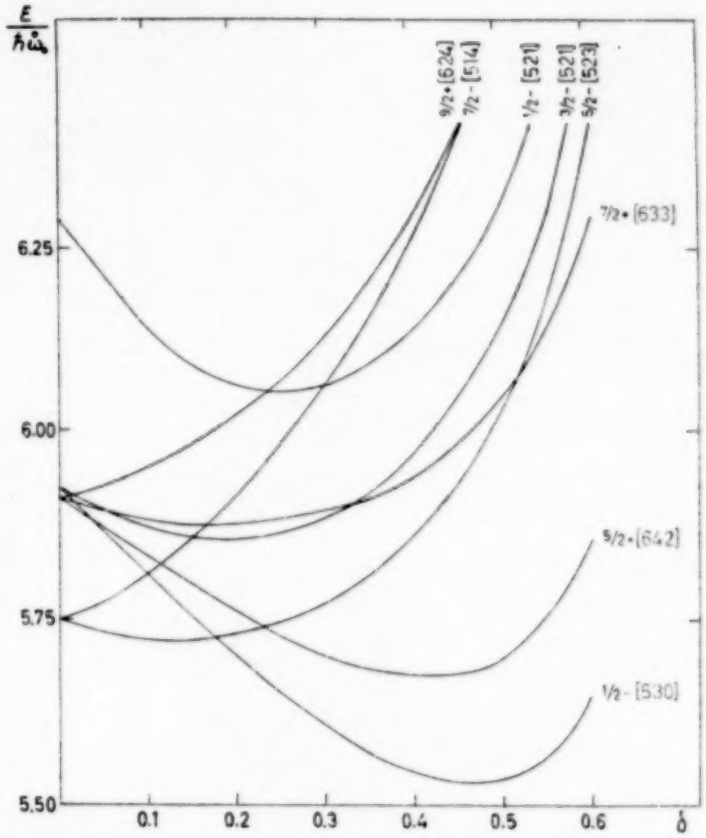

Fig. 3. Proton levels for proton numbers from 91 to 106. Spin, parity, and the asymptotic quantum numbers N, n_z and Λ are written beside each level.

The most important problem connected with the level diagram is the question how the nucleons behave at the level crossings. We first restrict the discussion to the case of paired nucleons. When δ is increased two paired nucleons move along a certain level. They might stay on the same level also after having passed a level crossing. The other possibility is that the interaction between the two nucleons makes it possible to change the K value and transfer to the crossing level. Since the nucleons still will be paired, spin and parity of the system will be conserved. One cannot calculate the transition probability with any certainty. Qualitatively, it can be said that if the

change in deformation is slow and the difference in slope of the two levels is small, there is a high probability for a transition to the crossing level. In this case, it is possible for the nucleus to change its configuration during the change in deformation so that the total energy is minimized. It is probable that this adiabatic approximation can be used in the case of spontaneous fission. If one makes the opposite assumption that every nucleon has to stay on a certain level all the time, it can be shown that this leads to consequences that do not seem to be in agreement with experimental facts.

In this connection, it is important to point out that the probability for the rearrangement of the nucleons at a level crossing is not necessarily 100 %. The fission barrier height is lowered if the energy can be minimized by the rearrangement. Each level crossing will on the average lower the barrier by an amount that corresponds to an increase in fission probability of almost one order of magnitude. Hence, even if the probability for the rearrangement is, let us say, only 30 %, the fission will mainly go via the path of minimum energy.

The foregoing discussion has been restricted to the case of two paired nucleons. If we have a single nucleon in a certain level, the situation is completely changed. Now, since spin and parity of the nucleus have to be conserved, the odd nucleon cannot in general transfer to other levels even if this would mean a gain in energy. Hence, the contribution to the fission barrier from a single nucleon will in general be greater than that of a paired nucleon. This fact might, as pointed out by Newton [8]) and Wheeler [9]), be an explanation to the fact that odd-mass nuclei have a considerably longer half-life than neighbouring even-nuclei. The detailed path of the odd nucleon in the level diagram depends on whether or not K is a good quantum number. It is known that Coriolis forces can couple states of different K. Hence, there is a certain probability for a transition from a level to another one having a lower K value with conservation of total spin and parity. One would expect such a transition to be retarded, however, and it is difficult to say if it would lead to a higher fission probability. For the odd-mass nuclei of interest in the present work, the ambiguity arising from these circumstances is small. For two of them, Pu^{239} and Cf^{249}, it so happens that parity conservation forbids all possible transitions to other levels. In the third case, U^{235}, there are two possible transitions, but they give only a small gain in energy. Hence, also in this case we have assumed that the odd nucleon stays in the original level.

One can then construct the path of a certain nucleon in the diagram. Fig. 4 shows, for example, the energy of the 145th neutron as a function of δ. For comparison is also shown the curve calculated on the basis of the drop model. Several conclusions can be drawn from this figure. One is that this particular level will lower the barrier considerably. Two neutrons occupying

this level will depress the fission barrier about 0.4 MeV in comparison with the smooth behaviour expected from the drop model. This shows that the single particle character of the nucleons will have a very decisive influence on the spontaneous fission rate. It will also be noted that the drop model curve in fig. 4 varies only little with δ compared to the single particle curve. Hence an error in the assumed shape of the barrier is not so essential in the comparison with the single particle levels.

The level diagrams shown in figs. 2 and 3 are not quite complete. Coming from below are a number of steeply rising levels from lower shells. They should have some influence on the calculations. The difficulty in taking them into account is that their exact position is not known. The systematic survey of Mottelson and Nilsson on the properties of the nuclei in this region does not give any indication for the presence of these levels. Hence, they must be somewhat depressed from their calculated positions.

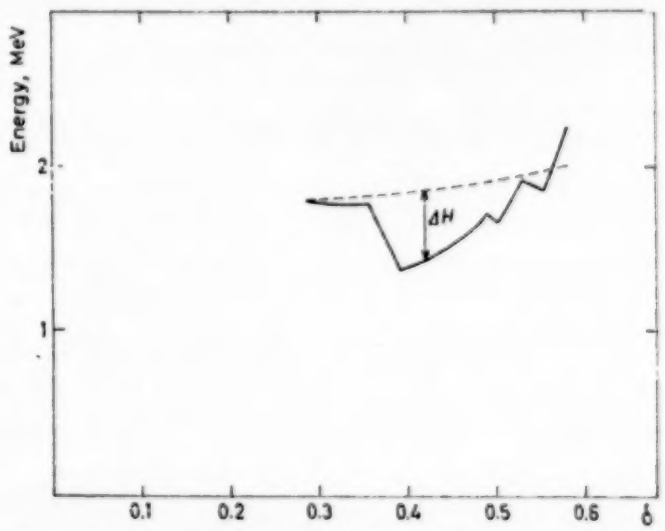

Fig. 4. As an example of the single particle effect, the energy of the 145th neutron is shown as a function of the deformation. Full line: the energy according to the present calculation, dashed line: the energy according to the liquid drop model.

Another important point in this connection is that the level diagram for $\delta = 0$ gives too small an energy gap at $Z = 82$ and $N = 126$. In both cases the diagram gives a gap of about 1 MeV, but according to various empirical facts (α decay systematics, binding energies, nuclear spectra etc.) it should be about twice as large. Hence, also from this point of view it seems to be necessary to depress the filled shells.

It is important to note that these levels from the lower shells will affect the calculation only if the nucleons originally in them transfer to crossing levels when the deformation is increased. There are some reasons to believe that the probability for these transitions is rather low. One is that there is a great difference in slope when these levels cross levels from the unfilled shells. Another effect working in the same direction is that the properties of the

rising levels of the filled shells are so different from those of the crossing levels of the unfilled shells. The former levels have $n_z = 0$ while the latter ones have rather large values of n_z. The wave functions will overlap only to a small extent and hence the probability for a transition will be small. If this is true, the filled shells will not be broken up, and they will not affect the calculations, regardless of their position.

The complication arising from the levels from the lower shells will not seriously disturb the calculations for curium and the heavier elements. It might be decisive for uranium and plutonium. It is impossible to take them into account, however, since nothing can be said with certainty about their position and how they influence the nucleonic configuration. We have therefore tentatively assumed that they do not interfere with the configuration of the unfilled shells. The results for uranium and plutonium are similar to those for the heavier elements. This might be an indication that the assumption is justified. The reason could be, as discussed above, that the filled shells are considerably depressed, or that they are not broken up when the deformation is increased.

An interesting application of the level scheme is to predict the spin values of the lowest fission channels for odd-mass nuclei. A comparison with experimental data gives a check on the scheme. The lowest fission channel should correspond to a state in which the total energy of the nucleons is minimized at a deformation corresponding to the saddle point shape. The K value of the odd nucleon should then give the spin of the lowest channel. Experimentally very little is known about the spin values. Wilets and Chase [10]) have analyzed the angular distribution in the neutron-induced fission of Th^{232}. They find that the distribution is in agreement with the assumption that the lowest channels are due to a rotational band with $K = \frac{3}{2}-$. To make a prediction from the level scheme one has to determine the level occupied by the odd neutron in Th^{233} at a deformation of about 0.6. It turns out that it will be the [752] level with $K = \frac{3}{2}-$. It will be noted that there is no other $\frac{3}{2}-$ level in this region of the diagram. This agreement is an indication that the level scheme might be fairly good also for large deformations.

4. The Fission Barrier

The most satisfactory treatment of the fission barrier problem would be to calculate the barrier from the single particle levels. This is possible in principle but involves great practical difficulties. First of all, the barrier is obtained as a fairly small difference between the surface energy and the Coulomb energy. The level diagram is probably not known well enough to give the surface energy with the required accuracy. Furthermore, one cannot use the level scheme calculated for an ellipsoidal potential, for

example the Nilsson level diagram. This is because the shape of the nuclei during the fission process is not quite ellipsoidal. This probably changes the energy enough to have a very great influence on the barrier height. An attempt to calculate the surface energy on the basis of the Nilsson level scheme showed that it rises too rapidly for large deformations, but that more reasonable values are obtained for smaller deformations.

For the present purpose the shape of the barrier has been taken from the drop model. In order to take into account the nuclear deformation it has been modified in a way suggested by Hill and Wheeler [11]). To the drop model potential a term $V = c\delta$ is added, where c is a constant and δ the deformation parameter. This term represents the deforming forces in the nucleus. Its size has been adjusted so that it gives the known ground-state deformation. The height of the barrier is then normalized to the known photofission thresholds of the uranium isotopes. The barrier is higher than the photofission threshold because of the penetrability of the barrier. The variation in barrier height with Z and N is calculated from the drop model.

This procedure is admittedly extremely crude. Its justification is that the influence of the exact shape of the barrier on the present calculations is rather small. We are not attempting any absolute calculation of the spontaneous fission rate, but are only calculating the changes introduced by a small change in barrier height. As a matter of fact, any reasonable shape of the barrier will give essentially the same results. The main uncertainties in the present work come from other sources. Therefore, it does not seem worthwhile to try to calculate the barrier shape in a more consistent and accurate way.

5. Penetration of the Fission Barrier

The problem of barrier penetration has been discussed in some detail by Bohr and Wheeler [12]). The formula they give for the probability per unit time of a fission process, λ_f is too complicated to be useful. For the present purpose we use a simplified expression

$$\lambda_f = 5\frac{\omega_f}{2\pi}\exp\left[-k\int_{\delta_1}^{\delta_2}\sqrt{H}\,\mathrm{d}\delta\right], \tag{1}$$

where ω_f is the frequency of the quadrupole oscillations, H the barrier height and δ the deformation parameter. The factor k is not constant but depends on the nuclear mass and the path of the nucleons in the fission process. The mean value of k for each element is calculated from the experimental fission rates. Values of H and δ are calculated from the drop model. Table 1 shows the result. It turns out that k increases slightly with increasing Z. This is partly due to the increase in mass but is probably also a consequence of the approximations in the penetration formula. The approximate constancy of

k is an indication that the penetration formula used is not too bad. As long as there are no sudden jumps in the value of k a small variation does not matter for our purpose. This seems to be the case.

TABLE 1

Mean values of H and k in the penetration formula

Element	H(MeV)	k
U	6.0	204
Pu	5.6	225
Cm	5.3	239
Cf	4.9	250
Fm	4.6	253

In the present work we want to calculate the change in fission rate corresponding to a small change in barrier height. For a certain nucleus we estimate the barrier height in two ways, using either the drop model or the single particle model. If the difference ΔH is small compared to H one gets for the ratio between the fission rates

$$\exp\left[-\tfrac{1}{2}k\int_{\delta_1}^{\delta_2}\frac{\Delta H}{\sqrt{H}}\,\mathrm{d}\delta\right]. \tag{2}$$

The lower limit of the integral is determined by the deformation in the ground state. Its value has been taken partly from the work of Mottelson and Nilsson [7]). For the nuclei not listed there, it has been determined by calculating the effect of the extra nucleons, starting from a nucleus having a known deformation. A slight shift in the lower limit of the integral is caused by the zero-point oscillations of the nucleus. The zero-point energy has been taken to be the same as in the drop model, namely 0.4 MeV.

The upper limit of the integral is determined by the barrier, which is calculated from the drop model as described above.

6. Results

The calculations have been made for a number of nuclei with known spontaneous fission rate. We first treat the case of addition of one or two neutrons to an even-Z nucleus. The quantity ΔH, the difference between the single particle curve and the drop model curve, is determined as a function of δ (see fig. 4). The exponent in (2) is then obtained by numerical integration and gives directly the change in fission rate. Table 2 shows the results. Listed there are also the equilibrium deformations and the deformation at the saddle point.

The comparison with the experimental data is made in the following way (shown in fig. 5). We start with a certain nucleus, for example U^{232}, and

consider the effect of addition of two extra neutrons to make U^{234}. The experimental value for the logarithmic difference in half-life between U^{234} and U^{232} is corrected by the correction term for U^{234} in table 2. This gives a

TABLE 2

Nucleus	Ground state deformation	Saddle point deformation	Spin, parity, and asymptotic quantum numbers for highest level	Correction factor (logarithmic change in half-life)
U^{234}	0.24	0.51	$\frac{5}{2}+[633]$	0.4
U^{235}	0.24	0.51	$\frac{7}{2}-[743]$	−0.6
U^{236}	0.25	0.52	$\frac{7}{2}-[743]$	0.7
U^{238}	0.26	0.53	$\frac{1}{2}+[631]$	1.9
Pu^{238}	0.25	0.47	$\frac{7}{2}-[743]$	0.6
Pu^{239}	0.26	0.48	$\frac{1}{2}+[631]$	−1.3
Pu^{240}	0.26	0.48	$\frac{1}{2}+[631]$	2.6
Pu^{242}	0.26	0.49	$\frac{5}{2}+[622]$	2.2
Pu^{244}	0.26	0.50	$\frac{9}{2}-[734]$	1.3
Cm^{242}	0.26	0.43	$\frac{1}{2}+[631]$	2.5
Cm^{244}	0.26	0.45	$\frac{5}{2}+[622]$	1.6
Cm^{246}	0.26	0.46	$\frac{9}{2}-[734]$	0.6
Cm^{248}	0.26	0.47	$\frac{7}{2}+[624]$	1.0
Cf^{248}	0.25	0.40	$\frac{9}{2}-[734]$	−0.1
Cf^{249}	0.25	0.41	$\frac{7}{2}+[624]$	−3.3
Cf^{250}	0.25	0.42	$\frac{7}{2}+[624]$	−0.2
Cf^{252}	0.24	0.43	$\frac{7}{2}+[613]$	4.3
Cf^{254}	0.24	0.44	$\frac{11}{2}-[725]$	2.3
Fm^{256}	0.24	0.40	$\frac{11}{2}-[725]$	3.7

point corresponding to U^{234} in fig. 5. This point is then the starting point for plotting the corrected difference between U^{236} and U^{234}, and so on. The resulting curve will therefore give the half-lives expected if there were no single particle effect. Fig. 5 shows that instead of having a more or less irregular curve for each element, we now get a fairly straight line. The lines for the various elements are roughly parallel. Even the isotopes of Cf and Fm, which deviate so strongly in fig. 1, follow the general trend fairly well but the correction is here apparently somewhat too small. The odd-mass nuclei are moved towards the lines, although the correction does not seem to be quite sufficient.

These straight lines are, of course, what we expect to get on the basis of the liquid drop model. It therefore seems that the calculated corrections for the single particle effect have the right size to explain the observed deviations from the drop model.

It is possible to go one step further and treat the single particle effect of the protons. In this case we study what happens when two protons are added to a certain nucleus. We can, for example, take U^{234} and add two protons to get Pu^{236}. The calculations are exactly analogous to those for the neutrons.

The correction for the single particle effect of the protons is essentially a parallel movement of the lines up or down. The correction factors are given in table 3. The comparison with the experimental data is made in a way analogous to that for the neutron case. Starting from U we get a corrected position for the Pu isotopes. This new position then is the starting point for the correction applied to the curium isotopes, and so on. The result is shown in fig. 6. Now the points fall rather nicely along a straight line.

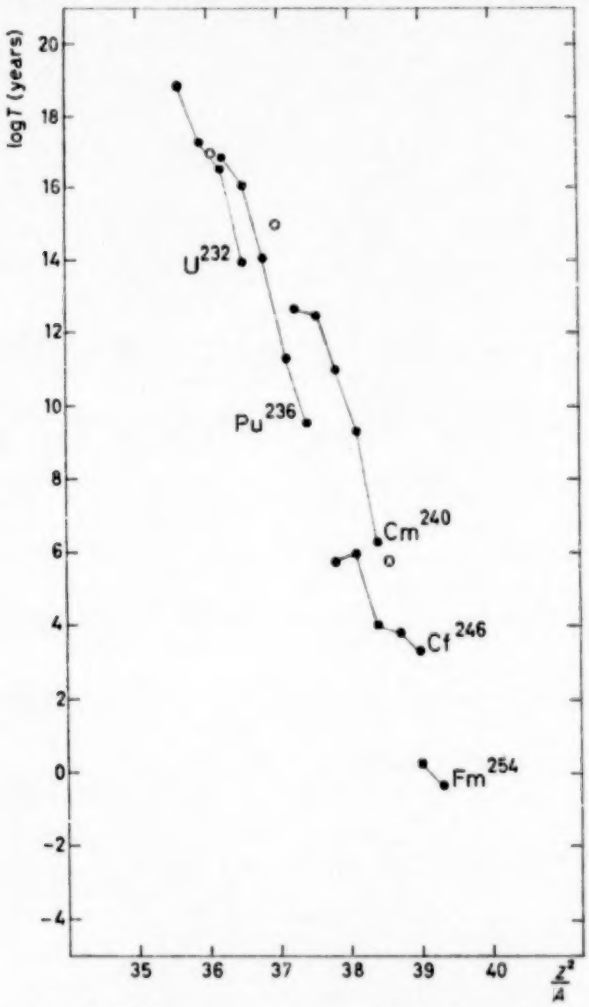

Fig. 5. Spontaneous fission half-lives corrected for the single particle effect of the neutrons. Dots: the even nuclei $U^{232-238}$, $Pu^{236-244}$, $Cm^{240-248}$ and $Fm^{254-256}$. Open circles: the odd-neutron nuclei U^{235}, Pu^{239} and Cf^{249}.

TABLE 3

Nucleus	Spin, parity, and asymptotic quantum numbers for highest level	Correction factor (logarithmic change in half-life)
Pu	$\frac{5}{2}+[642]$	1.2
Cm	$\frac{7}{2}-[523]$	−5.4
Cf	$\frac{9}{2}-[521]$	−2.1
Fm	$\frac{7}{2}-[633]$	−2.4

The result of the calculation is that the irregular behaviour of the spontaneous fission rates apparently can be explained as a single particle effect. In fig. 6 there are no systematic deviations left. The corrected values scatter along a straight line. The scattering is not greater than what can be expected from the various uncertainties and approximations of the calculation. It should also be borne in mind that the experimental values in several cases are rather uncertain. This also contributes to the scattering.

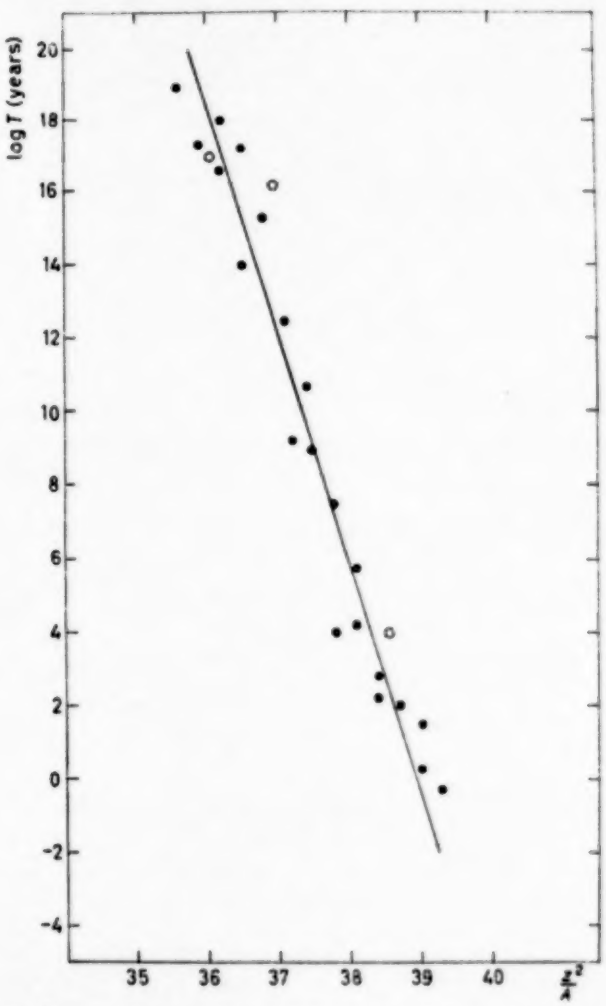

Fig. 6. Spontaneous fission half-lives corrected for the single particle effect of both neutrons and protons. The same nuclei as in fig. 5 are shown.

7. Discussion

The experimental deviations from the drop model are apparently quite well explained by the calculated single particle effect. It is somewhat surprising that the result of the calculation is so good. There are some reasons for this. The Nilsson level diagram is not purely theoretical, but the parameters are adjusted to get the best possible agreement with the experimental level order. Hence, the greatest uncertainty in the level diagram comes from

the uncertainty in the slope of the levels. In the asymptotic approximation, however, the slope is given by the asymptotic quantum numbers N and n_z and does not depend on the detailed shape of the potential. Since the asymptotic approximation should be good for the deformations of interest in the present work, the level diagram is perhaps better than one would expect.

There is, of course, still a faily large uncertainty in the position of a level. It is interesting to examine the consequences of a shift in level position. If the highest occupied level in a certain nucleus is moved upwards, for example, it means that the barrier will become lower. This is because the two nucleons in this level will jump to other levels with increasing deformation. Hence, the ground state energy will become higher without a corresponding increase in energy at larger deformations. The two highest nucleons will, by the level shift, acquire a tendency to lower the barrier. For the nucleus obtained by addition of two neutrons we shall get an opposite effect. The shift of the level in question will result in a tendency for the two highest nucleons to make the barrier higher. An error in the position of a level will therefore cause a positive error in the correction of a certain nucleus, followed by a negative error in the correction for the next nucleus or vice versa. An effect of this type seems to exist in fig. 5. The deviations from straight lines in fig. 5 are therefore partly due to the errors in the level scheme.

It must also be borne in mind that the present calculation is based on the rather extreme assumption of pure single particle states. The actual wave functions are not pure, however, but contain contributions from several configurations. This fact, if it could be taken into account, should make the lines in fig. 5 smoother. Hence, in figs. 5 and 6 only the general trend is significant but not the details.

In the present work the single particle level scheme is used to calculate the single particle effects in spontaneous fission. It has been necessary, however, to use the drop model to calculate some quantities, for example the shape of the potential barrier. The calculation is therefore not quite consistent. It must be emphasized, however, that the results obtained from the drop model enter the calculations in such a way that their influence is small. The final results depend essentially only on the single particle level scheme provided that the drop model is not entirely wrong.

8. Predictions for Heavier Nuclei

It is, for many reasons, of great interest to predict the spontaneous fission half-lives of the unknown, heavier isotopes of the transuranium elements. Such predictions are of great help in the search for these isotopes, since the spontaneous fission is often the major mode of decay. There are other problems in which a knowledge of spontaneous fission rates are of interest. Some of them will be discussed later.

The predictions are usually made by a straightforward extrapolation of the lines in fig. 1. The extrapolated parts of the curves are dashed in fig. 1. Fm^{258}, for example, is predicted to have a half-live of the order of one minute. Without knowledge about all the factors that influence the spontaneous fission rates such an extrapolation must be rather uncertain, however.

The present calculations can easily be extended to heavier nuclei. Fig. 2 can be used to $N = 160$. It turns out that the downward trend for the heavier Cf and Fm isotopes will not continue. The level corresponding to $N = 157, 158$ will have a rather small effect on the barrier height. The half-lives for the corresponding nuclei should therefore be those given by an extension of the trend in fig. 6. This will be the same as an estimate based on the drop model. The next level will even tend to increase the barrier height. The half-lives for the corresponding nuclei should be longer than the estimate from fig. 6. The spontaneous fission rates given by the present calculation will be slower than the ones estimated by the previously mentioned extrapolation. For Fm^{258}, for example, the half-life has previously been estimated to be of the order of a minute. The estimate from the present work is a half-life of the order of a day. In this region, however, the corrections seem to be too small with about one order of magnitude. Hence the half-life might be as short as about an hour. For Cf^{256} we get in the same way a half-life between a year and a month.

The general tendency for the heavier elements will be to follow the drop model estimate more closely. The reason is that the saddle point shapes become more spherical. For these smaller deformations the slope of the levels is smaller. This makes the single particle effect on the barrier height relatively less important. A consequence of this is also that the difference between the even- and odd-mass nuclei will diminish.

Knowledge of the half-life for spontaneous fission is of great importance for an attempt to produce heavier elements by multiple neutron capture in a very intense bombardment with slow neutrons. A possible path for production according to this method has been described by Seaborg [13]). This process works, however, only if the successive nuclei formed have a half-life long enough to permit absorption of a further neutron. It turns out that the decisive point is the spontaneous fission half-life of some isotopes e.g., Fm^{258}. If it is about a minute, as predicted previously, this method of production holds little promise. If it is considerably longer, as predicted by the present work, the method is more promising.

A related problem is the production of heavy elements in supernova explosions. They are assumed to be formed on a very short time scale (of the order of seconds) by multiple neutron absorption. Because of the extremely high neutron flux, heavier nuclei can be built in this way than in the corresponding process in the laboratory. However, the build-up of heavy nuclei

will also in this case stop when the fission half-lives become too short. The half-lives will therefore determine how far this process can proceed, thereby having influence on the abundance of the elements. A detailed discussion of this problem is found in the papers of Burbidge *et al.*[14]) and Cameron [15]). Burbidge *et al.* use the previously mentioned extrapolation and conclude that the build-up will stop at about $A = 260$. Cameron, on the other hand, assumes (without giving any reasons) that the half-lives are longer than those resulting from the straightforward extrapolation. The build-up can then proceed further to the closure of a major neutron shell at $N = 184$. This can explain some features in the abundance curve of the elements. The present work supports the second alternative.

References

1) G. T. Seaborg, Phys. Rev. **85** (1952) 157
2) W. Whitehouse and W. Galbraith, Nature **169** (1952) 494
3) A. Ghiorso, Geneva Conference Report no. 718 (1955)
4) J. R. Huizenga, Phys. Rev. **94** (1954) 158
5) W. J. Swiatecki, Phys. Rev. **100** (1955) 937
6) S. G. Nilsson, Mat. Fys. Medd. Dan. Vid. Selsk. **29**, No. 16 (1955)
7) B. N. Mottelson and S. G. Nilsson, Mat. Fys. Skr. Dan. Vid. Selsk. **1**, No. 8 (1959)
8) J. O. Newton, Progress in Nuclear Physics **4** (1955) 234
9) J. A. Wheeler, Nuclear Fission and Nuclear Stability in Niels Bohr and the Development of Physics (Pergamon Press, London 1955)
10) L. Wilets and D. M. Chase, Phys. Rev. **103** (1956) 1296
11) D. L. Hill and J. A. Wheeler, Phys. Rev. **89** (1953) 1102
12) N. Bohr and J. A. Wheeler, Phys. Rev. **56** (1939) 426
13) G. T. Seaborg, The Transuranium Elements (Yale University Press, New Haven 1958)
14) E. M. Burbidge *et al.*, Revs. Mod. Phys. **29** (1957) 547
15) A. G. W. Cameron, Chalk River Report CRL-41.

1.C *Nuclear Physics* **12** (1959) 465—484; © *North-Holland Publishing Co., Amsterdam*
Not to be reproduced by photoprint or microfilm without written permission from the publisher

THE GREEN'S FUNCTION METHOD IN QUANTUM STATISTICS

E. S. FRADKIN

P. N. Lebedev Physical Institute of USSR Academy of Sciences, Moscow

Received 7 January 1959

Abstract: A Green's function method in quantum statistics is developed. It is shown that the equations obtained contain in a simple approximation various methods encountered in statistical physics and in the theory of many particles as well as their extensions to cases of non-vanishing temperature (e.g., the Debye-Hückel, Hartree-Fock, Thomas-Fermi, Gell-Mann-Brueckner methods). A transition to time-dependent Green's functions is considered and a method for the determination of the energy spectrum of the system is proposed.

1. Introduction

Much effort has been spent lately in attempts to develop methods which would differ from the usual thermodynamic perturbation theory in statistics and the familiar perturbation theory procedure for many-particle systems. We shall not enumerate here the various investigations carried out in this direction †; it will suffice to mention that the existing methods are manifold and involve very cumbersome calculations.

It seems natural to attempt to find a more general approach to the solution of quantum statistical problems which would be independent of perturbation theory and, in particular, would yield in a simple and graphic approximation the same results as the existing methods.

The Green's function method is apparently an approach of precisely this type. It has been successfully applied for the case $T = 0$ [2]. Matzubara [3] was the first to formulate Feynman's method and to introduce the Green's function for $T \neq 0$. However, the problem of setting up closed equations for the Green's functions in x space still awaits its final solution. What is more important is that the transition to p space which eases the possibility of practical solution of the equations, has not been considered. On the other hand the development of high energy physics requires further elaboration of a formalism of quantum statistics in which, generally speaking, account should be taken of relativistic corrections or secondary quantization of the system Hamiltonian. Finally, for the investigation of the energy spectrum

† For relevant references see ref. [1]).

of the system a knowledge of the time dependence of the Green's function is also necessary.

The present paper is devoted to a study of the problems enumerated above †.

2. Green's Function Equations in Quantum Statistics

The density matrix for a canonical ensemble has the form

$$\rho = \exp -\beta(\hat{H}-\mu\hat{N}), \tag{1.1}$$

where $\beta = 1/kT$; $\hat{H}$ is the total Hamiltonian of the system, consisting of the free field Hamiltonian H_0 and interaction Hamiltonian H_1; μ is the chemical potential, $\hat{N}$ the operator of the total number of conserved particles (e.g. the difference between the number of particles and antiparticles).

Without loss of generality we can consider the interaction between a Fermi field ψ(mass m) and a Bose field φ(mass κ).

In this case the interaction Hamiltonian is

$$\begin{aligned} \hat{H}_1 &= -\int j(\mathbf{x})\varphi(\mathbf{x})\mathrm{d}^3x, \\ j(x) &= \tfrac{1}{2}ig\ \mathrm{tr}\ \gamma[\bar{\psi}(\mathbf{x})\psi(\mathbf{x})-\psi(\mathbf{x})\bar{\psi}(\mathbf{x})], \end{aligned} \tag{1.2}$$

$$\hat{N} = \tfrac{1}{2}\int \mathrm{tr}\ \gamma_4[\bar{\psi}(\mathbf{x})\psi(\mathbf{x})-\psi(\mathbf{x})\bar{\psi}(\mathbf{x})]\mathrm{d}^3x. \tag{1.3}$$

The form of the interaction γ and covariant properties of the field φ will not be specified in greater detail (e.g. in electrodynamics $\gamma = \gamma_\mu$, $\varphi = A_\mu$). By conventional field theory methods [3]) we obtain

$$\begin{aligned} \rho(\beta) &= \rho_0(\beta)S(\beta), \quad \rho_0(\beta) = \exp -\beta(\hat{H}_0-\mu\hat{N}), \\ S(\beta) &= \mathrm{T}\exp -\left[\int_0^\beta \mathrm{d}x_4 \int H_1(x_4, \mathbf{x})\mathrm{d}_4x\right], \\ H_1(\mathbf{x}, x_4) &= -(j(\mathbf{x}, x_4)\varphi(\mathbf{x}, x_4)), \end{aligned} \tag{1.4}$$

where T denotes a right to left time ordered arrangement of the operators, in the order of increasing time. Any operator $f(\mathbf{x}, x_4)$ is defined by the relation

$$f(\mathbf{x}, x_4) = \rho_0(-x_4)f(\mathbf{x})\rho_0(x_4). \tag{1.5}$$

By analogy with quantum field theory [4]) we generalize the interaction Hamiltonian by including an additional interaction between the external sources and the Bose and Fermi fields:

$$\begin{aligned} H_1(\mathbf{x}, x_4) = -\{&[j(\mathbf{x}, x_4)+J(\mathbf{x}, x_4)]\varphi(\mathbf{x}, x_4) \\ &+\bar{\eta}(\mathbf{x}, x_4)\psi(x, x_4)+\bar{\psi}(\mathbf{x}, x_4)\eta(x, x_4)\} \end{aligned} \tag{1.6}$$

† Some of the results of this paper are contained in a previous paper of the author [5]) and also (as we have recently learned) in ref. [12]).

The following relations follow from (1.4) and (1.6):
a) for x_4 in the interval between 0 and β,

$$\frac{\delta\rho(\beta)}{\delta J(\mathbf{x}, x_4)} = \rho_0(\beta)S(\beta)S(-x_4)\varphi(\mathbf{x}, x_4)S(x_4) = \rho(\beta)\tilde{\varphi}(\mathbf{x}, x_4),$$

$$\frac{\delta\rho}{\delta\bar{\eta}(\mathbf{x}, x_4)} = \rho\hat{\psi}(\mathbf{x}, x_4), \quad \frac{\delta\rho}{\delta\eta(\mathbf{x}, x_4)} = \rho\hat{\bar{\psi}}(\mathbf{x}, x_4), \tag{1.7}$$

$$\frac{\delta\rho}{\delta\bar{\eta}(\mathbf{x}, x_4)\delta\eta(\mathbf{x}', x'_4)} = \rho\mathrm{T}(\psi(\mathbf{x}, x_4)\hat{\bar{\psi}}(\mathbf{x}', x'_4));$$

b) for x_4 outside of the interval $(0, \beta)$ all functional derivatives vanish. Any operator $f(\mathbf{x}, x_4)$ is related to the operator $f(\mathbf{x})$ by the relation

$$\hat{f}(\mathbf{x}, x_4) = \rho^{-1}(x_4)f(\mathbf{x})\rho(x_4). \tag{1.8}$$

Variations with respect to η and $\bar{\eta}$ should be understood in the sense of variations from the right and left, respectively, i.e.

$$\delta\rho = \int \mathrm{d}^4x \left(\delta\bar{\eta}\frac{\delta\rho}{\delta\bar{\eta}} + \frac{\delta\rho}{\delta\eta}\delta\eta\right). \tag{1.9}$$

Employing the commutation rules for ψ and φ the following functional equations for the state integral can be obtained:

$$\left(i\hat{\not{p}} + m - ig\gamma\frac{\delta}{\delta J}\right)\frac{\delta z}{\delta\bar{\eta}(x)} = \eta(x)z,$$
$$\left(-\frac{\partial^2}{\partial x_\nu^2} + \kappa^2\right)\frac{\delta z}{\delta J(x)} = J(x)z - ig\,\mathrm{tr}\,\gamma\frac{\delta^2 z}{\delta\bar{\eta}(x)\delta\eta(x)}, \tag{1.10}$$

where

$$z = \mathrm{Tr}(\rho(\beta)), \quad i\hat{\not{p}} = \gamma_\nu\partial_\nu, \quad \partial_4 = \frac{\partial}{\partial x_4} - \mu, \quad \partial_k = \frac{\partial}{\partial x_k},$$
$$\hbar = c = 1, \quad \nu = 1, 2, 3, 4, \quad k = 1, 2, 3.$$

Here the functional derivatives do not vanish only for those values of x_4 which lie in the region from 0 to β.

With the aid of (1.10) and the method described in ref. [6]) we can find the following operator solution for the state integral †;

$$z = z_0 \exp\left[ig\,\mathrm{tr}\,\gamma\int \mathrm{d}^4x\frac{\delta}{\delta\eta(x)}\frac{\delta}{\delta\bar{\eta}(x)}\frac{\delta}{\delta J(x)}\right]\exp\int\{J(x)D_0(x-y)J(y)$$
$$+\bar{\eta}(x)G_0(x-y)\eta(y)\}\mathrm{d}^4x\mathrm{d}^4y, \tag{1.11}$$
$$z_0 = \prod_{r,k}(1+\exp\beta(\mu-\varepsilon_r))(1+\exp-\beta(\mu+\varepsilon_r))(1-\exp-\beta w_k)^{-1},$$

† Here and in the following the integral with respect to the fourth component is evaluated between 0 and β.

$$D_0(x-x') = \frac{1}{(2\pi)^3}\int \frac{d^3k}{2w_k}\{(f_k+1)\exp[i\mathbf{k}\cdot(\mathbf{x}-\mathbf{x}')-w_k|x_4-x'_4|] + f_k\exp[-i\mathbf{k}\cdot(\mathbf{x}-\mathbf{x}')+w_k|x_4-x'_4|]\}, \tag{1.12}$$

$$G(x-x') = (i\hat{p}-m)\frac{1}{(2\pi)^3}\int\frac{d^3k}{2\varepsilon_k}\begin{cases}(N_k^+-1)\exp[i\mathbf{k}\cdot(\mathbf{x}-\mathbf{x}')-(\varepsilon_k-\mu)(x_4-x'_4)]\\ N_k^+\exp[-i\mathbf{k}\cdot(\mathbf{x}-\mathbf{x}')-(\varepsilon_k-\mu)(x_4-x'_4)]\end{cases}$$
$$+\begin{cases}N_k^-\exp[-i\mathbf{k}\cdot(\mathbf{x}-\mathbf{x}')+(\varepsilon_k+\mu)(x_4-x'_4)] & (x_4>x'_4)\\ (N_k^--1)\exp[i\mathbf{k}\cdot(\mathbf{x}-\mathbf{x}')+(\varepsilon_k+\mu)(x_4-x'_4)] & (x_4<x'_4),\end{cases} \tag{1.13}$$

$$N_k^{\pm} = \frac{1}{1+\exp(\varepsilon_k\mp\mu)\beta}, \quad f = \frac{1}{\exp(w_k\beta)-1};$$
$$\varepsilon_k = \sqrt{\mathbf{k}^2+m^2}, \qquad w_k = \sqrt{\mathbf{k}^2+\kappa^2};$$

$N_k^+(N_k^-)$ is the mean number of particles (antiparticles) in a state of energy ε_k.

Eliminating the Boson derivatives we obtain [5]) from (1.11)

$$z = z_0\exp\int\left\{\left(J(x)+ig\gamma\frac{\delta}{\delta\eta(x)}\frac{\delta}{\delta\bar{\eta}(x)}\right)\tfrac{1}{2}D_0(x-y)\left(J(y)+ig\gamma\frac{\delta}{\delta\eta(y)}\frac{\delta}{\delta\bar{\eta}(y)}\right)\right\}$$
$$\cdot\, d^4x d^4y\exp\int\bar{\eta}(x)G_0(x-y)\eta(y)d^4xd^4y. \tag{1.14}$$

Differentiating $\ln z$ with respect to the "charge" we obtain the following operator solution for the thermodynamic potential

$$\Omega = \Omega_{|g=0} - \int_0^g \frac{i\,dg'}{g'\beta z}\,\mathrm{tr}\,\gamma\int d^4x\frac{\delta}{\delta\eta}\frac{\delta}{\delta\bar{\eta}}\frac{\delta}{\delta J}z. \tag{1.15}$$

Expressions (1.11) and (1.15) can be expanded in a power series in g, each term of the series coinciding with the corresponding approximation calculated by the Feynman method [3]).

Our method is more convenient, especially for higher approximations since not all Feynman graphs have to be tested and the whole problem reduces to a successive functional differentiation in the required order with respect to the charge and this is an easy operation.

The mean value of any T-ordered function of the field operators $f(\psi\bar{\psi}\varphi)$ can be calculated in accord with the rule

$$\langle f\rangle = \frac{\mathrm{tr}\,(\rho f)}{z} = \frac{1}{z}f\left(\frac{\delta}{\delta\bar{\eta}}\frac{\delta}{\delta\eta}\frac{\delta}{\delta J}\right)z_{|J=\eta=0}. \tag{1.16}$$

For example

$$\langle \mathrm{T}(\psi(x)\psi(x_1)\bar{\psi}(x')\bar{\psi}(x'))\rangle = \frac{1}{z}\frac{\delta^4 z}{\delta\bar{\eta}(x)\delta\bar{\eta}(x_1)\delta\eta(x')\delta\eta(x'_1)_{|J=\eta=0}}.$$

We introduce "single-particle" Green's functions for fermions G and bosons D; according to (1.16) they can be written down as †

$$G(x, y) = \frac{1}{z}\frac{\delta^2 z}{\delta\bar{\eta}(x)\delta\bar{\eta}(y)_{|J=\eta=0}},$$
$$D(x, y) = \frac{\delta^2}{\delta J(x)\delta J(y)}\ln z_{|J=\eta=0}. \tag{1.17}$$

With the help of (1.10) we obtain the following set of equations for G and D:

$$(i\hat{p}+m-ig\gamma\langle\varphi(x)\rangle)G(x, y)+\int\Sigma^*(x, z)G(z, y)\mathrm{d}^4z = \delta(x-y), \tag{1.18}$$

$$\left(-\frac{\partial^2}{\partial x_\nu^2}+\kappa^2\right)\langle\varphi(x)\rangle=-\tfrac{1}{2}ig\,\mathrm{tr}\gamma[G(\mathbf{x}, x_4; \mathbf{x}, x_4-\varepsilon)+G(x, x_4; x, x_4+\varepsilon)]_{|\varepsilon\to 0} \tag{1.19}$$

$$\left(-\frac{\partial^2}{\partial x_\nu^2}+\kappa^2\right)D(x, y)-\int\Pi(x, z)D(z, y)\mathrm{d}^4z = \delta(x-y); \tag{1.20}$$

$$\Sigma^*(x, y) = g^2\int\gamma G(x, z)\Gamma(z, y, y')D(y', x)\mathrm{d}z\,\mathrm{d}y',$$
$$\Pi(x, y) = g^2\,\mathrm{tr}\int\gamma G(x, z)\Gamma(z, y', y)G(y', x)\mathrm{d}z\,\mathrm{d}y', \tag{1.21}$$
$$\Gamma(x, y, y') = \gamma\delta(z-y')\delta(y-y')-\frac{\delta\Sigma^*(x, y)}{\delta ig\,\langle\varphi(y')\rangle}.$$

The "single-particle" Green's functions are defined by equations (1.19—1.21) only for x_4 in the interval $(-\beta, \beta)$. Outside this interval these functions can be defined in an arbitrary manner.

Let us impose on the functions the restriction that they be periodic with an interval 2β. We then expand these functions in a Fourier series:

$$G(x) = \frac{1}{\beta(2\pi)^3}\sum_{p_4}\int\mathrm{d}^3p\,G(\mathbf{p}, p_4)\exp -ip_\nu x_\nu,$$
$$D(x) = \frac{1}{\beta(2\pi)^3}\sum_{p_4}\int\mathrm{d}^3p\,D(\mathbf{p}, p_4)\exp -ip_\nu x_\nu, \tag{1.22}$$
$$\Gamma(x, y, z) = \Gamma(x-z, y-z) = \frac{1}{\beta^2(2\pi)^6}\sum_{p_4, p'_4}\int\Gamma(p, p')\exp[-ip_\nu(x-z)_\nu$$
$$+ip'_\nu(y-z)_\nu]\mathrm{d}^3p\,\mathrm{d}^3p'.$$

The following can be shown: 1) The frequencies p_4 assume the values $(2n+1)\pi/\beta$ †† for Fermi particles, whereas for Bose particles the frequencies

† Matzubara [3]) was the first to introduce Green's functions for $T \neq 0$. The distinctive feature of our Green's functions is the complete symmetry between $\hat{H}$ and μN, viz. all quantities depend on $(H-\mu N)$ (whereas in Matzubara's paper x_4 entered only in combination with the factor $\hat{H}$). It will be seen below that this circumstance permits one to change to the p representation in the Green's functions.

†† The fact that for $T \neq 0$ the thermodynamic quantities can be expressed in the form of a series in $\varepsilon_n = \varepsilon(2n\pi)/\beta$ has already been demonstrated under other circumstances in ref. [7]).

p_4 assume † only the values $2n\pi/\beta$, where n takes all integral values from $-\infty$ to $+\infty$.

2) For G and D the following relations hold:

$$G(x_4 = \pm 0) = -G(x_4 = \pm\beta),\quad \dot{D}(x_4 = \mp 0) = \dot{D}(x_4 = \pm\beta)\left(\dot{D} = \frac{\partial}{\partial x_4} D\right).$$

This follows from the spectral representations of G and D which have the form

$$G(x-x') = \begin{cases} \frac{1}{z}\sum_{m,n} \psi_{n,m}(0)\bar{\psi}_{m,n}(0)\exp[(\mu N_n - E_n)\beta + (E_n - E_m + \mu N_m - \mu N_n)(x_4 - x'_4) \\ \qquad + i(\mathbf{p_n} - \mathbf{p_m})(\mathbf{x}-\mathbf{x}')];\ (x_4 > x'_4) \\ -\frac{1}{z}\sum_{m,n} \bar{\psi}_{m,n}(0)\psi_{n,m}(0)\exp[(\mu N_m - E_m)\beta + (E_n - E_m + \mu N_m - \mu N_n)(x_4 - x'_4) \\ \qquad + i(\mathbf{p}_n - \mathbf{p}_m)(\mathbf{x}-\mathbf{x}')];\ (x_4 < x'_4) \end{cases} \tag{1.23}$$

$$D(x, x') = \frac{1}{z}\sum_{m,n} |\varphi_{n,m}(0)|^2 \exp[-\beta E_n + (E_n - E_m)|x_4 - x'_4| + i(\mathbf{p}_n - \mathbf{p}_m)(\mathbf{x}-\mathbf{x}')]. \tag{1.24}$$

The fact that only odd frequencies (in π/β units) are involved in the Green's function G and even frequencies in the D functions signifies that the Kronecker delta function † arises from integration over x_4 (law of conservation of "quasi energy" in each mode of the Feynman graphs).

The set of equations for the Green's functions in the p representation can be greatly simplified and has the form [5])

$$\begin{aligned} &[-ip_\nu\gamma_\nu - \gamma_4\mu + m + \Sigma^*(p)]G(p) = \sum_n \delta\left(p_4 - \frac{(2n+1)\pi}{\beta}\right), \\ &[k_\nu^2 + \kappa^2 - \Pi(k)]D(k) = \sum_n \delta\left(k_4 - \frac{2n\pi}{\beta}\right), \\ &\Sigma^*(p) = \frac{g^2}{(2\pi)^3\beta}\int\sum_{k_4} \gamma G(p+k)\Gamma(p+k, p)D(k)\,\mathrm{d}^3k, \\ &\Pi(k) = \frac{g^2}{(2\pi)^3\beta}\,\mathrm{tr}\int\sum_{p_4} \gamma G(p+k)\Gamma(p+k, p)G(p)\mathrm{d}^3p, \\ &\Gamma(p, p') = \sum_{n,m} \gamma\delta\left(p_4 - \frac{(2n+1)\pi}{\beta}\right)\delta\left(p_4 - \frac{(2m+1)\pi}{\beta}\right) + \Lambda(p, p'), \end{aligned} \tag{1.25}$$

where δ is the Kronecker delta function and Λ the set of all graphs of the vertex part excluding a simple vertex.

With the help of (1.15) we find that the thermodynamic potential can also be expressed in terms of "single-particle" functions:

† This point was previously mentioned in ref [8]) for $\mu = 0$. However, for $\mu \neq 0$ the Matzubara Green's functions would have even as well as odd frequencies and hence integration over x_4 would not always yield a Kronecker delta function and therefore transition to the p representation would not be effective.

$$\begin{aligned}\Omega &= \Omega_{|g=0} - \frac{v}{(2\pi)^3\beta}\sum_{k_4}\int\int_0^g \frac{dg'\,\Pi(k)}{g'(k^2+\Pi(k))}\,d^3k \\ &= \Omega_{|g=0} - \frac{v}{(2\pi)^3\beta}\,\mathrm{tr}\sum_{k_4}\int d^3k\int_0^g \frac{dg'}{g'}\,\Sigma^*(k)G(k).\end{aligned} \tag{1.26}$$

The set (1.25) was obtained with the aid of the unrenormalized Hamiltonian of the interacting fields. This can be seen, in particular, from the fact that all quantities are expressed in terms of the particle bare masses (m and $\varkappa$) and bare charge (g). However, already within the framework of mechanics of a single physical particle the experimental values of the indicated quantities differ from the bare values; this is a result of interaction between the particle and zero oscillation of the Bose and Fermi fields.

In view of the difficulties encountered in present day theory it is very important that this renormalization be performed in the Green's function equations themselves. To do this it is sufficient to employ the renormalized interaction field Hamiltonian. This is equivalent to the following renormalization procedure for the Green's functions [9]):

1) A change should be made to the new variables $G_1, D_1, \Gamma_1, \psi_1, \varphi_1, \eta_1, g_e$ related to the old ones as follows:

$$\begin{aligned}&\psi_1 = \psi/z_2^{\frac{1}{2}}, \quad G_1 = G/z_2, \quad \eta_1 = \eta z_2^{\frac{1}{2}}, \quad \Gamma_1 = z_1\Gamma, \\ &\varphi_1 = \varphi/z_3^{\frac{1}{2}}, \quad J_1 = z_3^{\frac{1}{2}}J, \quad D_1 = Dz_3, \quad g_e = z_1^{-1}z_2z_3^{\frac{1}{2}}g.\end{aligned} \tag{1.27}$$

2) Constants z_n and m_e are specified by the mass operator $\tilde{\Sigma}$, polarization operator $\tilde{\Pi}$ and vertex part $\tilde{\Lambda}$ for single particle Green's functions in quantum field theory:

$$\begin{aligned}&z_1^{-1} = 1+\tilde{\Lambda}(\hat{p}^0, \hat{p}^0), \quad z_2 = 1-\frac{\partial\tilde{\Sigma}(\hat{p}^0)}{\partial i\hat{p}^0}, \quad z_3 = 1-\frac{\partial\tilde{\Pi}(k^0)}{\partial(k^0)^2}; \\ &m_e = m+\frac{\tilde{\Sigma}(\hat{p}^0)}{z_2}, \quad \varkappa_e^2 = \varkappa^2-\frac{\Pi(k^0)}{z_3}, \quad (k^0)^2 = \mathbf{k}^2-k_0^2 = -\varkappa_e^2; \\ &i\hat{p}^0 = i\boldsymbol{\gamma}\cdot\mathbf{p}-\gamma_4 p_0 = m_e.\end{aligned} \tag{1.28}$$

It can be shown that the mass and polarization operators and also the vertex part of single-particle Green's functions in the quantum field theory are identical to the analytic continuation of the respective quantities for "single-particle" Green's functions in quantum statistics when $\beta = \infty$ and $\mu = 0$ (that is, when p_4 is replaced in the latter by $ip_0-\varepsilon p_0/|p_0|$).

Taking into account the last remark and substituting (1.27) and (1.28) in (1.25) we finally obtain the following set of renormalized equations for the Green's functions in quantum statistics:

$$G_1^{-1}(p) = (-ip_\nu\gamma_\nu - \gamma_4\mu + m_e + \Sigma_2^*(p)) \sum_n \delta\left(p_4 - \frac{(2n+1)\pi}{\beta}\right),$$

$$D_1^{-1}(k) = (k_\nu^2 + \kappa_e^2 - \Pi_2(k)) \sum_n \delta\left(k_4 - \frac{2n\pi}{\beta}\right),$$

$$\Sigma_2^*(\mathbf{p}, p_4) = \Sigma^*(\mathbf{p}, p_4) - \left\{\tilde{\Sigma}_1^*(\mathbf{p}, ip_0) + (i\gamma_\nu p_\nu + \gamma_4\mu - m_e)\frac{\partial\tilde{\Sigma}_1^*(\mathbf{p}, ip_0)}{\partial i\gamma\cdot\mathbf{p}}\right\},$$

$$\Gamma_1(p, p_2) = \gamma + [\Lambda_1(p_1, p_2) - \Lambda_1(\hat{p}_1^0\hat{p}^0)_{|_{\beta^{-1}=\mu=0}^{i\hat{p}^0=m_e}}],$$

$$\Pi_2(\mathbf{k}, k_4) = \Pi_1(\mathbf{k}, k_4) - \left\{\tilde{\Pi}_1(\mathbf{k}, ik_0) + (k_\nu^2 + \kappa_e^2)\frac{\partial\Pi_1(\mathbf{k}, ik_0)}{\partial\mathbf{k}^2}\right\}, \tag{1.29}$$

$$\Sigma_1^*(p) = \frac{g_e^2}{(2\pi)^3\beta}\int\sum_{k_4} z_1\gamma G_1(p+k)\Gamma_1(p+k, p)D_1(k)\mathrm{d}^3k,$$

$$\Pi_1(k) = \frac{g_e^2}{(2\pi)^3\beta}\,\mathrm{tr}\int\sum_{p_4} z_1\gamma G_1(p+k)\Gamma_1(p+k, p)G_1(p)\mathrm{d}^3p,$$

$$\tilde{\Pi}_1(\mathbf{k}, ik_0) = \Pi_1(\mathbf{k}, ik_0)_{|_{\beta^{-1}=\mu=0}^{k_0^2=\mathbf{k}^2+\kappa_e^2}}, \quad \tilde{\Sigma}_1^*(p, ip_0) = \Sigma_1^*(\mathbf{p}, ip_0)_{|_{\beta^{-1}=\mu=0}^{i\gamma_\mathbf{p}-\gamma_4 p_0=m_e}}$$

$$z_1 = 1 + \Lambda_1(\hat{p}^0, \hat{p}_1^0)_{|\beta^{-1}=\mu=0}, \quad \left(\sum_n{}_{|\beta\to 0} = \frac{\beta}{2\pi}\int_{-\infty}^{+\infty}\mathrm{d}p_4\right).$$

We see that after renormalization z_1 remains in Σ_1^* and Π_1 (and also in the vertex part); the function of z_1 (just as in quantum field theory) is to eliminate the so-called overlapping infinities which appear in the higher approximations in g_e^2. An effective procedure which can be applied to remove overlapping infinities is presented in ref.[9]) In the case of an electrodynamical system the analysis is much simpler since $z_1^{-1} = z_2$ and only z_3 is involved in the renormalization. In the non-relativistic approximation $z_3 = 1$ and only the Fermi particle mass is renormalized.

In concluding this section it may be pertinent to note that the transition to the non-relativistic approximation is performed as follows: $-i\gamma_\nu p_\nu - \gamma_4\mu + m$ should be replaced everywhere by $-ip_4 - \mu_1 + (\mathbf{p}^2/2m)$ and $G_{\alpha\beta}$ by $G\delta_{\alpha\beta}$ ($d, \beta = 1, -1$ are spin indices). Indeed it can readily be seen from equations (1.25) that it should be sufficient to consider the transition to the non-relativistic limit only for the interactionless Green's function

$$G_0 = \frac{\sum_n \delta\left(p_4 - \frac{(2n+1)\pi}{\beta}\right)}{-i\gamma_\nu p_\nu - \gamma_4\mu + m} = \frac{(i\gamma_\nu p_\nu + \gamma_4\mu + m)\sum_n \delta\left(p_4 - \frac{(2n+1)\pi}{\beta}\right)}{(p_4 - i\mu)^2 + p^2 + m^2}. \tag{1.30}$$

In the non-relativistic approximation we have $\mu = m + \mu_1$, $\gamma = 0$, $\gamma_4 = \delta_{\alpha\beta}$ and all the quantities are small compared with m. Retaining terms of first order of magnitude we obtain the aforementioned rule for transition to non-relativism.

3. Procedure for Obtaining the Time-Dependent Green's Function

Up to now we considered the temperature Green's function which permits one to evaluate all required thermodynamic characteristics. However, in order to determine the spectrum of the system etc. it is very important to know the time-dependent Green's function in quantum statistics.

For the sake of simplicity the analysis will be performed with the help of a non-relativistic Hamiltonian.

Our task, therefore, is to find the time-dependent Green's function in quantum statistics; the definition of this function will be somewhat different from that given by L.D. Landau [10]):

$$\bar{G}(\mathbf{x}, t;\ \mathbf{x}', t') = i\langle \mathrm{T}(\psi(\mathbf{x}, t)\psi^{+}(\mathbf{x}', t')\rangle. \tag{2.1}$$

Here the time dependence of any Heisenberg operator $f(\mathbf{x}, t)$ is generalized in the following way:

$$f(\mathbf{x}, t) = \mathrm{e}^{i(\hat{H}-\mu\hat{N})t} f(\mathbf{x}) \mathrm{e}^{-i(\hat{H}-\mu\hat{N})t}; \tag{2.2}$$

$\langle\ \rangle$ denotes averaging over a canonical ensemble. The spectral representation for the time function can easily be written down as follows:

$$\bar{G}(\mathbf{x}, t; \mathbf{x}', t') = \frac{i}{z}\begin{cases} \sum\limits_{n,m} |\psi_{n,m}(0)|^2 \exp(\mu N_n - E_n)\beta \\ \qquad +i(E_n - E_m - \mu N_n + \mu N_m)(t-t') - i(\mathbf{p}_n - \mathbf{p}_m)(\mathbf{x}-\mathbf{x}')\ (t > t') \\ -\sum\limits_{n,m} |\psi_{n,m}(0)|^2 \exp(\mu N_m - E_m)\beta \\ \qquad +i(E_n - E_m - \mu N_n + \mu N_m)(t-t') - i(\mathbf{p}_n - \mathbf{p}_m)(\mathbf{x}-\mathbf{x}')\ (t < t'). \end{cases} \tag{2.3}$$

Comparing (1.23) and (2.3) we see that the transition from G to $\bar{G}$ is connected with the analytic continuation with respect to x_4; namely, for $t - t' > 0$ the function $\bar{G}(\mathbf{x}-\mathbf{x}',\ t-t')$ is the analytic continuation with respect to $x_4 (x_4 \to it)$ of the function $G(\mathbf{x}-\mathbf{x}', x_4 - x'_4)$ defined in the interval $\beta > x_4 - x'_4 > 0$. The function $\bar{G}(\mathbf{x}-\mathbf{x}',\ t-t')$ in the interval $t-t' < 0$ is an analytic continuation of $G(\mathbf{x}-\mathbf{x}',\ x_4-x'_4)$ defined in the interval $-\beta > x_4 - x'_4 > 0$.

The problem thus reduces to finding the Green's function in the intervals $(0, \beta)$ and $(-\beta, 0)$. In order to do this we shall use the spectral representation of the Green's function $G(\mathbf{x},\ x_4)$. According to (1.23) we have

$$G(\mathbf{p}, p_4) = \frac{1}{z}\sum_{n,m} |\psi_{m,n}(0)|^2 \frac{\exp(\mu N_n - E_n)\beta + \exp(\mu N_m - E_m)\beta}{-ip_4 + (E_n - E_m) - \mu} \tag{2.4}$$

where $p_4 = (2n+1)\pi/\beta$, and n is any positive or negative number. From (2.4) it follows that G can always be represented in the form

$$G(\mathbf{p}, p_4) = \int_{-\infty}^{+\infty} \frac{f(w, \mathbf{p})\mathrm{d}w}{-ip_4 - \mu + w}. \tag{2.5}$$

With the help of (2.5) and (1.22) $G(\mathbf{p},\ x_4)$ can be obtained for values of x_4 lying in the interval from $-\beta$ to β:

$$G(\mathbf{p}, x_4) = \begin{cases} \int_{-\infty}^{+\infty} dw f(w, \mathbf{p}) \dfrac{\exp -(w-\mu)x_4}{1+\exp -(w-\mu)\beta} & (\beta > x_4 > 0) \\ -\int_{-\infty}^{+\infty} dw f(w, \mathbf{p}) \dfrac{\exp -(w-\mu)x_4}{1+\exp +(w-\mu)\beta} & (0 > x_4 > \beta). \end{cases} \tag{2.6}$$

For the time-dependent Green's function we obtain from here

$$\bar{G}(\mathbf{p}, t) = i \begin{cases} \int_{-\infty}^{+\infty} dw f(w, \mathbf{p}) \dfrac{\exp -i(w-\mu)t}{1+\exp -(w-\mu)\beta} & (t > 0) \\ -\int_{-\infty}^{+\infty} dw f(w, \mathbf{p}) \dfrac{\exp -i(w-\mu)t}{1+\exp +(w-\mu)\beta} & (t < 0). \end{cases} \tag{2.7}$$

Performing the Fourier transformation with respect to t we find the time-dependent Green's function in the p representation:

$$\bar{G}(\mathbf{p}, p_4) = i \int_{-\infty}^{+\infty} dw f(w, \mathbf{p}) \left[\frac{\delta+(p_4+\mu-w)}{1+\exp -(w-\mu)\beta} - \frac{\delta-(p_4+\mu-w)}{1+\exp (w-\mu)\beta} \right] \tag{2.8}$$

where

$$\delta_{\pm}(\alpha) = \int_{-\infty}^{+\infty} \exp \pm i\alpha t \, dt = \pi\delta(\alpha) \pm i\alpha$$

(here p_4 runs over the continuous set of values in the interval from $-\infty$ to $+\infty$). Employing (2.5) and (2.8) it can be shown that the energy spectrum of the system can be deduced from the temperature Green's function. The following rule holds in this case: in order to find the poles of the time-dependent Green's function (and hence the energy spectrum) it is sufficient to find the zeros of the analytic continuation of $G^{-1}(\mathbf{p}, p_4)$ in the complex plane of p_4. Thus E_n can be determined from the following equation:

$$-E_n + \frac{\mathbf{p}^2}{2m_e} + \Sigma_2^*(\mathbf{p}; p_4 = i(\mu - E_n)) = 0. \tag{2.9}$$

Here the real part of E_n corresponds to the energy and the imaginary part to damping of the n^{th} excitation. For $\beta \to \infty$ levels with $E_n < \mu$ correspond to holes in the Fermi distribution and levels with $E_n > \mu$ correspond to excitation of "quasiparticles" above the Fermi sphere.

For the case of weak damping, i.e. $\Gamma_n \ll E_n^0 (E_n = E_n^0 - i\Gamma_n)$, we get from (2.11)

$$\begin{gathered} -E_n^0 + \frac{\mathbf{p}^2}{2m_e} + \Sigma_2^{*(0)}(\mathbf{p}, ip_4 = E_n^0 - \mu) = 0, \\ \Gamma_n = \Sigma_2^{*(1)}(\mathbf{p}, p_4) \Big/ 1 - \frac{\partial \Sigma_2^{*(0)}(\mathbf{p}, p_4)}{\partial i p_4}\Bigg|_{ip_4 = (E_n^0 - \mu)}, \quad \Sigma_2^* = \Sigma_2^{*(0)} - i\Sigma_2^{*(1)}. \end{gathered} \tag{2.9'}$$

All results obtained here can easily be extended to the case of Bose statistics, namely

$$\bar{D}(\mathbf{p}, p_4) = i\int_{-\infty}^{+\infty} dw f_1(w, \mathbf{p})\left(\frac{\delta_+(p_4+\bar{\mu}-w)}{1-\exp-(w-\bar{\mu})\beta} + \frac{\delta_-(p_4+\bar{\mu}+w)}{\exp[(w-\bar{\mu})\beta]-1}\right) \quad (2.10)$$

where $\bar{\mu}$ is the chemical potential of the Bose particles.

In our case ($\bar{\mu} = 0$) the Bose excitation energy is specified by the equation

$$-E_n^2+\mathbf{p}^2+\kappa_e^2-\Pi_2(\mathbf{p}^2; -E_n^2) = 0. \quad (2.11)$$

For weak damping

$$\Gamma_n = \frac{\Pi_2^1(\mathbf{p}^2; p_4^2)}{2E_n\left(1-\dfrac{\partial\Pi^0}{\partial p_4^2}\right)_{|p_4^2=-(E_n^0)^2}}, \quad (2.12)$$

$$-(E_n^0)^2+\mathbf{p}^2+\kappa_e^2-\Pi_2^0(\mathbf{p}^2; p_4^2 = -(E_n^0)^2) = 0,$$

$$\Pi_2 = \Pi_2^0-i\Pi_2^1, \quad E_n = E_n^0-i\Gamma_n.$$

4. Systems of Ions and Electrons

Consider a system of electrons and ions interacting in accord with Coulomb's law. In this case, up to the neglect of unimportant self-energy terms the interaction Hamiltonian can be written as

$$H_1 = -\tfrac{1}{2}e^2\sum_{\lambda_1\lambda_2} z_{\lambda_1} z_{\lambda_2}\int j_4^{(\lambda_1)}(\mathbf{x})v(\mathbf{x}-\mathbf{x}')j_4^{(\lambda_2)}(\mathbf{x}')d^3x d^3x' \quad (3.1)$$

where z_λ is the charge of particles of type λ ($e^2/4\pi\hbar c = 1/137$).

It is not difficult to see from formula (1.14) that the system under consideration is equivalent to a system of charged particles interacting with the 4-component vector field φ_μ and

$$D_0(x-x') = v(\mathbf{x}-\mathbf{x}')\delta(x_4-x'_4). \quad (3.2)$$

We can therefore immediately write down the equations for Green's functions of a system of particles interacting according to Coulomb's law.

We shall consider two limiting cases.

4.1. UNIFORM DISTRIBUTION OF IONS

Suppose the ions are distributed uniformly (the system is translationally invariant). In this case the set of equations for the Green's functions has the form

$$[-i\gamma_\nu p_\nu-\gamma_4\mu_\lambda+m_\lambda-\Sigma_\lambda^*(p)]G_\lambda(p) = \sum_n \delta\left(p_4-\frac{(2n+1)\pi}{\beta}\right), \quad (3.3)$$

$$D(k) = D_0(\mathbf{k})+D_0(\mathbf{k})\Pi(k)D(k), \quad (3.4)$$

$$\Sigma_\lambda^*(p) = \frac{e^2 z_\lambda^2}{(2\pi)^3\beta}\int\sum_{k_4}\gamma_4 G_\lambda(p+k)\Gamma_4^{(\lambda)}(p+k, p)D(k)d^3k, \quad (3.5)$$

$$\Pi(k) = \sum_{\lambda} \frac{e^2 z_\lambda^2}{(2\pi)^3 \beta} \operatorname{tr} \int \sum_{p_4} \gamma_4 G_\lambda(p+k) \Gamma_4^{(\lambda)}(p+k, p) G_\lambda(p) \mathrm{d}^3 p, \quad (3.6)$$

$$\Gamma_4^{(\lambda)}(p, p') = \sum_{n,m} \gamma_4 \delta\left(p_4 - \frac{(2n+1)\pi}{\beta}\right) \delta\left(p' - \frac{(2m+1)\pi}{\beta}\right) + \Lambda_4^{(\lambda)}(p, p'), \quad (3.7)$$

where the G_m are "single-particle" Green's functions for particles of charge z_m (for electrons $z = -1$), and $D_{(k)}$ is the propagation function of a longitudinal photon, the presence of the plasma being taken into account.

a) In terms of the reduced equations the self-consistent field (Hartree-Fock) approximation corresponds to the approximation $\Pi = \Lambda = 0$.

b) Because of the singularity of $D_0(\mathbf{k}) = 1/\mathbf{k}^2$ at small momentum values, higher approximations (the so-called "correlation" corrections) become important.

To be more precise those approximations which remove the singularity in the D function at small momentum ($\mathbf{k}$) values are important.

The main part of the correlation energy can practically be taken into account by computing Π in the first approximation:

$$\Pi^{(1)}(k) = \sum_{\lambda} \frac{2e^2 z_\lambda^2}{(2\pi)^3 \beta} \int \sum_{p_4} G_\lambda^{(0)}(p+k) G_\lambda^{(0)}(p) \mathrm{d}^3 p,$$

$$G_\lambda^{(0)} = \frac{\sum_n \delta\left(p_4 - \frac{(2n+1)\pi}{\beta}\right)}{-ip_4 - \mu_\lambda + \mathbf{p}^2/2m_\lambda}. \quad (3.8)$$

In this approximation the following expression for the thermodynamic potential can be derived from (1.26):

$$\Omega = \Omega_{|e=0} + \frac{v}{2\beta(2\pi)^3} \sum_{k_4} \int \ln\left(1 - \frac{1}{\mathbf{k}^2} \Pi^{(1)}(k)\right) \mathrm{d}^3 k. \quad (3.9)$$

Separating the self-consistent part, i.e. $-\Pi^{(1)}(k)/\mathbf{k}^2$, we get the following expression for the correlation part of the thermodynamic potential:

$$\Omega_{\mathrm{corr}} = \frac{v}{2\beta(2\pi)^3} \sum_{k_4} \int \left[\ln\left(1 - \frac{1}{\mathbf{k}^2} \Pi^{(1)}(k)\right) + \frac{1}{\mathbf{k}^2} \Pi^{(1)}(k)\right] \mathrm{d}^3 k. \quad (3.10)$$

In the classical limit, $\hbar \to 0$, we get the results of the Debye-Hückel theory. This corresponds to the approximation when $\Pi(k) \approx \Pi(0)$. In this case we obtain the well known expressions for the Debye radius

$$r_{\mathrm{d}}^{-2} = -\Pi^{(1)}(0) = -\frac{2e^2}{(2\pi)^3} \sum_{\lambda} z_\lambda^2 \int \frac{\partial f_{\mathbf{k}}^{(\lambda)}}{\partial \varepsilon_{\mathbf{k}}} \mathrm{d}^3 k = e^2 \sum z_\lambda^2 \frac{\partial}{\partial \mu_\lambda} n_\lambda \quad (3.11)$$

where n_λ is the mean density of particles of the λ type.

From (3.8) and (3.10) we obtain, when $\beta \to 0$,

$$\Omega = \Omega_{e=0} - \tfrac{2}{3}\beta^{\frac{1}{2}} n_e^{\frac{3}{2}} (z+1)^{\frac{3}{2}} (e^2/4\pi)^{\frac{3}{2}} - \tfrac{1}{4} e^2 \beta \hbar^2 n_e^2 m_e^{-1}$$
$$+ \frac{e^4 \pi^{\frac{3}{2}}}{6\sqrt{2}(4\pi)^2} [3z + (2\sqrt{2}+1)(1+z^2(m_e/M)^{\frac{1}{2}}+c)] \beta^{\frac{3}{2}} n_e^2 m_e^{-\frac{1}{2}} + O(\beta^{\frac{3}{2}}). \quad (3.11')$$

c) It is significant that the indicated approximation for Π also encompasses another limiting case, when the Gell-Mann-Brueckner approximation is valid. $(me^2/\hbar n^{\frac{1}{3}} \ll 1)$.

Indeed, carrying out the necessary calculations we obtain from (3.10)

$$\Omega_{\text{corr}} = v \int \frac{d^3q}{2(2\pi)^3 \beta} \sum_{n=-\infty}^{\infty} \left[\ln \left(1 + \sum_\lambda \frac{2e^2 z_\lambda^2}{\mathbf{q}^2 (2\pi)^3} \int \frac{w_{\mathbf{p}} (f_{\mathbf{p}}^{(\lambda)} - f_{\mathbf{p}+\mathbf{q}}^{(\lambda)}) d^3p}{w_{\mathbf{p}}^2 + \left(\frac{2n\pi}{\beta}\right)^2} \right) \right.$$
$$\left. - \sum_\lambda \frac{2e^2 z_\lambda^2}{\mathbf{q}^2 (2\pi)^3} \int \frac{w_{\mathbf{p}} (f_{\mathbf{p}}^{(\lambda)} - f_{\mathbf{p}+\mathbf{q}}^{(\lambda)}) d^3p}{w_{\mathbf{p}}^2 + \left(\frac{2n\pi}{\beta}\right)^2} \right], \quad (3.12)$$

where

$$w_{\mathbf{p}} = \varepsilon_{\mathbf{p}+\mathbf{q}}^{(0)} - \varepsilon_{\mathbf{p}}^{(0)}, \quad \varepsilon_{\mathbf{p}}^{(0)} = \frac{\mathbf{p}^2}{2m_\lambda}, \quad f_{\mathbf{p}}^{(\lambda)} = \frac{1}{1+\exp(\varepsilon_{\mathbf{p}}^0 - \mu_\lambda)\beta'}.$$

From (3.12) we find by the usual methods

$$E_{(\text{corr})}^{(e)} = v \int \frac{d^4q}{2(2\pi)^4} \left\{ \ln \left(1 + \frac{2e^2}{(2\pi)^3 \mathbf{q}^2} \int \frac{w_{\mathbf{p}} (f_{\mathbf{p}}^0 - f_{\mathbf{p}+\mathbf{q}}^0)}{w_{\mathbf{p}}^2 + q_4^2} \right) \right.$$
$$\left. - \frac{2e^2}{\mathbf{q}^2 (2\pi)^3} \int \frac{w_{\mathbf{p}} (f_{\mathbf{p}}^0 - f_{\mathbf{p}+\mathbf{q}}^0) d^3p}{w_{\mathbf{p}}^2 + q_4^2} \right\} \quad (3.13)$$

where

$$f_{\mathbf{p}}^0 = \begin{cases} 0 \text{ when } \varepsilon_{\mathbf{p}}^0 > \mu\text{el} \\ 1 \text{ when } \varepsilon_{\mathbf{p}}^0 < \mu\text{el}. \end{cases} \quad (3.14)$$

Expanding (3.13) in a series in the smallness parameter we obtain the Gell-Mann-Brueckner results. Working as in § 2, we can find the time dependent $\bar{D}$-function.

d) It is not difficult to verify that $\bar{D}$ has a discrete pole corresponding to a plasmon. In this case equation (2.15), from which the poles of $\bar{D}$ can be determined, has the form

$$1 + \frac{2e^2}{q^2(2\pi)^2} \int \frac{2w_{\mathbf{p}} (f_{\mathbf{p}} - f_{\mathbf{p}+\mathbf{q}})}{w_{\mathbf{p}}^2 - E_n^2 - i\delta} d^3p \Big|_{E_n = E_n^0 - i\Gamma_n \frac{E_n^0}{|E_n^0|}} = 0. \quad (3.15)$$

The continuous spectrum corresponds to pair excitations, whereas the discrete pole yields the plasmon energy.

4.2. FIXED IONS

Another limiting case of interest is when the ions are so correlated with their electrons that translational invariance is strongly violated (as, for example, in the statistical theory of the atom). In this case, in a first approximation the ions can be considered to be motionless in their cells (atoms) and the problem can be reduced to the interaction of the electrons with the scalar component of the electromagnetic field (A_s before D_0 is defined by the equation $-\Delta D_0(\mathbf{x}, \mathbf{y}) = \delta(\mathbf{x}-\mathbf{y})$). Since the ion distribution is essentially non-uniform, the "single-particle" Green's functions do not depend only on the differences of the space coordinates (as before, the dependence on the fourth components is through a difference). For the sake of simplicity we shall consider the approximation $\Gamma = \gamma$. It can be shown that in this case the equations for the Green's functions have the following form:

$$\{-i(p_4-i\mu-ie\langle\varphi(\mathbf{x})\rangle)\gamma_4+\boldsymbol{\gamma}\boldsymbol{\nabla}_x\}G(p_4, \mathbf{x}, \mathbf{x}')+\int\Sigma^*(p_4, \mathbf{x}, \mathbf{y})G(p_4, \mathbf{y}, \mathbf{x}')\mathrm{d}^3y = \delta(\mathbf{x}-\mathbf{x}')\delta\left(p_4-\frac{(2n+1)\pi}{\beta}\right), \quad (3.16)$$

$$-\Delta\langle\varphi(\mathbf{x})\rangle = e\rho_{\text{ion}}+\frac{e}{\beta}\operatorname{tr}\gamma_4\sum_{p_4}G(p_4, \mathbf{x}, \mathbf{x}), \quad (3.17)$$

$$-\Delta D(k_4, \mathbf{x}, \mathbf{x}')-\int\Pi(k_4, \mathbf{x}, \mathbf{y})D(k_4, \mathbf{y}, \mathbf{x}')\mathrm{d}^3y = \delta(\mathbf{x}-\mathbf{x}'), \quad (3.18)$$

$$\Sigma^*(p_4, \mathbf{x}, \mathbf{y}) = \frac{e^2}{\beta}\sum_{k_4}\gamma_4G(p_4+k_4, \mathbf{x}, \mathbf{y})\gamma_4D(k_4, \mathbf{y}, \mathbf{x}), \quad (3.19)$$

$$\Pi(k_4, \mathbf{x}, \mathbf{y}) = \frac{e^2}{\beta}\operatorname{tr}\sum_{p_4}\gamma_4G(p_4+k_4, \mathbf{x}, \mathbf{y})\gamma_4G(p_4, \mathbf{y}, \mathbf{x}). \quad (3.20)$$

We change to the p representation with respect to the coordinate difference, i.e.

$$G(p_4, \mathbf{x}, \mathbf{y}) = \frac{1}{(2\pi)^3}\int G(p_4, \mathbf{x}, \mathbf{p})\mathrm{e}^{-i\mathbf{p}\cdot(\mathbf{x}-\mathbf{y})}\mathrm{d}^3p. \quad (3.21)$$

In the case under consideration the Green's functions have the form

$$[-i\gamma_\nu\tilde{p}_\nu-\gamma_4\mu+m-e\gamma_4\langle\varphi(\mathbf{x})\rangle+\Sigma^*(\mathbf{x}, \tilde{p})]G(\mathbf{x}, p) = \sum_n\delta\left(p_4-\frac{(2n+1)\pi}{\beta}\right), \quad (3.22)$$

$$-\Delta\langle\varphi(\mathbf{x})\rangle = e\rho_{\text{ion}}+\frac{e}{(2\pi)^3\beta}\operatorname{tr}\int\gamma_4\sum_{p_4}G(\mathbf{x}, p)\mathrm{d}^3p, \quad (3.23)$$

$$[(\mathbf{p}-i\boldsymbol{\nabla})^2-\Pi(\mathbf{x}, \tilde{p})]D(\mathbf{x}, p) = 1, \quad (3.24)$$

$$\Sigma^*(\mathbf{x}, p) = \frac{e^2}{(2\pi)^3 \beta} \int \sum_{k_4} \gamma_4 G(\mathbf{x}, \tilde{p}+k)\gamma_4 D(\mathbf{x}, k)\mathrm{d}^3 k, \tag{3.25}$$

$$\Pi(\mathbf{x}, k) = \frac{e^2}{(2\pi)^3 \beta} \sum_{p_4} \mathrm{tr} \int \gamma_4 G(\mathbf{x}, p+\tilde{k})\gamma_4 G(\mathbf{x}, p)\mathrm{d}^3 p \tag{3.26}$$

where $\tilde{p}_k = p_k - i\nabla_k$ for $k = 1, 2, 3$; $\tilde{p}_4 = p_4$ and the operator ∇ acts to the right.

a) Expressed in terms of the obtained equations, the Hartree approximation corresponds to $\Pi = \Sigma^* = 0$. In this case the following symbolic solution can be written for G:

$$G(\mathbf{x}, p) = \frac{\sum_n \delta\left(p_4 - \frac{(2n+1)\pi}{\beta}\right)}{-i\gamma_\nu \tilde{p}_\nu - \gamma_4 \mu + m - \gamma_4 \langle e\varphi(\mathbf{x})\rangle}. \tag{3.27}$$

It can readily be demonstrated that

$$-\frac{1}{\beta} \mathrm{tr} \sum_{p_4} G(\mathbf{x}, p) = 2(N^+ - N^-) \tag{3.28}$$

where

$$N_p^{\pm} = \frac{1}{1+\exp \beta\varepsilon_{\mathbf{p}}^{\pm}}, \tag{3.29}$$

$$\tilde{\varepsilon}_{\mathbf{p}}^{\pm} = \sqrt{(\mathbf{p} - i\nabla)^2 + m^2} \mp (\mu + e\langle\varphi(\mathbf{x})\rangle)$$

(in the quasi-classical approximation $\nabla = 0$).

Thus in the Hartree approximation we obtain the following symbolic equation for

$$\Delta\langle\varphi(x)\rangle = -e\rho_{\mathrm{ion}} + \frac{2e}{(2\pi)^3} \int \hat{\varrho}(\varepsilon_p)\mathrm{d}^3 p \tag{3.30}$$

where $\hat{\varrho}(\varepsilon_p) = \hat{N}_p^+ - \hat{N}_p^-$.

We have obtained the generalized Thomas-Fermi model with all quantum and relativistic correlations.

In the non-relativistic approximation equations (3.30) coincide with the operator equations derived by D. A. Kirzhnits [11]). If the mass operator is additionally taken into account in a first approximation, we obtain the generalized Thomas-Fermi-Dirac model in operator form, with all quantum and relativistic corrections (Hartree-Fock method).

5. Four Fermion Interactions

Consider now a system of particles for which the interaction Hamiltonian density is

$$\tfrac{1}{2} g\psi^+(\mathbf{x})\psi^+(\mathbf{y})v(\mathbf{x}-\mathbf{y})\psi(\mathbf{y})\psi(\mathbf{x})$$

where V is a short range potential.

In accord with § 1 the operator solution for the state integral (grand partition function) can be obtained in this case

$$z = z_0 \exp - \left\{ \tfrac{1}{2} g v \beta \sum_{p,p',q} \frac{\delta}{\delta \eta_s(p+q)} \frac{\delta}{\delta \eta_{s_1}(p'-q)} V(q) \frac{\delta}{\delta \eta_{s_1}(p')} \frac{\delta}{\delta \eta_s(p)} \right\} \cdot \exp \frac{1}{v\beta} \sum_p \bar{\eta}_s(p) G^0_{ss_1}(p) \eta_{s_1}(p) \qquad (4.1)$$

where

$$G^0_{ss_1}(p) = \frac{\delta_{ss_1} \delta \left(p_4 - \dfrac{(2n+1)\pi}{\beta} \right)}{-ip_4 - \mu + \dfrac{\mathbf{p}^2}{2m}}, \quad q_4 = \frac{2m\pi}{\beta}, \quad p'_4 = \frac{(2n+1)\pi}{\beta}. \qquad (4.2)$$

Expanding z or Ω (see (1.15)) in a series in g we get all the Feynman graphs of this interaction in the p representation.

From (4.1) and (1.14) it can be seen that any four-fermion interaction is equivalent to an interaction via an intermediate Bose field, the propagation function of the free Bose field being $D_0(q) = V(q)$. Therefore an equation set similar to (1.25) can also be deduced for the Green's functions in this case. However, for a short range potential higher order terms in g in the vertex part of Γ become important and it is therefore more convenient to express the mass operator in terms of the two-particle Green's function $G(x_1, x_2, x_3, x_4)$. The latter is determined by an equation of the Bethe-Saltpeter type.

The Green's functions equation set in this case has the form

$$\left(\frac{\partial}{\partial x_4} - \mu - \frac{\Delta}{2m} \right) G_{ss_1}(x-x') - g \int V(\mathbf{x}-\mathbf{y}) G_{ss_2s_2s_1}(x, y, y, x') \mathrm{d}^4 y = \delta(x-x') \delta_{ss_1}, \qquad (4.3)$$

$$G_{s_1s_2s_3s_4}(x_1, x_2, x_3, x_4) = G_{s_1s_3}(x_1-x_3) G_{s_2s_4}(x_2-x_4) - G_{s_1s_4}(x_1-x_4) G_{s_2s_3}(x_2-x_3) + g \int G_{s_1s_5}(x_1-x_5) G_{s_2s_6}(x_2-x_6) I_{s_5s_6s_7s_8}(x_5, x_6, x_7, x_8) \cdot G_{s_7s_8s_3s_4}(x_7, x_8, x_3, x_4) \mathrm{d}^4x_5 \mathrm{d}^4x_6 \mathrm{d}^4x_7 \mathrm{d}^4x_8, \qquad (4.4)$$

where

$$G(x_1, x_2, x_3, x_4) = \frac{\delta^4 z}{\delta \bar{\eta}(x_1) \delta \bar{\eta}(x_2) \delta \eta(x_3) \delta \eta(x_4)_{|\eta=0}} = \langle \mathrm{T}(\psi(x_1) \psi(x_2) \bar{\psi}(x_3) \bar{\psi}(x_4)) \rangle.$$

The effective potential can be determined in a general form [4]). In a first approximation when

$$I(x, y, x', y') = D(x-y) \delta(x-x') \delta(y-y') \approx V(\mathbf{x}-\mathbf{y}) \delta(x_4-y_4) \delta(x-x') \delta(y-y')$$

the set of equations (4.3)—(4.4) assumes the following form in the p-representation:

$$\left(-ip_4-\mu+\frac{p^2}{2m}\right)G_{s_1s_2}(p) \tag{4.5}$$

$$-\frac{g}{(2\pi)^6\beta^2}\sum_{p_4}\int V(\mathbf{q})G_{s_1ss_2}(p+q, p'-q, p', p)\mathrm{d}^3q\,\mathrm{d}^3p' = \sum_n \delta\left(p_4-\frac{(2n+1)\pi}{\beta}\right),$$

$$G_{s_1s_2s_3s_4}(p_1, p_2, p_3, p_4) = (2\pi)^3\beta(G_{s_1s_3}(p_1)G_{s_2s_4}(p_2)\delta(p_1-p_3)\delta(p_2-p_4)$$
$$-G_{s_1s_4}(p_1)G_{s_2s_3}(p_2)\delta(p_1-p_4)\delta(p_2-p_3)) \tag{4.6}$$
$$+G_{s_1s_5}(p_1)G_{s_2s_6}(p_2)\frac{g}{(2\pi)^3\beta}\sum_{q_4}\int \mathrm{d}\mathbf{q}V(\mathbf{q})G_{s_5s_6s_3s_4}(p_1+\mathbf{q}, p_2-\mathbf{q}, p_3, p_4).$$

Since $G(p)$ is diagonal with respect to the spin indices the two-particle Green's function will differ from zero when $s_1 = s_3$, $s_2 = s_4$ or $s_1 = s_4$; $s_3 = s_2$.

Let us consider in greater detail the case when $(s_1 = s_3) \neq (s_2 = s_4)$. Changing to the relative momenta p, p' and centre of mass momentum P:

$$p = \tfrac{1}{2}(p_1-p_2), \qquad p' = \tfrac{1}{2}(p_3-p_4), \qquad P = p_1+p_2 = p_3+p_4,$$

we obtain the equations

$$\bar{S}(p, p', P) \equiv G(\tfrac{1}{2}P+p, \tfrac{1}{2}P-p, \tfrac{1}{2}P+p', \tfrac{1}{2}P-p')G^{-1}(\tfrac{1}{2}P-p')G^{-1}(\tfrac{1}{2}P+p')$$
$$=\beta(2\pi)^3\delta(p-p')-G(\tfrac{1}{2}P+p)G(\tfrac{1}{2}P-p)\frac{g}{(2\pi)^3\beta}\sum_{q_4}\int \mathrm{d}^3qV(\mathbf{q})\bar{S}(p-q, p', P). \tag{4.7}$$

Since the potential $V(\mathbf{q})$ is independent of q_4 it should be sufficient to determine $\bar{S}(p, p', P)$ summed over the fourth coordinate p_4.

Denoting this function by $S(\mathbf{p}, \mathbf{p}', P)$ and summing (4.7) over p_4 we get

$$S(\mathbf{p}, \mathbf{p}', P)-\frac{g}{(2\pi)^3}\Phi(\mathbf{p}, P)\int V(\mathbf{q})S(\mathbf{p}-\mathbf{q}, p', P)\mathrm{d}^3q=\delta(\mathbf{p}-\mathbf{p}')(2\pi)^3 \tag{4.7'}$$

where

$$\Phi(\mathbf{p}, P) = \frac{1}{\beta}\sum_{p_4} G(\tfrac{1}{2}P+p)G(\tfrac{1}{2}P-p).$$

Solving simultaneously the equations (4.5) and (4.6) and putting $G = G^0$ in (4.6) we arrive at the results of the "gas approximation" at a non-zero temperature.

Omitting the computations we directly give the set of equations for the Green's functions in the "gas approximation".

$$\left(-ip_4-\mu+\frac{p^2}{2m}+\Sigma^*(p)\right)G(p)=\sum_n \delta\left(p_4-\frac{(2n+1)\pi}{\beta}\right),$$

$$\Gamma(\mathbf{p},\mathbf{p}',P)=(2\pi)^{-3}g\int d\mathbf{q}V(\mathbf{q})S(\mathbf{p}-\mathbf{q},\ \mathbf{p}',P),$$

$$\Sigma^*(p)=-\frac{2}{(2\pi)^3\beta}\sum_{P_4}\int G_0(P-p)\Gamma(\mathbf{p}+\tfrac{1}{2}\mathbf{P},\mathbf{p}-\tfrac{1}{2}\mathbf{P},P)d^3P \tag{4.8}$$

$$+\frac{1}{(2\pi)^3\beta}\sum_{P_4}\int G_0(P-p)\Gamma(\mathbf{p}-\tfrac{1}{2}\mathbf{P},\tfrac{1}{2}\mathbf{P}-\mathbf{p},P)d^3P;$$

$S(\mathbf{p},\mathbf{p}',P)$ is defined by equation (4.7) and

$$\Phi(\mathbf{p},P)=\frac{1}{\beta}\sum_{p_4}G_0(\tfrac{1}{2}P+p)G_0(\tfrac{1}{2}P-p)=\frac{N(\mathbf{p},\mathbf{P})}{iP_4-\dfrac{1}{4m}\mathbf{P}^2-\dfrac{\mathbf{p}^2}{m}-2\mu}, \tag{4.9}$$

$$N(\mathbf{p},\mathbf{P})=1-f^0_{\frac{1}{2}\mathbf{P}+\mathbf{p}}-f^0_{\frac{1}{2}\mathbf{P}-\mathbf{p}},\qquad f_{\mathbf{p}}{}^0=\left[1+\exp\left(\frac{p^2}{2m}-\mu\right)\right]^{-1}. \tag{4.10}$$

In superconductivity theory the potential $V(q)$ is only different from zero near the Fermi surface and is then approximately constant. It can be shown that for $\beta\to\infty$ a minimum energy bound state of two "holes" (particles) appears in the Fermi sphere when the spins and momenta are opposite in sign. Therefore, for $\beta\to\infty$, a "condensate" of such pairs is formed. For $\mathbf{P}=0$ a δ-like singularity appears in distribution $\Gamma(\mathbf{p},\mathbf{p}',P)$ and the set of equations for the Green's functions becomes much simpler. It is important that due to the change in the Fermi distribution in this case $G(p)$ cannot be replaced by $G^0(p)$.

The Fermi excitation spectrum can be obtained by investigating the poles of the analytic continuation of $G(p)$ for complex values of p_4. By investigating the poles of the analytic continuation of the D-function (set up on analogy with the Coulomb problem) we can obtain the Bose excitation spectrum. These questions will be discussed in greater detail elsewhere.

In conclusion the author expresses his appreciation to I. E. Tamm, V. L. Ginzburg and D. A. Kirzhnitz for interest in this work and useful discussion of the results.

Appendix

We shall discuss the method of calculating sums with respect to p_4, of the type

$$\mathcal{F}=\frac{1}{\beta}\sum_{p_4}F(\ldots p_4),\qquad p_4=\frac{(2n+1)\pi}{\beta}. \tag{1}$$

Two cases will be considered:

1) when there exists a unique analytic function coinciding with F in the entire p_4 plane (for example G_0, D_0),

2) when there is no such function.

1) In the first case, let us consider the contour integral $\oint F(\ldots z) f^{(\pm)}(z)\mathrm{d}z$, in which the contour is taken along the circle of infinite radius, and

$$f^{(\pm)}(z) = \frac{\pm i\beta}{1+\exp\mp i\beta z}.$$

It should be noted that the choice of $f^{(+)}$ or $f^{(-)}$ is determined by the condition that the integrand vanish at infinity. In this case $\oint = 0$, and since the poles of the function f lie at the points $(2n+1)\pi/\beta$, we obtain

$$\mathscr{F} = -\frac{1}{\beta}\sum_s f^{(\pm)}(z_s)\,\mathrm{Res}\,F(\ldots z_s). \tag{3}$$

2) An example of the second case is eq. (2.6), i.e., the sum of the kind

$$G(\mathbf{p}, x_4) = \frac{1}{\beta}\sum_{p_4} G(\mathbf{p}, p_4)\mathrm{e}^{-ip_4x_4}. \tag{4}$$

Generally speaking, there is no analytic function coinciding with G in the entire plane, but it follows from (2.5) that $G(\mathbf{p}, p_4) = g_1(\mathbf{p}, p_4)$ when $\mathrm{Re}\,p_4 > 0$ (i.e., in the right semi-plane) and $G(\mathbf{p}, p_4) = g_2(\mathbf{p}, p_4)$ when $\mathrm{Re}\,p_4 < 0$. The analytic function $g_1(g_2)$ has no poles in the right (left) semi-plane, so that the singularities of G lie on the imaginary axis p_4. [It will be noted that the poles determining the excitation spectrum arise from the analytic continuation of $g_1(g_2)$ in the left (right) semi-plane.] Thus,

$$G(\mathbf{p}, x_4) = \frac{1}{\beta}\sum_{p_4>0} g_1(\mathbf{p}, p_4)\mathrm{e}^{-ip_4x_4} + \frac{1}{\beta}\sum_{p_4<0} g_2(\mathbf{p}, p_4)\mathrm{e}^{-ip_4x_4}. \tag{5}$$

Each of these sums is reduced by the preceding method to an integral along a line infinitely neary to the imaginary axis p_4 and situated to the right (for $p_4 > 0$) or to the left (for $p_4 < 0$) of it. In the present case the contour for the first (second) sum is selected along the imaginary axis and an infinite semi-circle to the right (left) of it. If poles existed outside the imaginary axis, a sum with respect to the residues in these poles would have to be added.

Finally, we obtain

$$G(\mathbf{p}, x_4) = \frac{1}{2\pi\beta}\int_{-\infty}^{+\infty}\{g_1(\mathbf{p}, -iw+\varepsilon) - g_2(\mathbf{p}, -iw-\varepsilon)\}f^{(\pm)}(-iw)\mathrm{e}^{-wx_4}\mathrm{d}w. \tag{6}$$

Eq. (2.6) follows from (2.5) and (6).

In the same way, it may be shown in general that in calculations according to perturbation theory, when

$$F(\ldots p_4) = \int \frac{\rho(\ldots x_1 \ldots x_n)}{\prod_i (x_i - i p_4)} \, dx_1 \ldots dx_n,$$

one gets

$$\mathcal{F} = -\frac{1}{\beta} \int dx_1 \ldots dx_n \rho(\ldots x_1 \ldots x_n) f^{(\pm)}(z) \operatorname{Res} \left\{ \frac{1}{\prod_{i=1}^{n} (x_n - iz)} \right\}. \qquad (7)$$

All results obtained above are extended to the case of sums with respect to $p_4 = 2n\pi/\beta$ by taking for this case

$$f^{(\pm)} = \frac{\mp i\beta}{1 - \exp \pm i\beta z}. \qquad (8)$$

In conclusion, it will be noted that since for $\beta^{-1} = 0$ the sum with respect to p_4 goes over into an integral, it is more expedient not to turn the axis of integration, but to carry out all calculations in Euclidian four-dimensional space (where the separation of angular variables is very simple). For $\mu = 0$, for example, we obtain all results of the conventional field theory in Euclidian variables, while the transition to pseudo-Euclidian space is discussed in § 2.

References

1) E. W. Montroll and J. C. Ward, Physics of Fluids **1** (1958) 55
2) V. M. Galitsky and A. B. Migdal, JETP **34** (1957) 139;
A. Salam, Progr. Theor. Phys. **9** (1953) 550;
V. L. Bonch-Bruevich, JETP **30** (1956) 342
3) J. Matzubara, Prog. Theor. Phys. **14** (1955) 351
4) J. Schwinger, Proc. Nat. Acad. Sci. USA **37** (1951) 452;
E. S. Fradkin, Doklady **98** (1954) 47
5) E. S. Fradkin, Doklady **125** (1959) 66, 313
6) E. S. Fradkin, Doklady **100** (1955) 897
7) E. M. Lifshitz, JETP **29** (1955) 97
8) H. Ezawa, J. Tomozawa and H. Umezawa, Nuovo Cimento **5** (1957) 810
9) E. S. Fradkin, JETP **26** (1954) 751; **29** (1955) 121
10) L. D. Landau, JETP **34** (1958) 262
11) D. A. Kirzhnits, JETP **32** (1957) 115
12) A. A. Abrikosov, L. P. Gorkov and I. E. Dzyaluishinsky, JETP **36** (1959) 901

7.A *Nuclear Physics* **12** (1959) 485—493; © *North-Holland Publishing Co., Amsterdam*
Not to be reproduced by photoprint or microfilm without written permission from the publisher

CALCULATION OF THE MAGNETIC MOMENTS OF NUCLEONS BY USE OF A MODIFIED PROPAGATOR

JACK L. URETSKY † and PETER J. REDMOND

Lawrence Radiation Laboratory and Physics Department University of California, Berkeley, California ††

Received 29 April 1959

Abstract: Previous attempts to use modified propagators in field-theory calculations have been frustrated by the appearance of ghost states in the propagator when one tries to improve on conventional perturbation theory. Recently a method of eliminating these ghosts has been suggested. By following this suggested procedure it is possible to calculate the magnetic moments of nucleons by using a modified nucleon propagator, which should be an improvement on simple perturbation theory without introducing any spurious infinities. This calculation has been performed approximately and yields magnetic moments of $+1.2$ and -2.3 nuclear magnetons for the proton and neutron, respectively, compared with the experimental values of 1.8 and -1.9. The improvement over perturbation theory is achieved because of a strong damping of the nucleon recoil term.

1. Introduction

It has been conjectured for a great many years that it should be possible to understand the "anomalous" magnetic moments of the neutron and proton in terms of the strong interactions between nucleons and π mesons. Today this conjecture must still be regarded as unproved.

Early attempts to calculate the nuclear magnetic moments made use of the perturbation techniques that had been successfully applied to quantum electrodynamics [1, 2]). These attempts were regarded as unsuccessful inasmuch as low-order perturbation calculations are not in good agreement with experiment †††, and unfounded because the pseudoscalar coupling constant is not of the same order of smallness as the fine-structure constant of electrodynamics. We make bold to observe that the disagreement with experiment is not relevant until one is certain that pion-nucleon interactions really are responsible for the anomalous moments. And the question of the size of the coupling constant would be much more pertinent if one had more feel for the convergence properties of field-theory perturbation methods.

† Now at Imperial College of Science and Technology, London.

†† This work was done under the auspices of the U.S. Atomic Energy Commission and of the U.S. Army, Office of Ordnance Research.

††† Part of the perturbation calculation predicts, within experimental error, the results of three independent experiments measuring the electromagnetic structure of the nucleon. For a viewpoint that regards this agreement as fortuitous see ref. [2]).

More recently attempts have been made to calculate the electromagnetic form factors by means of an axiomatic approach [2]). The method attempts to relate S-matrix elements to one another as a consequence of the assumptions of unitarity, causality, and specified asymptotic conditions. Although such calculations have forsworn any knowledge of an underlying Lagrangian, a severe penalty is paid for this freedom. It is found that the integral relations among the S-matrix elements generally require a knowledge of non-physical scattering amplitudes, and one is led to the suspicion that additional postulates may be required in order to establish a satisfactory system of relations among experimental quantities.

In this paper, we once more attempt to calculate the nucleonic magnetic moments with the idea that a Lagrangian theory does in fact lead to unique predictions of their values and that one ought to know what these predictions are. In trying to do something better than perturbation theory we shall find ourselves repeating Feldman's "modified propagator" calculation [3]) †, but this time we shall exorcise the ghosts that haunted Feldman's work.

In section 2 we derive the integral equations that must be solved in order to obtain the electromagnetic form factors of the π meson and the nucleon. Section 3 describes an approximate calculation of the nucleonic magnetic moments. In section 4 we discuss some of the implications of gauge invariance. Section 5 is devoted to a brief summary of our conclusions. There is an appendix dealing with the magnitudes of the renormalization constants.

2. The Integral Equations

The Lagrangian is chosen to contain the usual pseudoscalar strong-coupling interaction. Explicitly, we write ††

$$\begin{aligned} L(x) = &-\tfrac{1}{2}[\bar{\psi}, \hat{\partial}\psi]-M\bar{\psi}\psi-\tfrac{1}{2}[\partial_\mu\boldsymbol{\phi}\cdot\partial_\mu\boldsymbol{\phi}+\mu^2\boldsymbol{\phi}\cdot\boldsymbol{\phi}]-\tfrac{1}{4}F_{\mu\nu}F_{\mu\nu} \\ &+\tfrac{1}{2}ie[\bar{\psi}, \hat{A}\tfrac{1}{2}(1+\tau_3)\psi]-\tfrac{1}{2}eA_\mu\varepsilon_{3ij}\{\phi_i, \partial_\mu\phi_j\}-\tfrac{1}{2}e^2(\boldsymbol{\phi}\cdot\boldsymbol{\phi}-\phi_3\phi_3)A_\mu A_\mu \quad (1) \\ &+\tfrac{1}{2}ig[\bar{\psi}, \gamma_5\boldsymbol{\tau}\psi]\cdot\boldsymbol{\phi}+\lambda\boldsymbol{\phi}^4-\bar{\eta}\psi-\bar{\psi}\eta+\boldsymbol{\varkappa}\cdot\boldsymbol{\phi}+J_\mu A_\mu, \end{aligned}$$

including the external sources ††† η, $\bar{\eta}$, J_μ, $\boldsymbol{\varkappa}$.

Next we obtain the equations of motion for the Green's functions G, $\mathscr{G}_{ij}$ of the fermion and meson fields. These are, to lowest order in e (with the external sources "turned off"),

† A brief summary is contained in ref. [2]), p. 295.

†† Our conventions, where applicable, are those of ref. [4]), except that we take $(\gamma_5)^2 = +1$. All Fourier transforms are defined by

$$F(x) = \frac{1}{(2\pi)^4}\int \mathrm{d}^4p\, \mathrm{e}^{ipx}\mathscr{F}(p).$$

Upper and lower indices are not distinguished from each other, and repeated indices imply summation from 0 to 3. Also, $\hat{A} = \gamma_\mu A_\mu = \boldsymbol{\gamma}\boldsymbol{A}-\gamma_0 A_0$ for any four-vector A.

††† The following derivation follows the prescriptions of ref. [5]).

$$G^{-1}(p) = S_F^{-1}(p) - \frac{ig^2}{(2\pi)^4}\gamma_5\tau^i \int dq G(q)\Gamma_5^j(q, p)\mathcal{G}_{ji}(q-p), \tag{2a}$$

$$\mathcal{G}_{ji}^{-1}(k) = \Delta_F^{-1}(k)\delta_{ji} - \frac{ig^2}{(2\pi)^4}\,\mathrm{Tr}\,\gamma_5\tau^j \int dq G(q)\Gamma_5^i(q, q-k)G(q-k). \tag{2b}$$

The photon-nucleon, meson-nucleon, and photon-meson vertex functions satisfy the respective equations

$$\begin{aligned}\Gamma_\mu(p, p') = {} & \tfrac{1}{2}(1+\tau_3)\gamma_\mu + \frac{ig^2}{(2\pi)^4}\tau^i\gamma_5 \int dq\{G(p+q)\Gamma_\mu(p+q, p'+q) \\ & \times G(p'+q)\Gamma_5^j(p'+q, p')\mathcal{G}_{ji}(q) + G(q)\Gamma_5^j(q, p')\mathcal{G}_{j\kappa}(q-p')C_\mu^{\kappa l}(q-p', q-p) \\ & \times \mathcal{G}_{li}(q-p) - G(q)V_\mu^j(q, p', q-p)\mathcal{G}_{ji}(q-p)\},\end{aligned} \tag{3a}$$

$$\begin{aligned}\Gamma_5^i(p, p') = {} & \gamma_5\tau^i + \frac{g^2}{(2\pi)^4}\gamma_5\tau^j \int dq\{G(p+q)\Gamma_5^i(p+q, p'+q)G(p'+q) \\ & \times \Gamma_5^\kappa(p'+\tau, p')\mathcal{G}_{\kappa j}(q) - G(q)U^{\kappa i}(q, p', q-p)\mathcal{G}_{\kappa i}(q-p)\},\end{aligned} \tag{3b}$$

$$\begin{aligned}C_\mu^{ij}(p, p') = {} & (p+p')_\mu\varepsilon^{ij3} + \frac{ig^2}{(2\pi)^4}\,\mathrm{Tr}\,\gamma_5\tau^i \int dq\{G(p+q)\Gamma_\mu(p+q, p'+q) \\ & \times G(p'+q)\Gamma_5^j(p'+q, q)G(q) \\ & + G(q)\Gamma_5^j(q, q-p')G(q-p')\Gamma_\mu(q-p', q-p) \\ & \cdot G(q-p) - G(q)V_\mu^j(q, q-p, p')G(q-p)\}.\end{aligned} \tag{3c}$$

In these expressions we have introduced the four-particle vertices V (photomeson production), and U (meson-nucleon scattering). These quantities are defined by the symbolic expressions

$$V_\mu^j = \frac{(2\pi)^4}{ie}\frac{\delta\Gamma_5^j}{\delta A_\mu}, \qquad U^{ji} = \frac{(2\pi)^4}{ig}\frac{\delta\Gamma_5^j}{\delta\phi_i}, \tag{4a, b}$$

and satisfy integral equations that involve five-particle vertices. The set of eqs. (2) and (3) may be closed by setting U and V equal to zero. This procedure can be shown to be equivalent to setting the photomeson production and meson-nucleon scattering *amplitudes* equal to their Born approximations. The equations obtained by neglecting the contributions of U and V are referred to as the "truncated equations" †.

It is probably well to remark at this point that there is no real reason to believe that solutions of the truncated set of equations (if they exist) bear any resemblance to the solutions of the original field equations (again presupposing existence). On the other hand, it has been shown that approximate solutions to eqs. (2a) and (2b) may be obtained in this way and that such solutions have plausible properties that could never be obtained from the usual perturbation theories [7]). In particular, one can deduce from these

† A somewhat different truncation procedure was proposed in ref. [6]).

solutions that they contain essential singularities in the limit of vanishing coupling constant. It is also suggestive to observe that it is possible to estimate the magnitudes of certain of the renormalization constants, and this is done in the appendix.

3. The calculation of the Magnetic Moments

The charge and magnetic structure of the nucleon is given by the generalized electromagnetic vertex function Γ_μ. If we had previously obtained a solution of the meson-nucleon problem, it would still be necessary to solve the coupled integral equations (3a) and (3c) in order to obtain Γ_μ in the truncation approximation. Lacking such a solution, we are constrained to find a systematic way of dealing with the five parts of eqs. (2) and (3).

The procedure we shall use is an obvious one. The *inverse* meson and nucleon propagators are calculated in lowest-order perturbation theory. The resultant propagators, after being modified in a manner to be described, are then inserted into eqs. (3), and the new approximations to the vertex functions obtained. This procedure may then, in principle, be iterated.

When Feldman attempted to carry out the calculation in the manner just suggested, he discovered that he obtained infinite contributions to Γ_μ from poles of the approximate propagators G and $\mathscr{G}$. These poles corresponded to discrete states of complex mass (often called "ghosts"). As we now know, the appearance of the ghost states was a warning that the perturbation approximation to the inverse propagators resulted in propagators that had incorrect analyticity properties. In order to sidestep this difficulty we use the eqs. (2) to compute the mass-spectral functions rather than the propagators themselves. The procedure for doing this has been described in detail by Redmond [7]) and need not be repeated here.

We write the propagators in the spectral forms

$$\mathscr{G}_{ij}(p) = \delta_{ij}\int \mathrm{d}l^2 \rho(l^2)(p^2+l^2)^{-1}, \tag{4a}$$

$$G(p) = \int \mathrm{d}l^2[i\hat{p}\rho_1(l^2)+M\rho_2(l^2)](p^2+l^2)^{-1}, \tag{4b}$$

and approximate the vertices Γ_μ, Γ_5, $C_\mu(p, p')$ by the "bare" values γ_μ, γ_5, $p_\mu+p'_\mu$ in the right-hand side of eq. (3a). The next higher approximation to Γ_μ may then be readily obtained by use of the usual Feynman techniques. We quote here our result for the magnetic moment part of Γ_μ:

$$\begin{aligned}\Gamma_\mu^{\mathrm{mag}}(p, p') = &-\frac{1}{2M}\frac{g^2}{8\pi^2}\sigma^{\mu\nu}q_\nu \int \mathrm{d}s^2\mathrm{d}n^2\mathrm{d}l^2 \int_0^1 \chi\mathrm{d}\chi \int_{-1}^1 \mathrm{d}z \frac{M^2}{a^2} \\ &\times\{\tau_3\rho(l^2)\rho(n^2)(1-\chi)[\chi\rho_1(l^2)+\rho_2(l^2)] \\ &-\tfrac{1}{8}(3-\tau_3)\rho(l^2)\chi[2(1-\chi)\rho_1(s^2)\rho_1(n^2)+\rho_1(s^2)\rho_2(n^2)+\rho_2(s^2)\rho_1(n^2) \\ &-z(\rho_1(s^2)\rho_2(n^2)-\rho_2(s^2)\rho_1(n^2))]\},\end{aligned} \tag{5a}$$

with the definitions

$$a^2 = \chi^2[M^2-\tfrac{1}{4}q^2(z^2-1)]+\chi[\tfrac{1}{2}(s^2-n^2)z+\tfrac{1}{2}(s^2+n^2)-M^2-l^2]+l^2, \qquad q_\mu = p_\mu - p'_\mu. \tag{5b}$$

The evaluation of the expression (5a) using only the "bubble" approximations for the various spectral functions is a formidable computational task. We have contented ourselves with a crude approximation that stems from the observation that the spectral functions are all strongly peaked. We have also observed that in our approximation the continuum contribution from the meson spectral function (which contributes only for masses greater than $2M$) is small and probably negligible. It follows that we may proceed directly to a numerical estimate by setting

$$\begin{aligned} \rho_1(l^2) &= \delta(l^2-M^2)+0.95\,\delta(l^2-5M^2), \\ \rho_2(l^2) &= -\delta(l^2-M^2)+1.85\,\delta(l^2-5M^2), \end{aligned} \tag{6}$$

where the numerical constants were determined from a graphical integration. We have also simplified the work by setting the meson mass equal to zero, a procedure that is probably no worse than the other approximations.

It is most convenient to quote our results in terms of the comparable second-order Feynman diagrams. We find, using the notation of Bethe (ref. [1]), p. 292),

$$B_1 = 0.2, \qquad B_2 = 0.75,$$

and it will be recalled that B_1 and B_2 refer to the "nucleon recoil" and "meson" diagrams, respectively (each divided by $g^2/8\pi^2$). In perturbation theory B_1 and B_2 are each equal to unity. The corresponding predictions for the anomalous moments, which can hardly be taken seriously, are

proton: $+1.2$ nuclear magnetons,
neutron: -2.3 nuclear magnetons,

compared with the respective experimental values of 1.7 and -1.9. We are, however, heartened by the very strong damping of the nucleon recoil term. It would be most interesting to see if this damping persists when a "better" approximation for the Γ_5 vertex function is used.

We are quite aware that our approximation or Γ_μ is not manifestly gauge-covariant, and we next discuss this point. It is some of interest to note, however, that the missing terms in Γ_μ (those not written down in eq. (5a)) do *not* contain any parts proportional to q_μ.

4. Gauge Invariance

It is a consequence of the principle of gauge invariance that the exact nucleon electromagnetic vertex function and the nucleon propagator are

related. They must satisfy the generalized Ward identity [8])

$$(p_\mu - p'_\mu)\Gamma_\mu(p, p') = \tfrac{1}{2}i(1+\tau_3)[G^{-1}(p) - G^{-1}(p')]. \tag{7a}$$

Similarly, the meson vertex function is constrained to obey the identity

$$-(p_\mu - p'_\mu)C_\mu{}^{ij}(p, p') = \mathcal{G}^{-1}_{i\kappa}(p)\varepsilon^{\kappa j 3} + \varepsilon^{i\kappa 3}\mathcal{G}^{-1}_{\kappa j}(p'). \tag{7b}$$

A little algebraic manipulation shows that these identities are not consistent with the truncation approximation that we have defined †. We are then obliged to inquire into the consequences of this inconsistency.

In order to gain some insight into the consequences of the Ward identity let us consider two different vertex functions, each of which obeys eq. (7a). Their difference $\delta\Gamma_\mu$ must obey

$$(p_\mu - p'_\mu)\delta\Gamma_\mu(p, p') = 0. \tag{8}$$

It is sufficient for our purposes to exhibit two vectors that satisfy eq. (8) identically and do not violate any invariance requirements that may be imposed upon Γ_μ. These are

$$\delta\Gamma_\mu{}^1(p, p') = (p-p')^2(p_\mu + p'_\mu) - (p_\mu - p'_\mu)(p^2 - p'^2)$$

and

$$\delta\Gamma_\mu{}^2(p, p') = \sigma_{\mu\nu}(p_\nu - p'_\nu).$$

One can readily see that a linear combination of $\delta\Gamma_\mu{}^1$ and $\delta\Gamma_\mu{}^2$ taken between Dirac spinors will give the most general possible form for the electromagnetic structure of a chargeless particle. We conclude that eq. (7a) by itself can only restrict the nucleonic charges (and guarantee charge-current conservation by eliminating terms proportional to $p_\mu - p'_\mu$).

5. Conclusions

We have of course no intention of suggesting that we have carried out a successful calculation of the nucleon magnetic moments. One reason is that so little is known of the mathematical structure of relativistic quantum field theory that one has no practicable criterion by which to measure the "success" of a calculation. By the same token we are permitted to entertain some hope that the method of computation outlined here may be in the right direction to deal with strong-coupling problems. To date, there does not appear to be any evidence that this is not the case.

Ideally, the problem is now one of carrying out a detailed mathematical investigation of the proposed approximation procedure. Unfortunately, we

† That is to say, one does not recover the lowest-order approximation to the inverse Green's functions on the right-hand side of eq. (3). In point of fact, after using the prescription of ref. [8]) to adulterate the propagator, one no longer knows the equation the propagator satisfies and the meaning of eq. (7) becomes obscure.

have no idea of how to go about this. It appears that all that can be suggested at this time is open to just the kind of objection referred to in the introduction. That is, we suggest a careful calculation of the electromagnetic form factors of the nucleon by use of our proposed techniques, and the success of the calculation would have to be judged on the basis of comparison with experiment. This, of course, is the spirit in which quantum electrodynamics is considered a successful theory. In this same spirit we might consider, despite the above remarks that we have successfully estimated the magnitudes of the nucleonic magnetic moments.

It may be thought strange that we have seen fit to present a calculation that is not meticulously consistent with gauge invariance. The position taken by us here is that gauge invariance is a principle that can be overworked. We are reasonably certain that our lack of gauge invariance has done violence only to the nucleon charges, and it was not our intention to calculate these. It seems to us that it may be asking too much of our approximate vertex functions to satisfy the Ward identity when they do not even satisfy the equations of motion.

We are indebted to Professor Geoffrey Chew, Professor Francis Low, Mr. Guido Sandri, and colleagues at the Lawrence Radiation Laboratory for many stimulating conversations.

Appendix

MAGNITUDES OF THE RENORMALIZATION CONSTANTS

In this appendix we calculate the magnitudes of the pion and nuclear wave-function renormalization constants and the nucleon mass renormalizations in the lowest order (the "bubble approximation"). In this approximation the meson-mass renormalization is infinite. For the sake of illustration we present the meson calculation in some detail.

To lowest order in the coupling constant the inverse meson propagator is given by

$$G^{-1}(p^2) = (p^2+\mu^2) - \frac{2ig^2}{(2\pi)^4}\int d^4q\ \mathrm{Tr}\{\gamma_5 S_F(q)\gamma_5 S_F(q-k)\}. \qquad (A.1)$$

After renormalizing and dropping superfluous terms in $(\mu/4M)^2$ one has

$$G^{-1}(p^2) = (p^2+\mu^2-i\varepsilon)\left\{1-\frac{g^2}{4\pi^2}\left[\left(\frac{2M}{\sqrt{-p^2}}-1\right)\ln\left(\frac{-p^2}{4M^2}-1\right)\right.\right.$$
$$\left.\left.+\frac{4M}{\sqrt{-p^2}}\ln\left(1+\frac{\sqrt{-p^2}}{2M}\right)-1-2\pi\theta(-p^2-4M^2)(1-2M/\sqrt{-p^2})\right]\right\}. \qquad (A.2)$$

The spectral function is obtained from the relation [7])

$$\rho(m^2) = \pi \operatorname{Im} G(p^2), \tag{A.3}$$

and the meson wave-function renormalization constant comes from Lehman's relation [9])

$$Z_3^{-1} = 1 + \int_{4M^2}^{\infty} \rho(m^2) \mathrm{d}m^2, \tag{A.4}$$

where the lower bound on the integral is obtained from the observation that lowest-order perturbation theory accounts only for the two-nucleon intermediate state.

The spectral function is very strongly peaked (see fig. 1) near the point

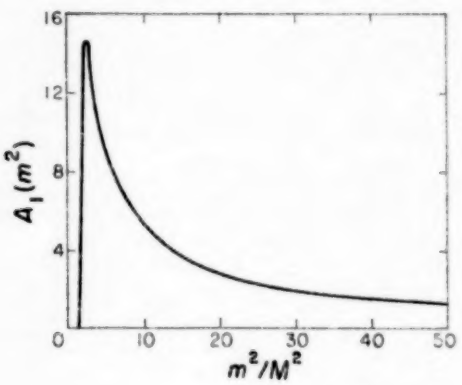

Fig. 1. Sketch of $A_1(m^2) = \dfrac{100}{0.298}\rho_1(m^2)$.

$$\rho \equiv m^2/4M^2 = 1.25,$$

and approximately 50 % of the contribution to the integral in eq. (A.4) comes from the region

$$1 \leqq \rho \leqq 4.$$

The integral was evaluated graphically for the interval below $\rho = 30$ and the contribution from the "tail" may then be obtained by using the asymptotic form of the spectral function in the integral. Thus, writing λ in place of $g^2/4\pi^2$, we have

$$\begin{aligned} Z_3^{-1} &= 1 + 0.18 + \pi\lambda \int_{30}^{\infty} \frac{\mathrm{d}\rho}{\rho} \{(\lambda-1)^2 + \lambda^2 + 4\lambda(\lambda-1)\ln\rho + 4\lambda^2 \ln^2\rho\}^{-1} \\ &\approx 1 + 0.18 + \frac{2}{\pi}(2\ln 30 + 1 - 1/\lambda)^{-1} = 1.20 \end{aligned} \tag{A.5}$$

to a precision of about 10 %. It will be observed that the integral just barely converges, so that

$$\int m^2 \rho(m^2) \mathrm{d}m^2,$$

which enters into the mass renormalization, is infinite.

A completely analogous calculation for the spinor field (somewhat complicated by the presence of the gamma matrices) gives the result

$$Z_2^{-1} \approx 1.9 \tag{A.6}$$

(for which the expression for the inverse nucleon propagator to second order in the coupling constant may be found in Feldman's paper). The mass renormalization for the nucleon is no less convergent than Z_2^{-1} and we have, in fact (M is the renormalized mass),

$$\frac{\delta M}{M} = 1 + Z_2 \int_{(M+\mu^2)}^{\infty} \mathrm{d}m^2 \rho_2(m^2) \approx 1.5. \tag{A.7}$$

References

1) H. A. Bethe and F. de Hoffman, Mesons and Fields, vol. 2 (Row Peterson and Co., Evanston Illinois, 1955) p. 289 ff
2) Federbush, Goldberger and Treiman, Phys. Rev. **112** (1958) 642
3) Feldman, Proc. Roy. Soc. A **223** (1954) 112
4) J. M. Jauch and F. Rohrlich, Theory of Photons and Electrons (Addison-Wesley, 1955)
5) Schwinger, Proc. Nat. Acad. Sci. **37** (1951) 452
6) R. Arnowitt and S. Gasiorowicz, Phys. Rev. **95** (1954) 538
7) P. J. Redmond, Phys. Rev. **112** (1958) 1404
8) Y. Takahashi, Nuovo Cimento **6** (1957) 371
9) H. Lehmann, Nuovo Cimento **11** (1954) 342

2.B *Nuclear Physics* **12** (1959) 494—509; © *North-Holland Publishing Co., Amsterdam*
Not to be reproduced by photoprint or microfilm without written permission form the publisher

THE POLARIZATION OF DEUTERONS AND PARTICLES OF ARBITRARY SPIN II

L. J. B. GOLDFARB and J. R. ROOK
Department of Theoretical Physics, University of Manchester

Received 31 March 1959

Abstract: General formulae are given for the polarization of charged particles of arbitrary spin emitted in an elastic scattering process in the neighbourhood of an isolated resonance, taking into account the specific Coulomb and potential contributions. These formulae also apply to the angular distributions associated with incoming polarized particles. The results are expressed in terms of the channel-spin and total angular-momentum representations.

Application is made to the elastic scattering of deuterons by He^4 at the deuteron laboratory energy of 1.069 MeV. Previous estimates of the polarization based on consideration of only resonance scattering require modification, particularly at low angles. Large values are found for the vector polarization which arise solely from the interference between resonance and non-resonance scattering.

1. Introduction

In a previous paper [1]) the possibility of the production or detection of a beam of polarized particles of arbitrary spin was examined, with special reference to deuterons. In particular, consideration was given to the process involving the elastic scattering of deuterons by He^4: $d+He^4 \rightarrow d+He^4$, which exhibits a sharp resonance for deuterons of energy 1.069 MeV and which can be interpreted [2]) in terms of only $l = 2$ waves. If one assumes that the contributions from Coulomb scattering and potential scattering can be treated as negligible, the resonance is described by a single matrix element †, and this leads to a polarization of the scattered deuterons. Indeed, under the assumption of a single matrix element large polarizations are found for a wide range of scattering angles of the deuterons, so that this process can serve either as a source of polarized deuterons or as an analyser of deuteron polarizations.

To give more reliable quantitative estimates of the polarization for this process, attention must be given to the influence of the potential and Coulomb scattering. We think it desirable to give general expressions for the polarization of charged particles in the neighbourhood of an isolated reso-

† This would not be the case if, instead of deuterons, there were spin-$\frac{1}{2}$ particles; here the polarization would vanish since it can only be associated with the interference between the matrix elements.

nance since such expressions may be useful for analyses of other scattering processes. This will serve to supplement the expressions for the unpolarized cross sections as given by Blatt and Biedenharn [3]). The results are also applicable to neutral particles if one ignores the Coulomb contributions. These expressions are given in section 2 in terms of both the channel-spin and total angular momentum representations.

The elastic scattering of deuterons by He^4 is then considered in section 3 and it is found that the original assumptions lead to polarizations which, although qualitatively the same as the re-calculated ones, differ in certain cases by a substantial amount. In addition, whereas first-rank (vector) polarization of the deuteron is ruled out for a single matrix element, it now arises by virtue of the interference between the resonance and the non-resonance scattering and can be quite large. Particular attention is given to the observation of this polarization in a double-scattering process.

2. General Formulae for Arbitrary Spin

The general expressions for the angular distributions of radiations of arbitrary spin which are prepared in a definite state of polarization or are detected by means of polarization-sensitive detectors already exist in the literature [1,4]). The scattering matrix S, or the reaction matrix $R(= S - 1)$ is expressed with respect to quantum numbers appropriate to the representation used for the coupling of the various angular momenta. The channel-spin representation provides the most usual method of designating nuclear reactions and it is this representation to which we shall mainly refer in the following section. We shall mention the corresponding results obtained for the total angular momentum representation near the end of the section.

Since the reaction matrix involves the potential, Coulomb and resonance contributions in essentially an additive fashion, we see that the angular distribution contains six terms in general — three from the scattering acting separately and three from the different types of interference. For uncharged particles there will be only three terms in all. These various terms are separately displayed in ref.[3]) for the unpolarized case. If we now consider polarization phenomena, we find that the angular distribution contains the unpolarized distribution, to which must be added three (not six) contributions, provided that we restrict potential scattering to a very general type presently to be specified. This is so because the Coulomb scattering, acting alone, will not yield any polarization. Neither will there be a contribution from potential scattering of the hard-sphere kind since there is no spin-orbit interaction. A potential scattering which includes the effects of levels of the compound system separated from the resonance level of interest may be represented in a phenomenological manner by phase-shifts which are not the

hard-sphere ones; however, as long as they are independent of the total angular momentum and the channel spin of the system, there will be no polarization arising purely from this type of scattering. To simplify the following discussion, we shall restrict ourselves to this latter type of potential scattering. Thus, the only contributions to the polarization will arise from the interference between the non-resonance and resonance scattering and from the resonance scattering, acting alone. (In the latter case, only even-rank polarization occurs, see ref.[1]).)

We first consider the detection of the polarization of the outgoing particles. The expression for the angular distribution $W(\Omega_1\Omega_2)\mathrm{d}\Omega_1\mathrm{d}\Omega_2$ is given by Devons and Goldfarb [4]):

$$W(\Omega_1\Omega_2) = \frac{\lambda^2}{4\hat{a}^2\hat{s}^2}\sum(-)^{S_1-b'}Z'(l_1bl_1'b';S_1k)\frac{\hat{s}\varepsilon^*_{k_s\kappa}(s)}{\varepsilon_{00}(s)}(k_s\kappa,k_l0|k\kappa):$$

$$\mathscr{D}^k_{\kappa 0}(\mathscr{R})(-)^{a-s+k_s-S'_2+l'_2}\hat{k}_s\hat{k}_l\hat{S}_2\hat{S}'_2\hat{l}_2\hat{l}'_2\hat{b}\hat{b}'(l_20,l'_20|k_l0)W(ssS_2S'_2;k_sa) \quad (1)$$

$$\begin{Bmatrix}S_2l_2b\\S'_2l'_2b'\\k_sk_lk\end{Bmatrix}\begin{cases}\mathrm{Re}(RR'^*)\ldots\text{even } k_s\\ i\,\mathrm{Im}(RR'^*)\ldots\text{odd } k_s\end{cases}$$

where the summation is over $l_1l_2l'_1l'_2bb'S_1S_2S'_2k_lk_sk$ and κ. The reader is referred to refs. [4]) or [1]) for an explanation of the symbols used. We shall merely point out the scheme used for the designation of the quantum numbers.

The initial and final spins of the target and the particle are represented by a and s_1 respectively. These are coupled together to yield the channel spins S_1 or S_2. The subscript 1 and 2 refer to the initial and final stages of the process, while the primed and unprimed symbols represent any two choices of the symbol that are not forbidden by the selection rules inherent in the different angular-momenta coefficients used above and consistent with the parity requirements. The total angular momentum b arises from the coupling of S to the orbital angular momentum l. Thus we have

$$\mathbf{b} = \mathbf{S}_1+\mathbf{l}_1 = \mathbf{S}_2+\mathbf{l}_2. \quad (2)$$

We use the notation $\hat{k}$ to mean $\sqrt{2k+1}$. The quantity $\varepsilon_{k_s\kappa}(s)$ is the efficiency tensor for the detection of the polarization [1]), and the angular dependence is contained in the rotation matrix $\mathscr{D}^k_{\kappa 0}(\mathscr{R})$. Finally, the matrix elements R and R' are meant to designate

$$\langle as(S_2)l_2b|R|\ as\ (S_1)l_1b\rangle \text{ and } \langle as(S'_2)l'_2b'|R|\ as\ (S'_1)l'_1b'\rangle$$

respectively. It might be pointed out here that the order of coupling of angular momenta, which is not usually of much significance for the unpolarized cases, is of importance in the general case. For example, an interchange of l and S will give rise to a phase factor. The expression for

$W(\Omega_1\Omega_2)$ is real since the quantity

$$\sum_{\kappa} \varepsilon^*_{k_s\kappa}(s)(k_s\kappa, k_l 0|k\kappa)\mathscr{D}^k_{\kappa 0}(\mathscr{R})$$

can be shown to be real or pure imaginary according as k_s is even or odd, and all the other quantities in (1), except for RR'^*, are real.

An alternative expression for the angular distribution in the angular-momentum representation can be found by using (2.14) and (2.14b) in ref. [1]).

The fact that neither Coulomb scattering nor potential scattering (without spin-orbit coupling) will give rise to polarization is evident from (1), if one sets $l_1 = l_2 = l$ and $S_1 = S_2 = S$, say. Expressing $Z'(lbl'b'; Sk)$ in terms of the 9-j symbol and summing over b and b', we find, by means of the identity

$$\sum_{bb'} \hat{b}^2\hat{b}'^2 \begin{Bmatrix} S & l & b \\ S' & l' & b' \\ 0 & k & k \end{Bmatrix} \begin{Bmatrix} S & l & b \\ S' & l' & b' \\ k_s & k_l & k \end{Bmatrix} = \delta_{kk_l}\delta_{k_s0}\delta_{SS'}\frac{1}{\hat{k}^4}, \tag{3}$$

that $k_s = 0$, and there is therefore no polarization.

We now use the Breit-Wigner one-level formula to represent the elastic scattering in the neighbourhood of a resonance corresponding to a specific parity and angular momentum b_0. The scattering matrix takes on the form

$$\langle S_2 l_2 b|S|S_1 l_1 b\rangle = e^{i(\zeta_{l_1}+\zeta_{l_2})}\langle S_2 l_2 b|I+K|S_1 l_1 b\rangle \tag{4}$$

where

$$\langle S_2 l_2 b|I|S_1 l_1 b\rangle = \delta_{S_1S_2}\delta_{l_1l_2} \tag{4a}$$

and

$$\langle S_2 l_2 b|K|S_1 l_1 b\rangle = \frac{ig_b(S_1 l_1)g_b(S_2 l_2)}{E_0 - E - \frac{1}{2}i\Gamma}\delta_{bb_0}. \tag{4b}$$

The energy shift is absorbed in the definition of the resonance level. Other quantities are as defined in ref.[3]). Thus, the level width is $\Gamma = \sum_{Sl}\Gamma_{b_0}(Sl)$ $= \sum_{Sl} g^2_{b_0}(Sl)$, omitting for convenience the channel index, and ζ_l is the phase shift arising from the combined effect of Coulomb and potential scattering. We shall assume that the latter is independent of b and S. The terms giving the effect of the screening of the Coulomb field are omitted, since they are independent of angular momentum and cancel in the final expressions. In accordance with ref.[3]), we introduce the Coulomb phase shifts σ_l and ψ_l and ϕ_l, the potential phase shift, such that

$$\zeta_l \equiv \sigma_l + \phi_l \equiv \psi_l + \sigma_0 + \phi_l, \tag{5}$$

where

$$\psi_l \equiv \sigma_l - \sigma_0. \tag{5a}$$

We then find that the reaction matrix R can be written as

$$\langle S_2 l_2 b|R|S_1 l_1 b\rangle = R_c(l_1) + R_{pot}(l_1) + \langle S_2 l_2 b|R_{res}|S_1 l_1 b\rangle \tag{6}$$

where

$$R_c(l_1) = I(e^{2i\sigma_{l_1}} - 1) \tag{6a}$$

$$R_{\text{pot}}(l_1) = I e^{2i\sigma_{l_1}}(e^{2i\phi_{l_1}} - 1) \tag{6b}$$

$$\langle S_2 l_2 b | R_{\text{res}} | S_1 l_1 b \rangle = e^{i(\sigma_{-1}+\sigma_{l_2}+\phi_{l_1}+\phi_{l_2})} \langle S_2 l_2 b | K | S_1 l_1 b \rangle, \tag{6c}$$

where the matrix elements for I are given in (4a).

We now consider the Coulomb term $R_c(l_1)$. Because of the slow convergence of the Coulomb phase shifts with l_1, we make use of the spherical expansion of the Coulomb wave-function [5]) $u_c(\mathbf{r})$ which is normalized to unit flux. This can be written as

$$u_c(\mathbf{r}) = \sum_l v_l(r) P_l(\cos\theta) \tag{7}$$

where $v_l(r)$ is asymptotically of the form

$$v_l(r) \xrightarrow[r\to\infty]{} \frac{\hat{l}^2 e^{i\sigma_l} i^l}{\sqrt{v}|\mathbf{k}|r} \sin\left[|\mathbf{k}|r - \tfrac{1}{2}l\pi - \eta \ln(2|\mathbf{k}|r) + \sigma_l\right]. \tag{7a}$$

Here v is the relative velocity and $|\mathbf{k}|$ the wave number in the centre-of-mass system, while η is the Coulomb parameter, $\eta = zZe^2/\hbar v$, where ze and Ze are the charges of particle and nucleus. We may put $v_l(r)$ in the form

$$\begin{aligned} v_l(r) \xrightarrow[r\to\infty]{} \frac{\hat{l}^2 i^l}{\sqrt{v}2i|\mathbf{k}|r} \big[&2i \sin\{|\mathbf{k}|r - \tfrac{1}{2}l\pi - \eta \ln(2|\mathbf{k}|r)\} \\ &+ (e^{2i\sigma_l} - 1) e^{i\{|\mathbf{k}|r - \frac{1}{2}l\pi - \eta \ln(2|\mathbf{k}|r)\}}\big], \end{aligned} \tag{7b}$$

so that

$$u_c(\mathbf{r}) \to \frac{1}{\sqrt{v}} \left[u_c\{\text{"plane wave"}\} + \frac{e^{i|\mathbf{k}|r}}{2i|\mathbf{k}|r} \sum_l R_c(l) \hat{l}^2 P_l(\cos\theta) \right], \tag{7c}$$

where the first term corresponds to a plane wave, except for the distortion associated with the logarithmic phase factors. This is to be compared with the alternative expression for $u_c(\mathbf{r})$,

$$u_c(\mathbf{r}) \to \frac{1}{\sqrt{v}} \left[u_c\{\text{"plane wave"}\} - f_c(\theta) \frac{e^{i|\mathbf{k}|r}}{r} \right], \tag{8}$$

where

$$f_c(\theta) = \frac{\eta}{2|\mathbf{k}|} \operatorname{cosec}^2 \tfrac{1}{2}\theta e^{2i\sigma_0 - 2i\eta \ln(\sin\frac{1}{2}\theta)}. \tag{8a}$$

This leads to the relation

$$\sum_l R_c(l) \hat{l}^2 P_l(\cos\theta) = -2i|\mathbf{k}| f_c(\theta) \equiv R_c(\theta). \tag{9}$$

Because of the orthogonality of the Legendre polynomials, the explicit value of $R_c(l)$ is

$$R_c(l) = \tfrac{1}{2} \int_{-1}^{+1} R_c(\theta) P_l(\cos\theta) \mathrm{d}\cos\theta. \tag{9a}$$

We may readily show that (9) leads to the Rutherford cross-section if we use the expression for the angular distribution when the scattering matrix

is diagonal in l and s †

$$W_{\text{Coul}}(\theta) = \tfrac{1}{4}\lambda\!\!\!^{-2} \sum_{kll'} \hat{l}^2 \hat{l}'^2 (l0, l'0|k0)^2 R_c(l) R_c^*(l') P_k(\cos\theta). \tag{10}$$

Using the relation for the product of two rotation matrices, which are each of the form $\mathscr{D}^L_{00}(000) = P_L(\cos\theta)$:

$$P_l(\cos\theta) P_{l'}(\cos\theta) = \sum_k (l0, l'0|k0)^2 P_k(\cos\theta), \tag{10a}$$

it follows that

$$W_{\text{Coul}}(\theta) = \tfrac{1}{4}\lambda\!\!\!^{-2} |\sum_l R_c(l) \hat{l}^2 P_l(\cos\theta)|^2 = \left(\frac{zZe^2}{2mv^2}\right)^2 \operatorname{cosec}^4 \tfrac{1}{2}\theta, \tag{10b}$$

where m is the reduced mass of the incident particle.

The angular distribution given in (1) may now be rewritten by separating R into its three components according to (6). The result is

$$W(\Omega_1\Omega_2) = W_0(\theta) + W_{\text{Coul; res}}(\Omega_1\Omega_2) + W_{\text{pot; res}}(\Omega_1\Omega_2) + W_{\text{res; res}}(\Omega_1\Omega_2), \tag{11}$$

where $W_0(\theta)$ is the unpolarized angular distribution, given by Blatt and Biedenharn [3]), and the remaining terms on the right-hand side of (11) represent the contributions to the polarization arising from the interference of the scattering with the resonance scattering. The authors of ref.[3]) present their results for the case corresponding to 'true' elastic scattering, i.e. scattering without change of the energy or the channel spin. The experimentally observed 'elastic' scattering cross-sections allow for the possibility of channel-spin change and therefore we shall present our results to include such terms. The only necessary modification required of their formulae in this case is to change the single term in $W_0(\theta)$ which corresponds to pure resonance scattering to one in which the channel spins may change, i.e. to relax the condition that (in their notation) $s' = s$ in the quantity $R_L(\alpha' s'; \alpha s)$ which is used in their equation (6.1).

The two middle terms may be simplified:

$$\begin{aligned} W_{\substack{\text{Coul; res}\\ \text{pot; res}}}(\Omega_1\Omega_2) &= \frac{\lambda\!\!\!^{-2}}{2\hat{a}^2\hat{S}^2} \sum_{k_s \neq 0} (-)^{a-s+k_s+l'_2-b'+S_1-S'_2} Z'(l_1 b l'_1 b'; S_1 k) \frac{\hat{s}\varepsilon^*_{k_s\kappa}(s)}{\varepsilon_{00}(s)} (k_s\kappa,\ k_l 0|k\kappa) \\ &\times \mathscr{D}^k_{\kappa 0}(\mathscr{R}) \hat{k}_s \hat{k}_l \hat{S}_1 \hat{S}'_2 \hat{l}_1 \hat{l}'_2 \hat{b}\hat{b}' W(ssS_1S'_2; k_s a)(l_1 0, l'_2 0|k_l 0) \\ &\times \begin{Bmatrix} S_1 l_1 b \\ S'_2 l'_2 b' \\ k_s k_l k \end{Bmatrix} \begin{cases} \operatorname{Re}[R_{\substack{c\\ \text{pot}}}(l_1) \langle S'_2 l'_2 b' | R_{\text{res}} | S_1 l'_1 b' \rangle^*] \ldots \text{even } k_s \\ i \operatorname{Im}[R_{\substack{c\\ \text{pot}}}(l_1) \langle S'_2 l'_2 b' | R_{\text{res}} | S_1 l'_1 b' \rangle^*] \ldots \text{odd } k_s \end{cases} \end{aligned} \tag{12}$$

with the summation over $l_1 l'_1 l'_2 b b' S_1 S'_2 k_l k_s k$ and κ. After some manipulation of the angular-momentum coefficients as shown in the appendix, one finds

† See for example ref. [3]), section 2, or ref. [4b]), section 38.

$$W_{\text{pot; res}}(\Omega_1\Omega_2) = \frac{\hat{\lambda}^2}{2\hat{a}^2\hat{s}^2}\sum_{k_s\neq 0}(-)^{a-s+k_s+l'_2-b'+S_1-S'_2}\frac{\hat{s}\varepsilon^*_{k_s\kappa}(s)}{\varepsilon_{00}(s)}(k_s\kappa,\, k_l 0|k\kappa)\mathscr{D}^k_{\kappa 0}(\mathscr{R})$$

$$\hat{k}_s\hat{k}_l\hat{S}_1\hat{S}'_2\hat{l}'^2_1\hat{l}'_1\hat{l}'_2\hat{b}'^2(l_1 0,\, l'_1 0|k0)(l_1 0,\, l'_2 0|k_l 0)W(l_1 l'_2 k k_s;\, k_l l'_1)W(S_1 l'_1 S'_2 l'_2;\, b' k_s)$$

$$W(ssS_1S'_2;\, k_s a)\begin{cases}\operatorname{Re}[R_{\text{pot}}(l_1)\langle S'_2 l'_2 b'|R_{\text{res}}|S_1 l'_1 b'\rangle^*]\ \ldots \text{ even } k_s\\ i\operatorname{Im}[R_{\text{pot}}(l_1)\langle S'_2 l'_2 b'|R_{\text{res}}|S_1 l'_1 b'\rangle^*]\ \ldots \text{ odd } k_s\end{cases} \tag{13}$$

where the summation is as in (12), except for no summation over b. The Coulomb-term is reduced still further by using $R_c(l)$ given in (9). One finds

$$W_{\text{Coul; res}}(\Omega_1\Omega_2) = \frac{\hat{\lambda}^2}{2\hat{a}^2\hat{s}^2}\sum_{k_s\neq 0}(-)^{a-s+S_1-S'_2-l'_1-b'}\frac{\hat{s}\varepsilon^*_{k_s\kappa}(s)}{\varepsilon_{00}(s)}(l'_2 0,\, k_s\kappa|l'_1\kappa)\mathscr{D}^{l'_1}_{\kappa 0}(\mathscr{R})$$

$$\hat{b}'^2\hat{k}_s\hat{S}_1\hat{S}'_2\hat{l}'_2 W(ssS_1S'_2;\, k_s a)W(S_1 l'_1 S'_2 l'_2;\, b' k_s) \tag{14}$$

$$\begin{cases}\operatorname{Re}[R_c(\theta)\langle S'_2 l'_2 b'|R_{\text{res}}|S_1 l'_1 b'\rangle^*]\ \ldots \text{ even } k_s\\ i\operatorname{Im}[R_c(\theta)\langle S'_2 l'_2 b'|R_{\text{res}}|S_1 l'_1 b'\rangle^*]\ \ldots \text{ odd } k_s\end{cases}$$

where the summation is now restricted to be only over $l'_1 l'_2 b' S_1 S'_2 k_s$ and κ. If one performs the summation over κ the coefficient of the matrix elements in (13) and (14) is split into real and imaginary parts. For example, for (14) we have

$$\sum_\kappa \varepsilon^*_{k_s\kappa}(s)\mathscr{D}^{l'_1}_{\kappa 0}(\mathscr{R})(l'_2 0,\, k_s\kappa|l'_1\kappa) = \varepsilon_{k_s 0}(s)(l'_2 0,\, k_s 0|l'_1 0)P_{l'_1}(\cos\theta)$$

$$+2\sum_{\kappa>0}(-)^\kappa\sqrt{\frac{(l'_1-\kappa)!}{(l'_1+\kappa)!}}(l'_2 0,\, k_s\kappa|l'_1\kappa)P^\kappa_{l'_1}(\cos\theta)\begin{cases}\operatorname{Re}[\varepsilon_{k_s\kappa}(s)e^{i\kappa\chi}]\ \ldots \text{ even } k_s\\ -i\operatorname{Im}[\varepsilon_{k_s\kappa}(s)e^{i\kappa\chi}]\ \ldots \text{ odd } k_s.\end{cases} \tag{15}$$

Here; χ is the angle between the y-axis describing the detector of the polarization and $-\mathbf{n}$, where $\mathbf{n} = \mathbf{k}_1\times\mathbf{k}_2$, and $\mathbf{k}_1$ and $\mathbf{k}_2$ are propagation vectors along radiations 1 and 2.

At this stage, we can present the results of the alternative polarization measurement, where the incoming beam is polarized with spin tensors $\rho_{k_s\kappa}(s)$ and this polarization is detected through the angular distribution of the subsequent scattering process. Then the above expressions for $W(\Omega_1\Omega_1)$ are still appropriate provided that we interchange suffices 1 and 2 and we change $\varepsilon^*_{k_s\kappa}(s)\mathscr{D}^k_{\kappa 0}$ to $\rho_{k_s\kappa}(s)\mathscr{D}^{k*}_{\kappa 0}$. The second operation is equivalent to using an expression such as in (15), but where ρ replaces ε and $-i\operatorname{Im}(\ldots)$ is changed to $i\operatorname{Im}(\ldots)$. Also, χ is to be interpreted as the angle between $\mathbf{n} = \mathbf{k}_1\times\mathbf{k}_2$ and the y-axis describing the polarization of the incident beam.

We can use the expressions for the matrix elements given in (6b), (6c) and (9) and, if we introduce the following notation:

$$\begin{aligned} G &\equiv g_b(S_1 l_1)g_b(S_2 l_2), \qquad \tan\beta \equiv \frac{2(E-E_0)}{\Gamma}\ (0\leqq\beta\leqq\pi),\\ G' &= g_{b'}(S'_1 l'_1)g_{b'}(S'_2 l'_2), \qquad \varepsilon \equiv +\sqrt{(E-E_0)^2+\tfrac{1}{4}\Gamma^2}, \end{aligned} \tag{16}$$

we find

$$\begin{matrix}\mathrm{Re}\\ \mathrm{Im}\end{matrix}[\langle S_2 l_2 b|R_{\mathrm{res}}|S_1 l_1 b\rangle\langle S_2' l_2' b'|R_{\mathrm{res}}|S_1' l_1' b'\rangle^*]$$
$$=\frac{GG'}{\varepsilon^2}\delta_{b'b_0}\delta_{bb_0}\begin{matrix}\cos\\ \sin\end{matrix}(\psi_{l_1}+\phi_{l_1}+\psi_{l_2}+\phi_{l_2}-\psi_{l_1'}-\phi_{l_1'}-\psi_{l_2'}-\phi_{l_2'}), \quad (16a)$$

$$\begin{matrix}\mathrm{Re}\\ \mathrm{Im}\end{matrix}[R_{\mathrm{pot}}(l_1)\langle S_2' l_2' b'|R_{\mathrm{res}}|S_1' l_1' b'\rangle^*]$$
$$=\pm\frac{2G'I}{\varepsilon}\delta_{b'b_0}\sin\phi_{l_1}\begin{matrix}\sin\\ \cos\end{matrix}(2\psi_{l_1}+\phi_{l_1}-\psi_{l_1'}-\psi_{l_2'}-\phi_{l_1'}-\phi_{l_2'}-\beta), \quad (16b)$$

$$\begin{matrix}\mathrm{Re}\\ \mathrm{Im}\end{matrix}[R_{\mathrm{c}}(\theta)\langle S_2' l_2' b'|R_{\mathrm{res}}|S_1' l_1' b'\rangle^*]$$
$$=\frac{G'I\eta}{\varepsilon}\,\mathrm{cosec}^2\tfrac{1}{2}\theta\,\delta_{b'b_0}\begin{matrix}\sin\\ \cos\end{matrix}(\psi_{l_1'}+\phi_{l_1'}+\psi_{l_2'}+\phi_{l_2'}+\beta+2\eta\ln\sin\tfrac{1}{2}\theta). \quad (16c)$$

The general formula for the angular distribution is then given by (11), where $W_0(\theta)$ is given by Blatt and Biedenharn, modified in the above manner. The quantities $W_{\mathrm{Coul;\,res}}(\Omega_1\Omega_2)$, $W_{\mathrm{pot;\,res}}(\Omega_1\Omega_2)$ and $W_{\mathrm{res;\,res}}(\Omega_1\Omega_2)$ are to be found by using (12) and (16b), (13) and (16c) and (1) and (16a), respectively.

We illustrate the above results by the particular case of the pure elastic scattering of charged spin-$\frac{1}{2}$ particles by spinless nuclei. The explicit expression for the unpolarized distribution is to be found in eq. (7.13) of ref. [3]). The other contributions to $W(\Omega_1\Omega_2)$ are as follows:

$$W_{\mathrm{pot;\,res}}(\Omega_1\Omega_2)=-\tfrac{1}{8}\lambda^2\sum_{l'b'k}\frac{\hat{b}'^2\hat{l}^2(l0,\,l'0|k0)^2}{l'(l'+1)k(k+1)}[k(k+1)+l'(l'+1)-l(l+1)]$$
$$[\tfrac{3}{4}+l'(l'+1)-b'(b'+1)]P_k^1(\cos\theta)\mathbf{P}^{\mathrm{d}}\cdot\mathbf{n}\,\mathrm{Im}[R_{\mathrm{pot}}(l)\langle\tfrac{1}{2}l'b'|R_{\mathrm{res}}|\tfrac{1}{2}l'b'\rangle^*], \quad (17a)$$

$$W_{\mathrm{Coul;\,res}}(\Omega_1\Omega_2)=-\tfrac{1}{4}\lambda^2\sum_{l'b'}\frac{\hat{b}'^2}{l'(l'+1)}[\tfrac{3}{4}+l'(l'+1)-b'(b'+1)]P_{l'}^1(\cos\theta)\mathbf{P}^{\mathrm{d}}\cdot\mathbf{n}$$
$$\times\,\mathrm{Im}[R_{\mathrm{c}}(\theta)\langle\tfrac{1}{2}l'b'|R_{\mathrm{res}}|\tfrac{1}{2}l'b'\rangle^*]. \quad (17b)$$

If we assume that there is a single isolated resonance level contributing to the process only a single term, b', contributes. In this case, there is no term corresponding to $W_{\mathrm{res;\,res}}(\Omega_1\Omega_2)$.

We also quote the expressions which obtain in the total angular momentum representation. The general expression for the angular distribution corresponding to detection of the polarization of the outgoing particles is given in ref. [1]):

$$W(\Omega_1\Omega_2)=\frac{\lambda^2}{4\hat{a}^2\hat{s}^2}\sum(-)^{s+l'_2-L_2+k}\hat{b}^2\hat{b}'^2\hat{l}_2\hat{l}'_2\hat{L}_2\hat{L}'_2\hat{k}_l\hat{k}_s Z'(l_1L_1l'_1L'_1;sk)$$

$$\times W(L_1L'_1bb';ka)W(L_2L'_2bb';ka)(l_20,l'_20|k_l0)(k_l0,k_s\kappa|k\kappa)\begin{Bmatrix}l_2 & l'_2 & k_l\\ s & s & k_s\\ L_2 & L'_2 & k\end{Bmatrix}\frac{\hat{s}\varepsilon^*_{k_s\kappa}(s)}{\varepsilon_{00}(s)} \quad (18)$$

$$\times\mathscr{D}^k_{\kappa 0}(\mathscr{R})\begin{cases}\mathrm{Re}[\langle al_2s(L_2)b|R|al_1s(L_1)b\rangle\langle al'_2s(L'_2)b'|R|al'_1s(L')b'\rangle^*]\ \ldots\ \text{even } k_s\\ i\,\mathrm{Im}[\langle al_2s(L_2)b|R|al_1s(L_1)b\rangle\langle al'_2s(L'_2)b'|R|al'_1s(L'_1)b'\rangle^*]\ \ldots\ \text{odd } k_s\end{cases}$$

where the summation is over $l_1l'_1l_2l'_2L_1L'_1L_2L'_2bb'k_lk_sk$ and κ. Here, the intrinsic spin of the particle s is coupled with l to give L, which is then coupled with a to finally yield b, i.e.

$$\mathbf{b}=\mathbf{a}+\mathbf{L}=\mathbf{a}+(\mathbf{l}+\mathbf{s}). \quad (18a)$$

The expression for $W_0(\theta)$ given in ref. [3]) may be used provided that we replace the term corresponding to the pure resonance contribution by the above expression where we put $k_s=0$. The derivation of $W_{\mathrm{Coul;\,res}}(\Omega_1\Omega_2)$ and $W_{\mathrm{pot;\,res}}(\Omega_1\Omega_2)$ is essentially similar to that used for the channel-spin representation and the results are as follows:

$$W_{\mathrm{pot;\,res}}(\Omega_1\Omega_2)=\sum_{k_s\neq 0}(-)^{l'_2+L'_2-s}\hat{b}'^2\hat{l}_1^2\hat{l}'_1\hat{l}'_2W(sl'_1sl'_2;L'_1k_s)W(kl'_1k_ll'_2;l_1k_s)$$

$$(l_10,l'_10|k0)(l_10,l'_20|k_l0)(k_l0,k_s\kappa|k\kappa)\frac{\hat{s}\varepsilon^*_{k_s\kappa}(s)}{\varepsilon_{00}(s)}\mathscr{D}^k_{\kappa 0}(\mathscr{R}) \quad (18b)$$

$$\begin{cases}\mathrm{Re}[R_{\mathrm{pot}}(l_1)\langle aL'_2b'|R_{\mathrm{res}}|aL'_1b'\rangle^*]\ \ldots\ \text{even } k_s\\ i\,\mathrm{Im}[R_{\mathrm{pot}}(l_1)\langle aL'_2b'|R_{\mathrm{res}}|aL'_1b'\rangle^*]\ \ldots\ \text{odd } k_s,\end{cases}$$

$$W_{\mathrm{Coul;\,res}}(\Omega_1\Omega_2)=\sum_{k_s\neq 0}(-)^{l'_2+L'_2-s+k_s}\hat{b}'^2\hat{l}'_2\hat{k}_sW(sl'sl'_2;L'_1k_s)(l_20,k_s\kappa|l'_1\kappa)$$

$$\frac{\hat{s}\varepsilon^*_{k_s\kappa}(s)}{\varepsilon_{00}(s)}\mathscr{D}^{l'_1}_{\kappa 0}(\mathscr{R})\begin{cases}\mathrm{Re}[R_c(\theta)\langle aL'_2b'|R_{\mathrm{res}}|aL'_1b'\rangle^*]\ \ldots\ \text{even } k_s\\ i\,\mathrm{Im}[R_c(\theta)\langle aL'_2b'|R_{\mathrm{res}}|aL'_1b'\rangle^*]\ \ldots\ \text{odd } k_s.\end{cases} \quad (18c)$$

The expression for $W_{\mathrm{res;\,res}}$ is given by (18) if R is replaced by R_{res} and $k_s\neq 0$.

3. The Polarization of Deuterons in the Resonance Scattering by He^4

We reconsider† the resonance scattering of deuterons by He^4 at $E_d=1.069$ MeV (laboratory system), taking into account the potential and Coulomb scattering which cannot be dismissed even if the scattering is through large angles. The analysis of Galonsky *et al.* [6]), who investigated the scattering over an extensive range of angles and over deuteron energies ranging

† An independent calculation of the polarization phenomena associated with this particular process has been made by R. J. N. Phillips (private communication) and we thank him for letting us see his results. These are essentially in agreement with the results quoted in this section.

from 0.28 to 4.62 MeV, enabled them to conclude that the potential scattering was not well-represented at the resonance energy by hard sphere scattering, as originally considered by Lauritsen *et al.*[2]). Rather it is sufficient to use a S-phase shift corresponding to a radius of $\approx 5\times10^{-13}$ cm and to put the P and D phase shifts equal to zero.

The quantum numbers for this process are therefore $a = 0$, $S = 1$ and $l_1 = l_2 = 2$, $b_0 = 3$ for the resonance and $l_1 = l_2 = 0$, $b = 1$ for the potential scattering. It is also necessary to know the resonance width † which is taken to be $\Gamma = 25$ keV. This is a case of 'true' elastic scattering and the formulae of ref. [3]) may be used for finding the unpolarized angular distribution, $W_0(\theta)$, which is shown in fig. 1. The angular distribution corresponding to

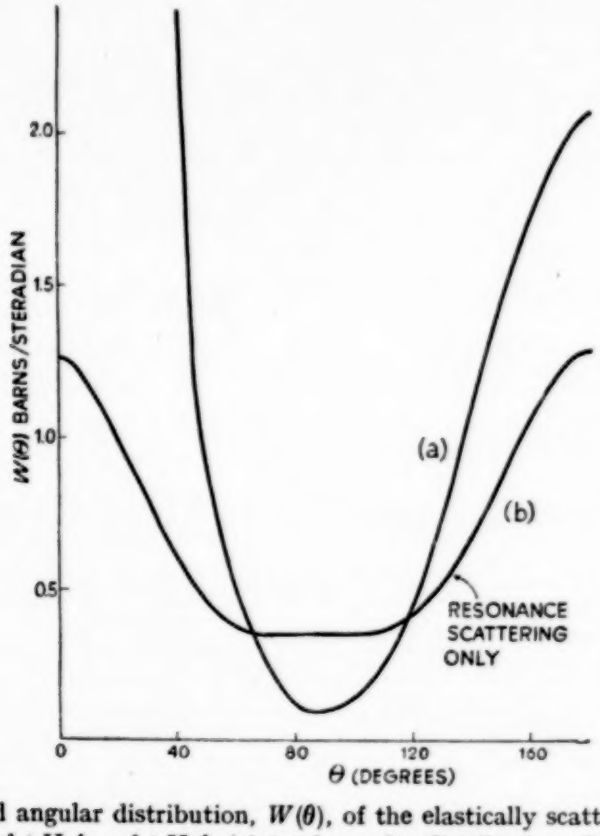

Fig. 1. Unpolarized angular distribution, $W(\theta)$, of the elastically scattered deuterons in the resonance reaction $d+He^4 \rightarrow d+He^4$. (a) total angular distribution; (b) angular distribution corresponding to resonance scattering only.

pure resonance scattering is also included for comparison. It is to be noted that, even allowing for the expected Coulomb scattering at small angles, there is considerable deviation over the entire angular range.

We now present the results of the calculation of the polarization of the deuterons. This is represented by the quantities P_{ij} which characterize polarization of rank 2 and the component of vector polarization P_2 (see

† The dependence on Γ arises only for angular distributions off resonance which are considered later in this section.

ref. [1])) which now arises because of the interference with non-resonance scattering. The added quantities to $W_0(\theta)$ in the angular distribution are given below:

$$W_{\text{Coul; res}}(\Omega_1\Omega_2) = -\tfrac{7}{12}\lambda^2 P_2^1(\cos\theta)\cos\chi P_2^{\text{d}}\,\text{Im}\,[R_c(\theta)R_{\text{res}}^*]$$
$$+\tfrac{1}{6}\lambda^2[-P_2(\cos\theta)P_{33}^{\text{d}} - \tfrac{1}{3}P_2^1(\cos\theta)\cos\chi P_{13}^{\text{d}} + \tfrac{1}{6}P_2^2(\cos\theta)\cos 2\chi(P_{11}^{\text{d}} P_{22}^{\text{d}})] \quad (19)$$
$$\times \text{Re}[R_c(\theta)R_{\text{res}}^*];$$

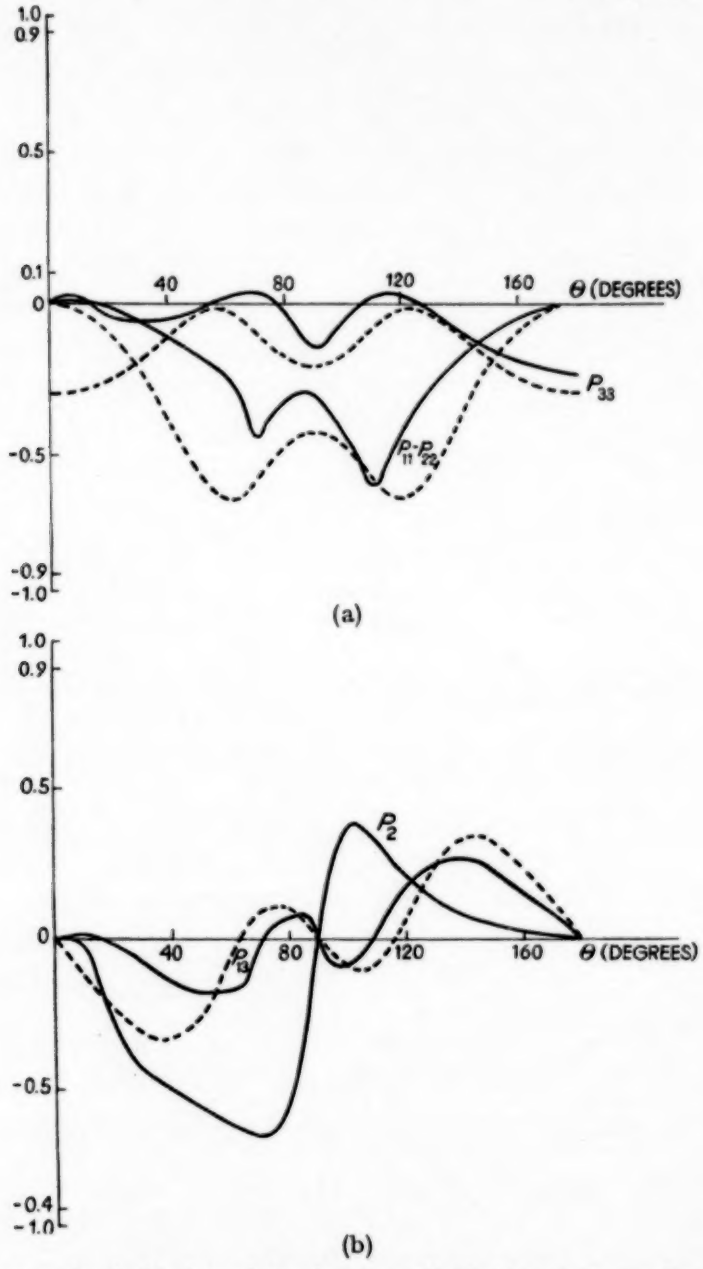

Fig. 2. Components of polarization of the deuteron divided by their maximum magnitude in any state of polarization. The dashed curves are those corresponding to resonance scattering only.

(a) P_{33} and $P_{11}-P_{22}$

(b) P_{13} and P_2.

the quantities $W_{\text{pot; res}}(\Omega_1\Omega_2)$ may be found from (19) by changing $R_c(\theta)$ to $R_{\text{pot}}(l_1 = 0)$. The polarization arising from pure resonance scattering is to be found † in ref. [1]). Using eq. (2.28b) of ref. [1]), we can easily read off the values of the polarization from (19). The efficiency of the scattering process when used as a detector of polarization can also be obtained from (19) by replacing P_{ij}^{d} by P_{ij} and P_2^{d} by $-P_2$, and re-interpreting χ. The polarization corresponding to a deuteron energy just at resonance are shown in fig. 2, where one has plotted the quantities P_{ij} and P_2, divided by their maximum magnitudes in any state of polarization. The latter quantities are shown in table 1 of ref. [1]), except for P_2 which is characterized by $(P_2)_{\substack{\max \\ \min}} = \pm 1$. The polarization parameters, computed by neglecting potential and Coulomb scattering, are also shown in fig. 2 and it is to be noted that these previous estimates are not greatly modified for angles greater than 90°. For smaller angles, the potential and Coulomb effects are quite large. In addition, high values are found for the quantity P_2 in the angular range from 30° to 80° and again from 100° to 120°.

It is possible †† in principle to observe these polarization parameters by performing a double scattering. This is achieved by allowing α-particles to impinge on deuterium with an energy of 2.14 MeV. The deuterons corresponding to scattering through angles greater than 80° with respect to their original motion in the first centre-of-mass system, now have laboratory energies exceeding the resonance energy and therefore a double scattering process through the resonance is possible. The angular distribution may be expressed as

$$W(\theta_1, \theta_2, \phi) = W_0(\theta_1, \theta_2)[1+l(\theta_1, \theta_2)\cos\phi+m(\theta_1, \theta_2)\cos 2\phi] \qquad (20)$$

where ϕ is the angle between the two planes of scattering.

In fig. 3, are plotted the 'left-right' symmetry

$$\frac{L-R}{L+R} \equiv \frac{W(\phi = 0°)-W(\phi = 180°)}{W(\phi = 0°)+W(\phi = 180°)}$$

and the 'left-up' asymmetry

$$\frac{L-U}{L+U} \equiv \frac{W(\phi = 0°)-W(\phi = 90°)}{W(\phi = 0°)-W(\phi = 90°)}$$

as functions of $\theta(= \theta_1 = \theta_2)$, the scattering angle in each of the centre-of-

† There is an overall sign in the expressions for P_{13} and P_{23} given in (2.29), and also plotted in fig. 1 of ref.[1]).

†† A more attractive possibility is to measure the polarization of the outgoing deuterons through either of the processes $d+He^3 \rightarrow He^4+p$ or $d+H^3 \rightarrow He^4+n$. The resultant angular distributions will serve to detect only tensor polarization. (See A. Galonsky, H. B. Willard and T. A. Welton, Phys. Rev. Lett. **2** (1959) 349; L. J. B. Goldfarb, Nuclear Physics, to be published shortly.)

mass systems. Large values are obtained for the left-up asymmetry ($\approx$0.5—0.6) at 70° and 110°, while the left-right asymmetry is not significant except for angles less than 90°.

In any experiment of this kind it would be difficult to arrange the second scattering to occur precisely at the resonance energy. To test the effect of the variation of energy from the value E_0, the polarization parameters as fractions of their maximum magnitudes are plotted in fig. 4 against $E-E_0$,

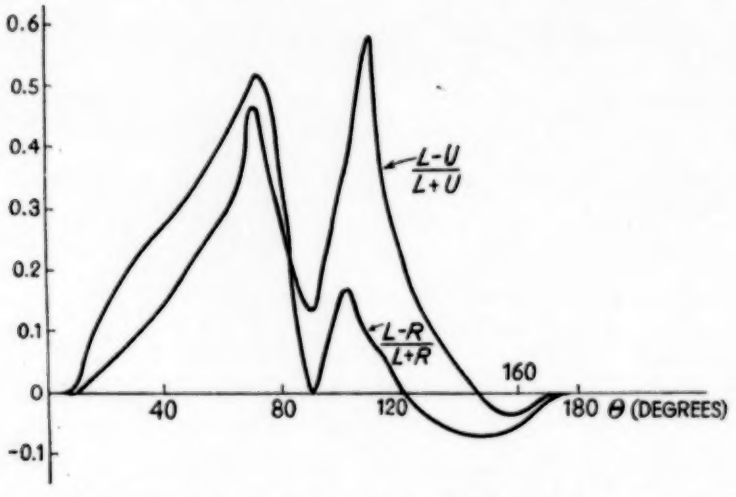

Fig. 3. Left-right asymmetry $(L-R)/(L+R)$ and left-up asymmetry $(L-U)/(L+U)$ corresponding to a double scattering process each occurring at the deuteron resonance energy.

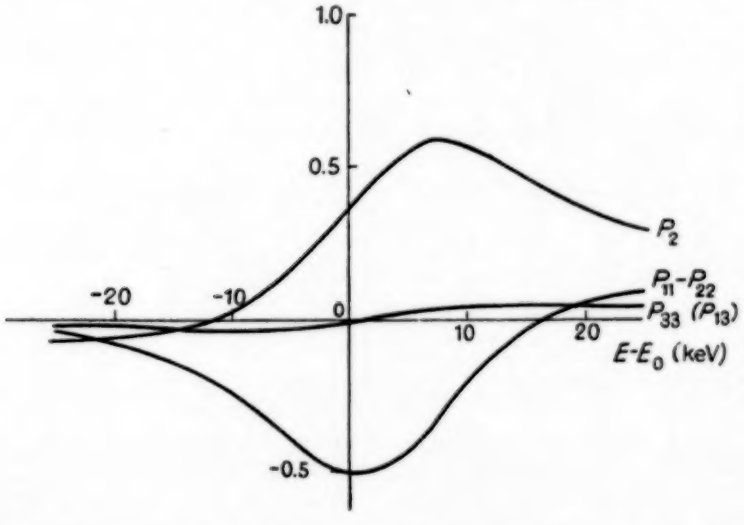

Fig. 4. Variation with incident deuteron energy of the components of polarization of the deuteron divided by their maximum magnitude in any state of polarization. E and the resonance energy E_0 are with reference to the centre-of-mass system. The quantity corresponding to P_{13} is not drawn, but it essentially coincides with P_{33}.

where $|E-E_0| < \Gamma$. The only significant parameters are P_2 and $P_{11}-P_{22}$. The vector polarization is relatively small for energies less than E_0, but rises to large values ($\approx 0.5-0.6$) for energies greater than E_0. The tensor polari-

zation, $P_{11}-P_{22}$, on the other hand, falls off sharply on either side of the resonance energy.

Finally, the asymmetries corresponding to $\theta_1 = \theta_2 = \theta = 105°$ are plotted in Fig. 5 as functions of the centre-of-mass energy of the deuterons and according to two possibilities. In one case, equal energies are assumed for each process and these energies can vary in the interval $(E_0-\Gamma, E_0+\Gamma)$, while in the second case, the first energy is assumed to be E_0, and the second varies in the same energy interval. The left-up asymmetry is essentially the same for both cases, while the left-right asymmetry is enhanced in the second case for energies greater than E_0.

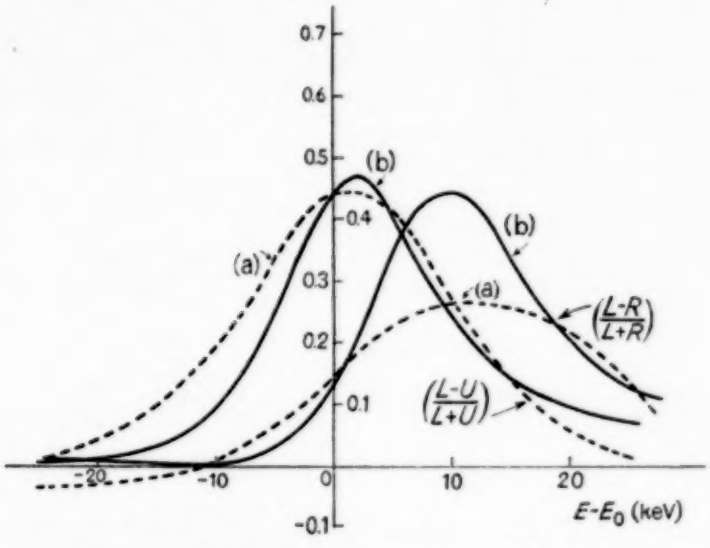

Fig. 5. Variation with incident deuteron energy of the left-right asymmetry and the left-up asymmetry corresponding to a double-scattering process for two cases: (a) equal deuteron energies for each process, (b) first deuteron energy = E_0, second deuteron energy = E.

Summarizing these results, the effect of Coulomb and potential scattering in the resonance scattering of deuterons by He^4 at $E_d = 1.069$ MeV is to modify seriously the polarization predictions given in ref. [1]). There is a tendency for the polarization to decrease, particularly for small scattering angles; although the vector polarization, which is solely attributed to the interference with resonance scattering, attains very large values for energies slightly higher than the resonance energy. The measurement of such a polarization can serve as a sensitive test of the assumptions concerning potential scattering.

Appendix

We require the evaluation of eq. (12). First, we note that since b is not included in the reaction matrix, we can sum over it. This involves

$$\sum_b Z'(l_1 b l_1' b'; S_1 k)\hat{b}\begin{Bmatrix} S_1 l_1 b \\ S_2' l_2' b' \\ k_s k_l k \end{Bmatrix}$$

$$= \sum_b \hat{b}^2 \hat{b}' \hat{l}_1 \hat{l}_1' (l_1 0, l_1' 0|k0) W(l_1 b l_1' b'; S_1 k)(-)^{S_1+l_1+b+S_2'+l_2'+b'+k_s+k_l+k} \begin{Bmatrix} S_1 l_1 b \\ k_s k_l k \\ S_2' l_2' b' \end{Bmatrix}$$

$$= \hat{b}' \hat{l}_1 \hat{l}_1' (l_1 0, l_1' 0|k0) \sum_b \hat{b}^2 (-)^{2S_1+l_1-l_1'+S_2'+l_2'+b'+k_s+k_l} W(S_1 l_1 b' k; b l_1') \sum_x \hat{x}^2 W(S_1 l_1 b' k; bx)$$

$$\times W(k_s k l_2' l_1; k_l x) W(S_1 k_s b' l_2'; S_2' x)$$

which by the orthogonality properties of the Racah coefficient reduces to

$$\hat{b}' \hat{l}_1 \hat{l}_1' (l_1 0, l_1' 0|k0) W(l_1 l_2' k k_s; k_l l_1') W(S_1 l_1' S_2' l_2'; b' k_s).$$

Hence

$$W_{\substack{\text{Coul} \\ \text{res}}}(\Omega_1 \Omega_2) = \frac{\hat{\lambda}^2}{2\hat{a}^2 \hat{s}^2} \sum (-)^{a-s+k_s+l_2'-b'+S_1-S_2'} \frac{\hat{s}\varepsilon^*_{k_s \kappa}(s)}{\varepsilon_{00}(s)} (k_s \kappa, k_l 0|k\kappa) \mathscr{D}^k_{\kappa 0}(\mathscr{R})$$

$$\hat{k}_s \hat{k}_l \hat{S}_1 \hat{S}_2' \hat{l}_1^2 \hat{l}_2' \hat{b}'^2 \hat{l}_1' (l_1 0, l_2' 0|k_l 0)(l_1 0, l_1' 0|k0) W(l_1 l_2' k k_s; k_l l_1') W(S_1 l_1' S_2' l_2'; b' k_s)$$

$$W(ss S_1 S_2'; k_s a) \begin{cases} \operatorname{Re}[R_{\substack{\text{Coul} \\ \text{pot}}}(l_1) \langle S_2' l_2' b' | R_{\text{res}} | S_1 l_1' b' \rangle^*] \ldots \text{even } k_s \\ i \operatorname{Im}[R_{\substack{\text{Coul} \\ \text{pot}}}(l_1) \langle S_2' l_2' b' | R_{\text{res}} | S_1 l_1' b' \rangle^*] \ldots \text{odd } k_s, \end{cases}$$

The summation is as in (12). We now consider the Coulomb interference term. We first expand $(l_1 0, l_1' 0|k0) W(l_1 l_2' k k_s; k_l l_1')$ as follows:

$$(l_1 0, l_1' 0|k0) W(l_1 l_2' k k_s; k_l l_1') = \frac{1}{l_1' \hat{k}_l} \sum_\Lambda (l_1 0, l_2' -\Lambda|k_l -\Lambda)(k_l -\Lambda, k_s \Lambda|k0)(l_2' -\Lambda, k_s \Lambda|l_1' 0).$$

Then, the summation over k is easily carried out for

$$\sum_k (k_s \kappa, k_l 0|k\kappa)(k_s -\Lambda, k_l \Lambda|k0) \mathscr{D}^k_{\kappa 0} = \mathscr{D}^{k_s}_{\kappa -\Lambda} \mathscr{D}^{k_l}_{0\Lambda}.$$

We may further sum over k_l since

$$\sum_{k_l} (l_1 0, l_2' 0|k_l 0)(l_1 0, l_2' \Lambda|k_l \Lambda) \mathscr{D}^{k_l}_{0\Lambda} = \mathscr{D}^{l_2'}_{0\Lambda} P_{l_1}(\cos\theta).$$

Expression (9) allows us to sum over l_1 since

$$\sum_{l_1} \hat{l}_1^2 R_c(l_1) P_{l_1}(\cos\theta) = R_c(\theta).$$

Assembling the various remaining terms we have

$$W_{\text{Coul; res}}(\Omega_1 \Omega_2) = \frac{\hat{\lambda}^2}{2\hat{a}^2 \hat{s}^2} \sum_{k_s \neq 0} (-)^{a-s+k_s+l_2'-b'+S_1-S_2'} \frac{\hat{s}\varepsilon^*_{\kappa_s \kappa}(s)}{\varepsilon_{00}(s)} \hat{b}'^2 \hat{k}_s \hat{S}_1 \hat{S}_2' \hat{l}_2' W(S_1 l_1' S_2' l_2'; b' k_s)$$

$$W(ss S_1 S_2'; k_s a) \mathscr{D}^{k_s}_{\kappa_s -\Lambda} \mathscr{D}^{l_2'}_{0\Lambda}(l_2' -\Lambda, k_s \Lambda|l_1' 0) \begin{cases} \operatorname{Re}[R_c(\theta) \langle S_2' l_2' b' | R_{\text{res}} | S_1 l_1' b' \rangle^*] \ldots \text{even } k_s \\ i \operatorname{Im}[R_c(\theta) \langle S_2' l_2' b' | R_{\text{res}} | S_1 l_1' b' \rangle^*] \ldots \text{odd } k_s. \end{cases}$$

Finally we sum over Λ making use of the fact that

$$\sum_{\Lambda} (l_2'-\Lambda, k_s\Lambda|l_1'0)\mathscr{D}^{k_s}_{\kappa-\Lambda}\mathscr{D}^{l_2'}_{0\Lambda} = (-)^{l_2'-l_1'-k_s}(l_2'0, k_s\kappa|l_1'\kappa)\mathscr{D}^{l_1'}_{\kappa 0},$$

so that our final expression for $W_{\text{Coul; res}}$ is

$$W_{\text{Coul; res}}(\Omega_1\Omega_2) = \frac{\lambda^2}{2\hat{a}^2\hat{s}^2}\sum_{k_s\neq 0}(-)^{a-s+S_1-S_2'-l_1'-b'}\frac{\hat{s}\varepsilon^*_{k_s\kappa}(s)}{\varepsilon_{00}(s)}(l_2'0, k_s\kappa|l_1'\kappa)\mathscr{D}^{l_1'}_{\kappa 0}(\mathscr{R})$$

$$\hat{b}'^2\hat{k}_s\hat{S}_1\hat{S}_2'\hat{l}_2'W(ssS_1S_2'; k_sa)W(S_1l_1S_2'l_2'; b'k_s)$$

$$\begin{cases} \operatorname{Re}[R_c(\theta)\langle S_2'l_2b'|R_{\text{res}}|S_1l_1'b'\rangle^*] \ldots \text{even } k_s \\ i\operatorname{Im}[R_c(\theta)\langle S_2'l_2'b'|R_{\text{res}}|S_1l_1'b'\rangle^*] \ldots \text{odd } k_s. \end{cases}$$

References

1) L. J. B. Goldfarb, Nuclear Physics **7** (1958) 622
2) T. Lauritsen, T. Huus and S. G. Nilsson, Phys. Rev. **92** (1953) 1501
3) J. M. Blatt and L. C. Biedenharn, Revs. Mod. Phys. **24** (1952) 258
4) A. Simon, Phys. Rev. **92** (1953) 1050;
S. Devons and L. J. B. Goldfarb, Angular Correlations, Handbuch der Physik Vol. **42** (Springer, 1957)
5) L. I. Schiff, Quantum Mechanics (McGraw-Hill, 1949) p. 118
6) A. Galonsky and M. T. McEllistrem, Phys. Rev. **98** (1955) 590;
A. Galonsky, R. A. Douglas, W. Haeberli, M. T. McEllistrem and K. T. Richards, Phys. Rev. **98** (1955) 586

1.E.1:
3.A

Nuclear Physics **12** (1959) 510—520; © *North-Holland Publishing Co., Amsterdam*
Not to be reproduced by photoprint or microfilm without written permission from the publisher

THE SPIN ASSIGNMENTS OF THE 9.16-MeV and 6.44-MeV STATES IN N^{14}

H. J. ROSE, W. TROST and F. RIESS

Institute of Physics, Freiburg University, Freiburg, Germany †

Received 13 May 1959

Abstract: A study has been made of the gamma-ray cascade emitted by the 9.16-MeV state to the 6.44-MeV state and from this to the ground state of N^{14}, using the reaction $C^{13}(p,\gamma)N^{14}$ at the 1.75 MeV resonance. By means of angular correlation and distribution measurements, using different geometrical arrangements relative to the beam, the 9.16-MeV state was assigned $J = 2$ and the 6.44-MeV state $J = 3$.

1. Introduction

The reported decay modes [1]) of the 9.16-MeV state in N^{14} lead to the $J^\pi = 1^+$ ground state and the $T = 0$, 6.44-MeV excited state. From the measured anisotropies of these transitions [1]) a spin assignment cannot be made with certainty. For the anisotropy of the 9.16 MeV → ground-state transition given by Woodbury, Day and Tollestrup as $A = -(0.48 \pm 0.03)$, agreement is possible with the assignments of $J^\pi = 1^+$, 2^+ and 2^- if one considers various mixtures of channel spins or p—f waves in the formation of the 9.16-MeV state by proton capture, and interference of different multipole orders in the gamma transition to the ground state. The gamma width of the 9.16 MeV → ground-state transition is $(2I+1)\Gamma_\gamma = 29$ eV [2]). A comparison of M1 transitions in light, self-conjugate nuclei [3]) shows that the intensity of the 10 % branch to the $T = 0$, 6.44-MeV state determines the isobaric spin of the 9.16-MeV state as $T = 1$. The strength of the 9.16 MeV → ground-state transition confirms this assignment; however, as has been previously suggested [3]), no preference for E1 radiation — as opposed to M1 — should be made from this transition strength. In fact, Elliott [4]) †† has calculated that a gamma width of 25 eV for the 9.16 MeV → ground state transition is predicted from theory if the 9.16-MeV level is 2^+, resulting from the p^{-2} configuration with a $^{31}D_2$ eigenfunction. Such a level would be expected around 10-MeV excitation energy in N^{14} from the

† This work was supported in part by the German Ministerium für Atomkernenergie.

†† Besides J. P. Elliott, the authors would like to thank E. K. Warburton and W. T. Pinkston for communicating their results on the M1 and E2 transition strenghs connecting the six lowest levels resulting from the p^{-2} configuration.

theoretical results of Elliott [5]), which explain the long lifetime of the C^{14} beta decay. An experimental location of this $^{31}D_2$ state and its corresponding $T = 0$ partner $^{13}D_2$ (which should be expected around 6-MeV excitation energy in N^{14}) would be highly desirable since their excitation energies would give direct information on the strength of the tensor force in the interaction of the two p-holes in the p^{-2} configuration of N^{14}.

Recently Strassenburg, Hubert, Krone and Prosser [6]) obtained a definite even parity assignment for the 9.16-MeV state, thus requiring as assignment for this state 1^+ or 2^+. Therefore, a decision between these two possible values would be the next step in considering wether or not the 9.16-MeV level could be the expected $^{31}D_2$ state. In the present paper it is not intended to follow up this question in further detail. More detailed investigations of the 9.16-MeV resonance level have been made by one of the present authors and will be discussed in a forthcoming paper [7]). The results of these investigations — using three-crystal pair spectrometer and coincidence techniques — shall be mentioned here only as far as being in connection with the spin assignment to the 9.16-MeV state. Besides the known transitions to the ground state and the 6.44-MeV state, there are several other transitions involved in the decay of the 9.16-MeV state; among them is one leading to the 5.83-MeV excited state. This level recently was assigned $J = 3$ with a preference for an odd parity assignment [8]). However, the decay mode of the 9.16-MeV state to the 5.83-MeV excited state has only an intensity of a few percent of the intensity of the transition to the ground state. Since deductions from experimental intensities of lower energy gamma rays in the presence of a high energy ground-state transition are inaccurate if their yields are only a few percent of the ground-state transition, the experimental values of the matrix elements for the lower energy transitions must be relatively inaccurate. The lower limit on the intensity given in ref. [7]) for the 9.16 → 5.83 MeV transition is 1 % and the upper limit 5 % of the intensity of the ground-state transition. From this and the known gamma width of the ground-state transition, one obtains as lower limits for the E2 and M2 matrix elements of the transition — if the 9.16-MeV state were $J = 1$ — the values 60 and 500, respectively. Therefore, an assignment of $J^\pi = 1^+$ to the 9.16-MeV level seems most unlikely, since at such high values for the quadrupole matrix elements the transition should be expected to be at least partially dipole. This is especially true since the quadrupole transition would be more likely M2 than E2 in as much as the 5.83-MeV state is more likely 3^- than 3^+ (ref. [8]).

The value for the anisotropy of the 2.72-MeV gamma ray (resulting from the decay of the 9.16-MeV state to the 6.44-MeV level) was given by Woodbury *et al.* as $A = -(0.05 \pm 0.10)$. This value was confirmed by three-crystal pair-spectra measurements and will be discussed in greater detail in

ref. [7]). Since the transition from the 9.16-MeV to the 6.44-MeV state must be dipole with negligible quadrupole admixture (the matrix elements for E2 and M2 are larger than 10^3, as can be easily calculated using results of refs.[1]) and [2]), this measurement of the anisotropy conclusively shows that both the 9.16-MeV state and the 6.44-MeV state cannot have spin 2. In this case the resulting anisotropy of the 2.72-MeV gamma ray should be 0.64, assuming p-wave formation for the 9.16-MeV state. An *f*-wave admixture corresponding to a relative intensity ratio $|M(\mathrm{f})|^2/|M(\mathrm{p})|^2 = 0.67$ and $M(\mathrm{f})/M(\mathrm{p}) = = -0.82$ yields $A = 0.32$ as the lowest theoretical value possible for the anisotropy of the 2.72-MeV gamma ray, which is by no means comparable with the measured value $A = -(0.05 \pm 0.10)$. Now, by comparison of the 2.72-MeV gamma-ray intensity with the 6.44-MeV gamma-ray intensity, there was found a disagreement by a factor two in the three-crystal pair-spectra measurements of ref. [7]); the 2.72-MeV gamma ray is about twice as strong as needed for the population of the 6.44-MeV excited state if this state decays to the ground state only. This suggests that the 6.44-MeV level branches to some other state. The 2.79-MeV gamma ray resulting from the decay mode 9.16 → 5.83 → 5.10 → 2.31 MeV → ground state cannot account for the strong intensity of the 2.72-MeV gamma ray seen in the three-crystal pair-spectra measurements. Taking the upper limit of 5 % (of the intensity of the 9.16 MeV → ground state transition) for the intensity of the branch to the 5.83-MeV state and considering the branching ratio of the 5.10 MeV → ground state and the 5.10 → 2.31 MeV transitions [8]), only about 20 % of the 2.72-MeV gamma-ray intensity could be due to a contamination by 2.79-MeV gamma rays. From several coincidence runs (which will also be described in ref. [7])) there is indication, from the observation of 1.64 and 2.49 MeV gamma rays, that the 6.44-MeV state branches to the 3.95-MeV excited state. This again indicates that the 6.44-MeV state would have to be given a favoured assignment of $J = 2$, which, combined with the impossibility of the 9.16-MeV and the 6.44-MeV levels having the same spin, disagrees with an assignment of $J^\pi = 2^+$ to the 9.16-MeV excited state.

Of course, this argument is based on the fact that a factor E_γ^5 occurs in the transition probability for quadrupole radiation. This factor would suppress the transition to the 3.95-MeV excited state compared with the transition to the ground state. However, the eigenfunctions of the ground state and the 3.95-MeV excited state are different (the eigenfunction of the 3.95-MeV state contains about 96 % $^{13}S_1$ while the ground-state eigenfunction has only about 0.6 % $^{13}S_1$, if one calculates the roots from Elliott's energy matrices of ref. [5]) fitting the first two excited states of N^{14} and the cancellation of the beta decay matrix element of C^{14}). This difference possibly could give an explanation for the occurrence of a branch to the 3.95-MeV excited state from the 6.44-MeV level if the 6.44-MeV level were found to have

$J = 3$. In view of these considerations it was felt worthwhile to find spin assignments for the 9.16-MeV and the 6.44-MeV excited states in N^{14} which are independent of arguments based on the decay modes of these levels.

2. Experimental Methods and Results

In order to obtain a spin assignment for the 9.16-MeV state which would be independent of the decay modes of this level, angular correlation and angular distribution measurements have been made of the gamma rays from the 9.16 → 6.44 MeV → ground-state cascade and of the 2.72-MeV and 6.44-MeV gamma rays produced in the reaction $C^{13}(p, \gamma)N^{14}$. The proton bombarding energy was $E_p = 1.75$ MeV, corresponding to the excited state at 9.16 MeV in N^{14}. The protons were accelerated in the Freiburg University 6-MeV research Van de Graaff. The target used was approximately 10 keV thick and consisted of 70 % enriched C^{13} deposited on a 0.005-in. platinum foil. It was proved that the 6.44-MeV (and hence the 2.72-MeV gamma ray) is resonant and that off-resonance contributions are less than 2 percent with the target used. In another way it has been proved that the 9.16-MeV level can be treated as a well isolated level. This was by making accurate angular distribution measurements at slightly different energies. These measurements showed symmetry with respect to the plane perpendicular to the beam. [9])

Three different sets of correlation measurements have been made for the present work. First a 3 by 3 in. NaI(Tl) crystal was placed at 0° to the beam at a distance of 5.5 cm from the target. This detector was used as a gate to detect gamma rays between 5.30 MeV and 6.65 MeV. The coincidence setup and the method of setting the gate window at a definite energy was essentially the same as described in a previous paper [10]). A 2 by 2 in. NaI(Tl) crystal was used to detect the 2.72-MeV gamma radiation in coincidence with the gate signals and this spectrum was displayed on an RIDL Model 3300 100-channel pulse-height analyzer. To obtain the anisotropy of the 2.72-MeV gamma rays with respect to the beam, i.e. the ratio of the counting rates at 0° and 90° to the beam minus one, the 2 by 2 in. crystal was mounted to rotate around the target at a distance of 5 cm and irradiated at 90°, 150° and 90° to the beam. If we denote by $(\theta_1\phi_1)$, $(\theta_2\phi_2)$, and $(\theta_{12}\phi_{12})$ the polar angles of the beam, the second (6.44-MeV) gamma rays, and the first (2.72-MeV) gamma rays, the notation of this distribution would be $W(00; 00; \theta 0)$.

In a second set of measurements the gate crystal detecting the 6.44-MeV gamma rays was placed at 90° to the beam and the 2 by 2 in. crystal was irradiated at 0°, 90°, and 0° to the beam in the plane containing the beam and the gate crystal. The notation of this distribution is $W(00; \frac{1}{2}\pi 0; \theta\pi)$.

A third set of measurements was carried out in the plane perpendicular to the beam for which the gate crystal was kept as for the second set of measurements; however, the 2 by 2 in. crystal could be rotated in the plane perpendicular to the beam, and was irradiated at $\phi = \pi$, $\phi = \frac{1}{2}\pi$, and $\phi = \pi$. The notation of this distribution is $W(00; \frac{1}{2}\pi 0; \frac{1}{2}\pi\phi)$.

All the correlation measurements were done with a beam of approximately 8 μA using the window counts of the fixed gate crystal in each set for monitoring. The results of the different measurements are given in table 1 together with the results for the anisotropies of the distributions of

TABLE 1

Experimental anisotropies of the 2.72-MeV and 6.44-MeV gamma-ray distributions

Gamma ray (MeV)	Specification	Notation	Anisotropy
2.72	distribution relative to beam, uncorrelated	$W(00; \theta_{12})$	$\frac{W(00;0)}{W(00;\frac{1}{2}\pi)} - 1 = -(0.02 \pm 0.15)$
	correlated to 6.44, gate at 0° to beam	$W(00; 00; \theta 0)$	$\frac{W(00;00;\pi 0)}{W(00;00;\frac{1}{2}\pi 0)} - 1 = -(0.09 \pm 0.12)$
	correlated to 6.44 MeV, gate at 90° to beam, 2.72 MeV observed in plane containing the beam	$W(00; \frac{1}{2}\pi 0; \theta\pi)$	$\frac{W(00;\frac{1}{2}\pi 0;0\pi)}{W(00;\frac{1}{2}\pi 0;\frac{1}{2}\pi\pi)} - 1 = +(0.36 \pm 0.20)$
	correlated to 6.44 MeV, gate at 90° to beam, 2.72 MeV observed in plane perpendicular to the beam	$W(00; \frac{1}{2}\pi 0; \frac{1}{2}\pi\phi)$	$\frac{W(00;\frac{1}{2}\pi 0;\frac{1}{2}\pi\pi)}{W(00;\frac{1}{2}\pi 0;\frac{1}{2}\pi\frac{1}{2}\pi)} - 1 = -(0.35 \pm 0.12)$
6.44	distribution relative to beam, uncorrelated	$W(00; \theta_2)$	$\frac{W(00;0)}{W(00;\frac{1}{2}\pi)} - 1 = +(0.61 \pm 0.32)$

the 2.72-MeV and the 6.44-MeV gamma rays, the latter ones having been obtained from the three-crystal pair-spectra measurements taken at 0° and 90° to the beam [7]) and normalized by singles measurements of the anisotropy of the 9.16 MeV → ground-state transition [9]). All values have been corrected for finite solid angle (except those obtained by pair spectra measurements, where this correction was found negligible in view of the errors). The errors given are mostly due to maximum errors in background subtraction and partially due to statistics. Since the target-holder used was constructed to be symmetrical around the axis of rotation and since the target backing was put at 45° to the beam, absorption corrections could be eliminated in most of the measurements. However, they were taken into account where necessary, but in no case required more than a few percent correction to the counting rates.

3. Comparison with Theoretical Results for the Anisotropies

It was shown in the introduction that the 9.16-MeV state and the 6.44-MeV state cannot both have $J = 2$. Since it was found that the $T = 1$, 8.90-MeV $J^\pi = 3^-$ state branches to the 6.44-MeV excited state, the latter state must have $J \geqq 2$ (ref. [8])). The possible assignments of the 9.16-MeV level are $J^\pi = 1^+$ or 2^+, and since the transition 9.16 → 6.44 MeV must be predominantly dipole (cf. ref. [3]) and sec. 1), the possible spin assignments to the states involved in the cascade 9.16 → 6.44 MeV → ground state are 1—2—1 or 2—3—1.

For the case 1—2—1 the 9.16-MeV excited state could be formed by p-wave protons only with channel spins $s = 0$ and $s = 1$. The 6.44 MeV → ground-state transition could be any mixture in $L_2 = 1$ or 2, since no lifetime measurement was made on the 6.44-MeV excited state. The theoretical distributions for the 2.72-MeV gamma ray resulting from p-wave formation of the 9.16-MeV excited state are given in table 2 for different channel spin mixtures and in dependence on $\delta = M(L_2 = 2)/M(L_2 = 1)$, the relative matrix element for the dipole-quadrupole mixture in the final (6.44-MeV) transition. The phase conventions on δ are those used by Sharpe, Kennedy, Sears and Hoyle in their tables of coefficients for angular distribution analysis [11]). The sign of δ as it occurs in table 2 is correct for M1—E2 mixture, the opposite sign should be used for E1—M2 mixture in the 6.44 MeV → ground state transition.

The numerical evaluations of the anisotropies obtained from the formulae

TABLE 2

The theoretical distributions for the first (γ_{12}) and second (γ_2) gamma rays in a gamma ray cascade from a $j_1 = 1$ state formed by p-wave protons on C^{13} and decaying by γ_{12} to a $j_2 = 2$ state and from this by γ_2 to a $I_2 = 1$ state; γ_{12} pure dipole, γ_2 mixture of dipole and quadrupole radiation †.

$W(00;\theta_{12}) = \lvert A(0)\rvert^2(1-0.100\,P_2)+\lvert A(1)\rvert^2(1+0.050\,P_2)$
$W00;\,00;\theta 0) = \lvert A(0)\rvert^2[(0.650+0.025\,P_2)+2\delta(-0.782+0.279\,P_2)+\delta^2(1.250-0.875\,P_2)]$ $+\lvert A(1)\rvert^2[(1.175+0.250\,P_2)+2\delta(0.391+0.447\,P_2)+\delta^2(0.875+0.250\,P_2)]$
$W(00;\tfrac{1}{2}\pi 0;\theta\phi) = \lvert A(0)\rvert^2[(1.175-0.162\,P_2+0.055\,P_2^2\cos 2\phi)$ $+2\delta(0.391-0.139\,P_2+0.125\,P_2^2\cos 2\phi)+\delta^2(0.875-0.312\,P_2+0.032\,P_2^2\cos 2\phi)]$ $+\lvert A(1)\rvert^2[(0.913-0.050P_2+0.037\,P_2^2\cos 2\phi)$ $+2\delta(-0.195-0.233\,P_2+0.083\,P_2^2\cos 2\phi)+\delta^2(1.062+0.250\,P_2-0.062\,P_2^2\cos 2\phi)]$
$W(00;\theta_2) = \lvert A(0)\rvert^2[(1-0.350\,P_2)-\delta 1.565\,P_2+\delta^2(1+0.250\,P_2)]$ $+\lvert A(1)\rvert^2[(1+0.175\,P_2)+\delta 0.782\,P_2+\delta^2(1-0.125\,P_2)]$

† $P_1^m(\cos\theta)$ denotes the usual Legendre function of the first kind. $\lvert A(0)\rvert^2$ and $\lvert A(1)\rvert^2$ represent the contributions from different channel spins and δ is the ratio of the matrix elements of different multipole orders in γ_2 (about the sign and the phase conventions on δ see sec. 3).

in table 2 are given in the figs. 1—4. These figures show the dependence of the anisotropy on the channel spin mixture $x = |A(0)|^2/[|A(0)|^2+|A(1)|^2]$ and on the multipole mixture δ for each of the distributions (with the exception of the 2.72-MeV gamma ray distribution if it is uncorrelated with the 6.44-MeV transition; in this case the anisotropy depends on x only). Furthermore, the experimental results on the anisotropies, given in table 1, have been included in figs. 1—4. The anisotropy of the uncorrelated distribution of the 2.72-MeV gamma ray is within the experimental errors in agreement for all

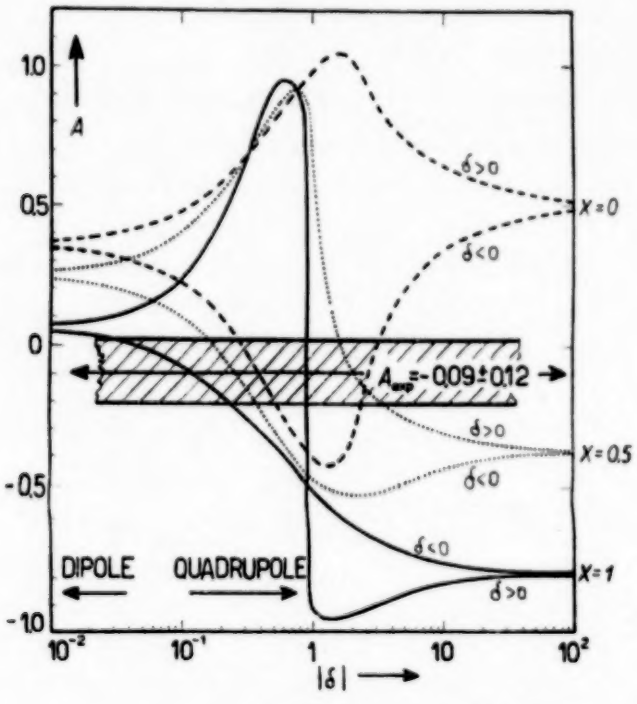

Fig. 1. The anisotropy of the distribution $W(00; 00; \theta 0)$ of the 9.16 → 6.44 MeV transition correlated to the 6.44 MeV → ground state transition following the formation of the N^{14} 9.16-MeV level by p-wave protons and assuming a spin sequence 1—2—1 for the transition 9.16 → 6.44 MeV → ground state. The 6.44 MeV → ground state transition is assumed to be a mixture of dipole and quadrupole radiation with an intensity ratio δ^2. The figure shows as a function of $|\delta|$ the anisotropy A of the angular distribution of the first gamma transition (9.16 → 6.44 MeV) relative to the proton beam if the second transition (6.44 MeV → ground state) is observed in the direction of the proton beam. Each pair of curves corresponds to a certain value of the channel spin mixture $x = |A(0)|^2/[|A(0)|^2+|A(1)|^2]$ and each curve of a pair to a definite sign of δ. The curves were calculated from the formula for $W(00; 00; \theta 0)$ given in table 2. The measured value for the anisotropy given in table 1 has been included in the figure. A certain region of $x-\delta$ values can be obtained from the figure which contains $x-\delta$ values consistent with the measured value for A within the experimental errors.

possible channel-spin mixtures with the measured value. Therefore, no information can be gained from this measurement for the case 1—2—1; however, the experimental value for this anisotropy was useful in excluding the possibility 2—2—1.

It is seen from the figures that for each single measurement agreement

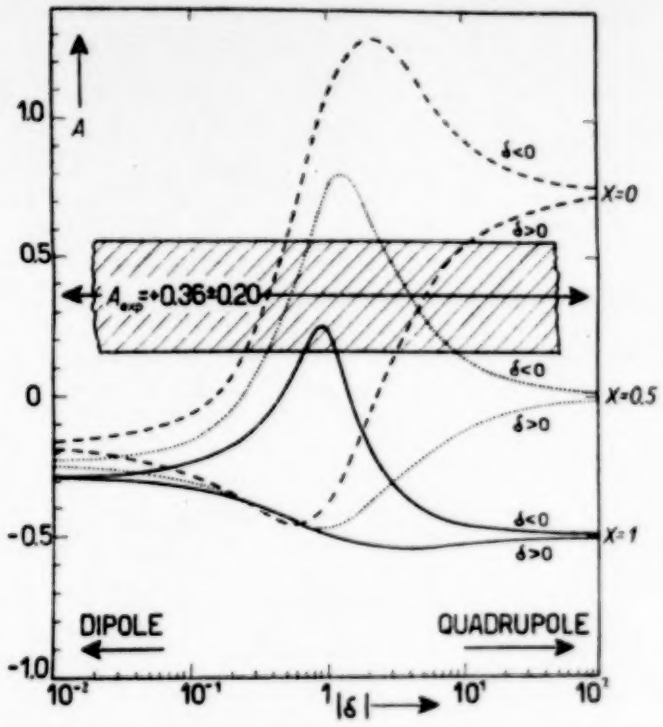

Fig. 2. The anisotropy of the distribution $W(00; \frac{1}{2}\pi 0; \theta\pi)$ of the 9.16 → 6.44 MeV transition correlated to the 6.44 MeV→ground state transition following the formation of the N^{14} 9.16-MeV level by p-wave protons and assuming a spin sequence 1—2—1 for the transition 9.16 → 6.44 MeV → ground state. Explanation as for fig. 1.

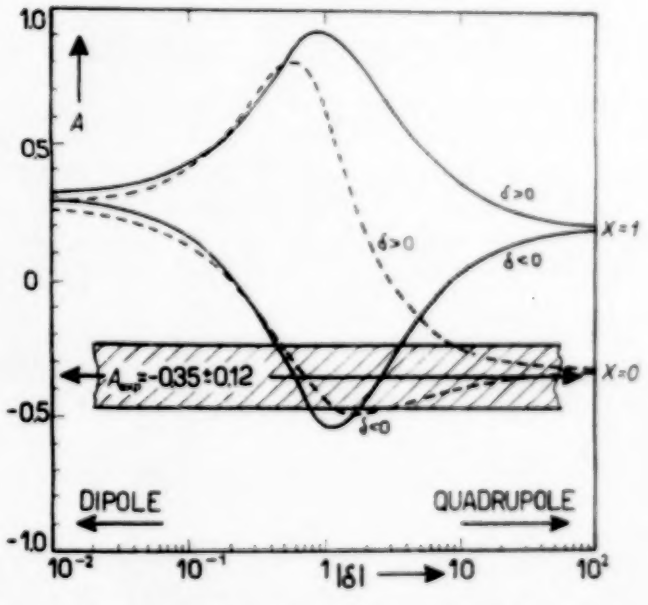

Fig. 3. The anisotropy of the distribution $W(00; \frac{1}{2}\pi; \frac{1}{2}\pi\phi)$ of the 9.16 → 6.44 MeV transition correlated to the 6.44 MeV→ground state transition following the formation of the N^{14} 9.16-MeV level by p-wave protons and assuming a spin sequence 1—2—1 for the transition 9.16 → 6.44 MeV → ground state. Explanation as for fig. 1.

can be obtained between the theoretically predicted and the experimentally determined anisotropy with an appropriate choice of x and δ. From each of the figs. 1—4 a certain region of x and δ values is determined for which the experiment agrees within the errors with the theoretically predicted anisotropy. These $x-\delta$ regions have been plotted in fig. 5 and it is seen from

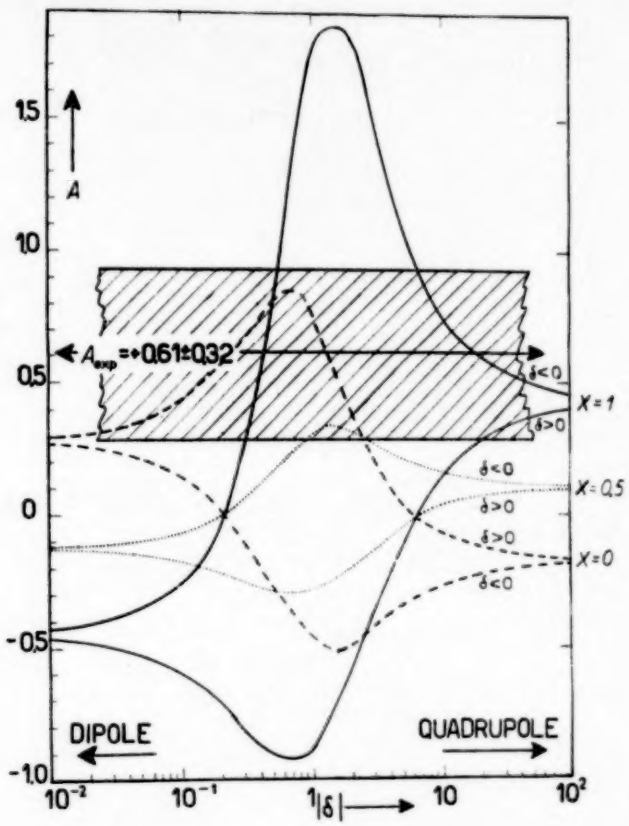

Fig. 4. The anisotropy of the distribution $W(00; \theta_2)$ of the 6.44 MeV → ground state transition after the formation of the N^{14} 9.16-MeV level by p-wave protons and assuming a spin sequence 1—2—1 for the transition 9.16 → 6.44 MeV → ground state. Explanation as for fig. 1.

this figure that in no point of the $x-\delta$ plane do all four $x-\delta$ regions overlap. This in turn means that there is no pair of (x, δ) values which would agree with all measurements. Therefore the case 1—2—1 is excluded. The only remaining possibility for the spin assignment for the 9.16-MeV level is $J = 2$ and for the 6.44-MeV level $J = 3$.

Table 3 gives a comparison of the experimental values for the anisotropies with the calculated ones for the spin sequence 2—3—1. The calculated values are valid for p-wave formation of the 9.16-MeV state and decay of the 6.44-MeV excited state to the ground state by quadrupole radiation. It is seen that all experimental values agree with the calculated values.

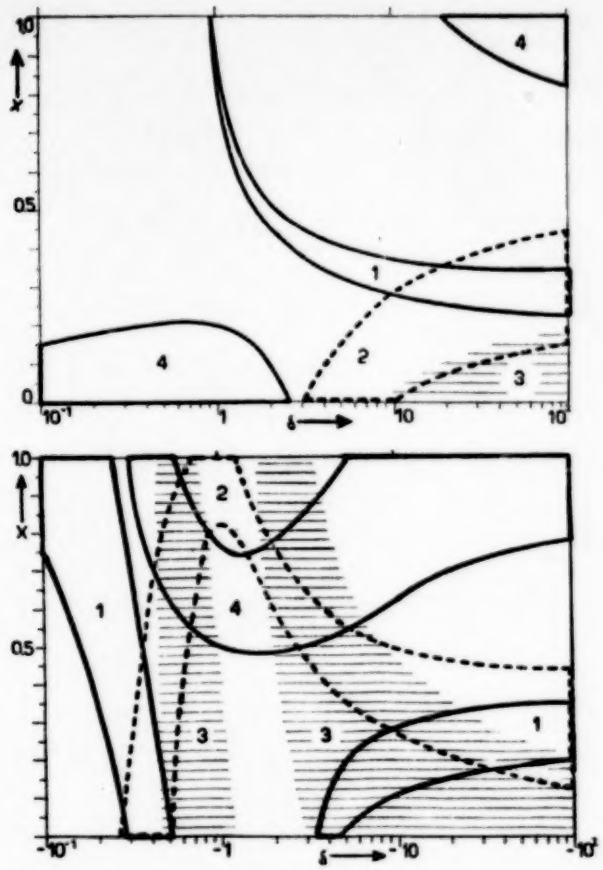

Fig. 5. The limits imposed on the channel spin mixture x and the dipole-quadrupole mixture δ in the 6.44 MeV → ground state transition assuming a spin sequence 1—2—1 in the gamma-ray cascade 9.16 → 6.44 MeV → ground state. The areas 1, 2, 3 and 4 show the values for x and δ consistent with the quoted uncertainties of the measured anisotropies for the distributions shown in the figures 1, 2, 3 and 4 respectively. The two parts of the figure correspond to different signs of δ as indicated on the abscissae.

TABLE 3

Comparison of the experimental and theoretical anisotropies corresponding to a spin sequence of 2—3—1 in the gamma-ray cascade from the 9.16-MeV state formed by p-wave protons on C^{13} and decaying by γ_{12} to the 6.44-MeV state and from here by γ_2 to the ground state; γ_{12} dipole γ_2 quadrupole

Gamma ray (MeV)	Notation	Anisotropy experimental	calculated
2.72	$W(00;\theta_{12})$	$-(0.02\pm0.15)$	-0.14
	$W(00;00;\theta 0)$	$-(0.09\pm0.12)$	-0.05
	$W(00;\frac{1}{2}\pi 0;\theta\pi)$	$+(0.36\pm0.20)$	$+0.43$
	$W(00;\frac{1}{2}\pi 0;\frac{1}{2}\pi\phi)$	$-(0.35\pm0.12)$	-0.42
6.44	$W(00;\theta_2)$	$+(0.61\pm0.32)$	$+0.62$

4. Conclusion

It was shown that the 9.16-MeV excited state in N^{14} must have a total angular momentum $J = 2$. Since the parity of this state is even [6]), the level has an assignment of $J^{\pi} = 2^{+}$. The measurements described in the present paper agree with p-wave formation of the 9.16-MeV state in the reaction $C^{13}(p, \gamma)N^{14}$. Furthermore, it was shown that the 6.44-MeV excited state in N^{14} has a total angular momentum $J = 3$.

The authors like to thank E. N. Hatch for suggestions regarding the manuscript of this paper. It is a pleasure to acknowledge the communications with E. K. Warburton and J. P. Elliott concerning the energy levels of N^{14}.

References

1) Woodbury, Day and Tollestrup, Phys. Rev. **92** (1953) 1199
2) S. S. Hanna and L. Meyer-Schützmeister, Phys. Rev. **108** (1957) 1644
3) E. K. Warburton, Phys. Rev. **113** (1959) 595
4) J. P. Elliott, private communication
5) J. P. Elliott, Phil. Mag. **1** (1956) 503
6) A. A. Strassenburg, R. E. Hubert, R. W. Krone and F. W. Prosser, Bull. Am. Phys. Soc. **3** (1958) 372
7) H. J. Rose, to be published
8) E. K. Warburton, H. J. Rose and E. N. Hatch, Phys. Rev. (1959)
9) H. J. Rose, F. Riess and W. Trost, to be published
10) E. K. Warburton and H. J. Rose, Phys. Rev. **109** (1958) 1199
11) W. T. Sharpe, J. M. Kennedy, B. J. Sears and M. G. Hoyle, CRT-556

8.B *Nuclear Physics* **12** (1959) 521—526; © *North-Holland Publishing Co., Amsterdam*
Not to be reproduced by photoprint or microfilm without written permission from the publisher

K^+-MESON—NUCLEON SCATTERING AND K^+-Y RELATIVE PARITY

L. K. PANDIT and S. N. BISWAS
Tata Institute of Fundamental Research, Bombay

Received 2 April 1959

Abstract: A covariant integral equation in the ladder approximation has been set up for the Feynman amplitude describing the K^+-nucleon scattering through a strong direct K-Y-N interaction. The two possibilities of the relative $K-Y$ parities have been considered, it being assumed that both K^0 and K^+ have identical parity. The equation has been solved by the Fredholm method employing the prescription of McCarthy and Green to obtain a divergence-free solution.

Our calculations favour *even* relative $K-Y$ parity. For best fit with (K^+-p) scattering experiments, the coupling constants required are $G_{NK\Lambda} = \sqrt{3}G_{NK\Sigma}$, $G^2_{NK\Sigma}/4\pi = 0.5$.

1. Introduction

In recent times the moderately strong interactions between the strange particles have become an important field of research. One of the most direct ways of investigating these is to study the scattering of the particles concerned. With this in view, we are interested in the present work in calculating covariantly the K^+-nucleon scattering through a direct K-Y-N interaction. Calculations [1]) using non-relativistic models have been performed by Stapp, Vitale and Amati, and Ceolin and Taffara.

In formulating the interaction [2]), conservation of the total isobaric spin T and the strangeness number S is taken into account, the T and S assignments being according to the Gell-Mann-Nishijima scheme. One also needs, of course, the knowledge of the spins and parities of the particles. Regarding these, one could make assumptions which may then be directly confronted with the experiments. We shall assume that the spins of $Y(\Lambda, \Sigma)$ are $\frac{1}{2}$ and the spin of K is 0. We shall further consider both possibilities of relative K^+-Y parity, it being assumed that Λ and Σ have the same parity relative to the nucleons. If one uses the convention that the parity of the hyperons is the same as that of the nucleons, our parity nomenclature (i.e. relative K^+-Y parity even or odd) refers directly to the parity of the K^+-meson. Our calculation is, of course, quite general, since, as seen below, only the relative parity of $K-Y$ enters the discussion on account of "associated production".

2. Interaction Hamiltonian

In the isobaric spin notation, the interaction between the hyperons, nucleons and K-mesons can be written as

$$H_I = G_{NK\Lambda}\bar{N}\Gamma\Lambda K + G_{NK\Sigma}\bar{N}\Gamma\tau_i\Sigma_i K + \text{h.c.}$$

This form of the interaction assures the conservation of strangeness. For parity invariance we have $\Gamma = 1$ or γ_5 according as (K^+—Y) relative parity is even or odd. The τ_i are the usual operators for isobaric spin $\frac{1}{2}$.

3. Feynman Diagrams

In the Nishijima-Gell-Mann scheme the $K^{+,0}$-meson has isobaric spin $\frac{1}{2}$ with strangeness $+1$ and the nucleon has isobaric spin $\frac{1}{2}$ with strangeness zero. Therefore, there are two isobaric spin states, namely the triplet ($T = 1$) and the singlet ($T = 0$), of the K^+-meson-nucleon system. If a^T denotes the amplitude for the scattering of K^+-mesons by nucleons in the isobaric spin state T, the $K^+ + p \to K^+ + p$ scattering amplitude is a^1; while the $K^+ + n \to$ $\to K^+ + n$ amplitude is $\frac{1}{2}(a^1 + a^0)$ and the charge-exchange $K^+ + n \to K^0 + p$ amplitude is $\frac{1}{2}(a^1 - a^0)$.

The lowest-order Feynman diagram in accordance with the above interaction is drawn in fig. 1. In view of strangeness-conservation, only the

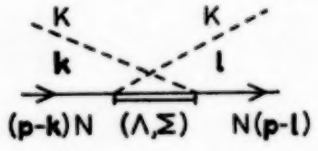

Fig. 1

diagram with crossed K-meson lines can occur. Besides this diagram, we include a whole series of higher order diagrams of the type shown in fig. 2.

Fig. 2

This means that we shall be working in the "ladder-approximation." The ladder approximation scattering amplitude in the total isobaric spin state $T(= 1, 0)$ is given by

$$M_T = C_T \bar{u}_2 \Phi_T(l) u_1 \tag{1}$$

where $\Phi_T(l)$ satisfies the integral equation

$$\Phi_T(l) = F_T(l) + \lambda_T \int K(l, l')\Phi_T(l')\mathrm{d}^4 l'. \tag{2}$$

Here u_2 and u_1 are the Dirac-spinors describing the final and initial nucleon, and we have ($\hbar = c = 1$) †

$$C_T = \frac{i}{(2\pi)^2} G^2 c_T \frac{m}{2\sqrt{E_1 E_2 \omega_1 \omega_2}} \delta^4(p_1 - p_f) \tag{3a}$$

where p_1, p_f denote the initial and final four-momenta of the system, E_1, E_2 being the initial and final energy of the nucleon, ω_1, ω_2 those of the K-meson;

$$\begin{aligned} F(l) &= \Gamma\{\gamma \cdot (p-k-l) - M\}^{-1}\Gamma, \\ K(l,l') &= \Gamma\{\gamma \cdot (p-l'-l) - M\}^{-1}\Gamma\gamma \cdot (p-l') - m\}^{-1}(l'^2-\mu^2)^{-1}, \\ \lambda_T &= -\frac{i}{(2\pi)^4} G^2 c_T. \end{aligned} \tag{3b}$$

Here we have taken

$$G_{NK\Lambda} = \alpha G_{NK\Sigma} = \alpha G,$$

in which case

$$c_T = \begin{cases} 1+\alpha^2 & \text{for } T = 1, \\ 3-\alpha^2 & \text{for } T = 0. \end{cases}$$

As stated earlier we shall put $\Gamma = 1$ or γ_5 according as the K⁺—Y relative parity is even or odd. M is the mass of Λ, Σ (neglecting their mass difference), m the nucleon mass and μ the K-meson mass.

The integral equation (2) is of the Fredholm type and hence the solution may be obtained by means of the Fredholm's resolvent kernel. A modification of this solution, developed by Green and McCarthy [3]), will be used here.

4. Fredholm Solution

Writing equation (2) in the operator form

$$\Phi = F + \lambda K \Phi$$

the Fredholm solution is

$$\Phi = \frac{F + \lambda(K - \operatorname{tr} K)F + \dots}{1 - \lambda \operatorname{tr} K + \frac{1}{2}\lambda^2\{(\operatorname{tr} K)^2 - \operatorname{tr} K^2\} \dots}, \tag{4}$$

where

$$\begin{aligned} \operatorname{tr} K &= \int K_{rr}(t,t)\mathrm{d}^4 t, \\ \operatorname{tr} K^2 &= \int\int K_{rs}(t,l)K_{sr}(l,t)\mathrm{d}^4 l \mathrm{d}^4 t, \\ KF &= \int K_{rs}(l,t)F_s(t)\mathrm{d}^4 t. \end{aligned} \tag{5}$$

Actually, tr K diverges logarithmically. This divergence is eliminated here by using the prescription of McCarthy and Green [3]), which results in the

† The notations used here for Dirac operators, the space-time metric etc. are the same as used in Schweber, Bethe and de Hoffmann, Mesons and Fields, Vol. 1 (New York, 1955).

replacement of tr K, tr K^2 etc. by tr' K, tr' K^2, where tr' K, for example, is obtained by substracting from tr K the value it assumes when $p = 0$ (p = = resultant 4-vector energy-momentum).

The solution of (2), in the first Fredholm approximation, is then given by

$$\Phi = F/(1-\lambda u'_1)$$

where

$$u'_1 = \mathrm{tr}'\, K,$$

$$u_1 = \mathrm{tr}\, K = \int \mathrm{tr}[\Gamma\{\gamma \cdot (p-2l')-M\}^{-1}\Gamma\{\gamma \cdot (p-l')-m\}^{-1}](l'^2-\mu^2)^{-1}\mathrm{d}^4 l'.$$

5. Cross Sections

Using (6), the scattering cross section is obtained in the usual manner. The differential cross section in the centre of mass system is given by ($g^2 = G^2/4\pi$)

$$\frac{\mathrm{d}\sigma_T^{\pm}}{\mathrm{d}\Omega} = \tfrac{1}{2}(g^2 c_T)^2 \frac{1}{W^2} \frac{A^{\pm}+B^{\pm}\cos\theta}{[a+b\cos\theta]^2} \frac{1}{(1+g^2 c_T\, \xi^{\pm})^2}, \tag{7}$$

and the total cross section by

$$\sigma_T^{\pm}(E) = (g^2 c_T)^2 \frac{\eta^{\pm}}{W^2} \frac{1}{(1+g^2 c_T \xi^{\pm})^2}. \tag{8}$$

The + sign is for relative K^+-Y parity even and the − sign for the relative parity odd. The various quantities occurring in (7) and (8) are listed in the appendix. In the above cross section formulae, if we drop the last factor (containing $\xi^{\pm}$) we get the result one obtains from the first Born-approximation.

If we take $\alpha = 1 (G_{NK\Lambda} = G_{NK\Sigma})$, the scattering amplitudes for the $T = 1$ and $T = 0$ states become equal ($c_1 = c_0 = 2$), and hence we get no charge-exchange scattering. Experiments give a value of 0.2 to 0.3 for the ratio of charge-exchange to no-charge-exchange scattering [4]). We have therefore taken the value $\alpha = \sqrt{3}$, ($G_{NK\Lambda} = \sqrt{3} G_{NK\Sigma}$), so that $c_1 = 4$ and $c_0 = 0$, and hence the scattering takes place only through the $T = 1$ state. This leads to a value of 0.2 for the ratio of charge-exchange to no-charge-exchange scattering.

In fig. 3 the total cross section for the scattering of K^+-mesons from protons is plotted as a function of the kinetic energy E of the incident K^+-mesons in the laboratory system. The value $g^2 = 0.5$ has been used along with $\alpha = \sqrt{3}$. It is seen that the Fredholm curve with relative K^+-Y parity *even* gives the experimentally found increase with energy, and also the magnitude of the cross section in the region $E = 50$ to 300 MeV. Thus, from this calculation it appears that, within the framework of the interaction scheme used, relative K^+-Y parity *even* is preferred.

Regarding the angular distribution, both experiments and our calculations at 50 MeV give a more or less isotropic distribution in the centre of mass system. The angular dependence alone does not provide any information on the relative parity of K^+ and Y.

Experiments [4]) seem also to point to a repulsive potential between K^+ and proton. From the cross sections alone, one cannot make any statement regarding the nature of the potential. A separate investigation, using, for example, dispersion relations, is needed to determine unambiguously the sign of the potential. We hope to present the results of such an investigation in the near future.

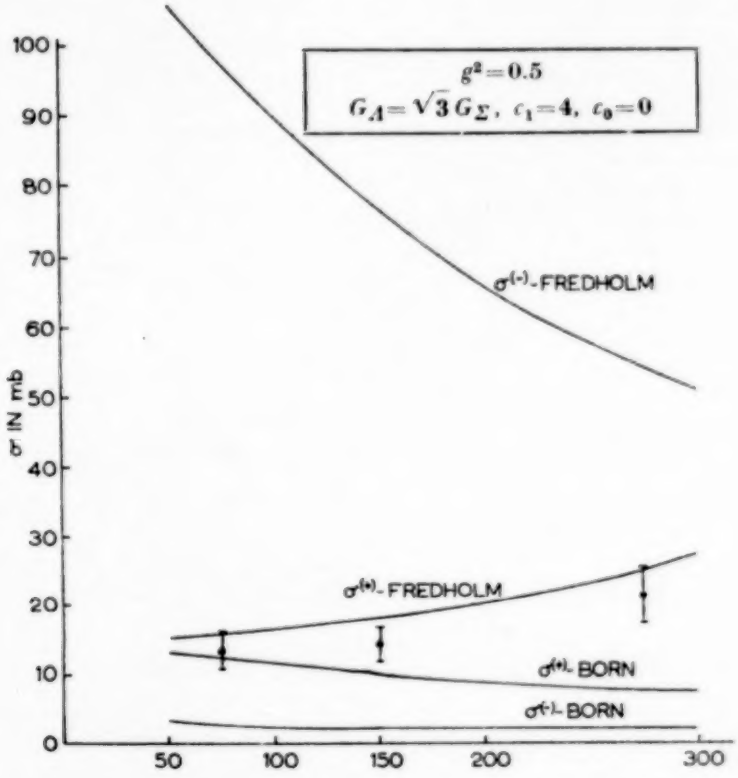

Fig. 3. Total cross section σ for (K^+-p) scattering plotted as a function of E, the kinetic energy of the incident K^+-meson in the laboratory system. The + or − signs refer to relative K^+-Y parity even or odd, respectively.

Recently, Pais [5]) has put forward the conjecture that K^+ and K^0 might have opposite parities, making it possible to formulate a direct ($K^+\bar{K}^0\pi^+$) interaction, which may contribute substantially to the K^+-N scattering. Work is now being done also to take this possibility into account.

We should like to express our thanks to Dr. Yash Pal and Dr. M. S. Swamy for useful discussions on various experimental points.

Appendix

$$W^2 = (\mu+m)^2+2mE, \quad \Delta^{\pm} = m \pm M.$$

$$A^{\pm} = -\mu^2(W^2-\omega^2-2\Delta^{\pm}m-m^2)+2\omega W(\omega W-\omega^2-2\Delta^{\pm}m) + 2\Delta^{\pm}m\omega^2+(\Delta^{\pm})^2\{(W-\omega)^2+m^2\},$$

$$B^{\pm} = k^2[-\mu^2+2\omega W-2\Delta^{\pm}m-(\Delta^{\pm})^2].$$

$$\omega = \sqrt{k^2+\mu^2}, \quad k^2 = \tfrac{1}{4}\left[W^2+\frac{(m^2-\mu^2)^2}{W^2}-2(m^2+\mu^2)\right].$$

$$\eta^{\pm} = \pi\left\{\frac{2(A^{\pm}b-B^{\pm}a)}{b(a^2-b^2)}+\frac{B^{\pm}}{b^2}\log\left|\frac{a+b}{a-b}\right|\right\},$$

$$\xi^{\pm} = \frac{1}{4\pi}\left\{\mathscr{I}_1+\mathscr{I}_2+\mathscr{I}_3-\frac{(2m\pm M)^2}{W^2}(\mathscr{I}_3+\mathscr{I}_4)\right\},$$

$$a = \mu^2+m^2-M^2-2\omega\sqrt{k^2+m^2}, \quad b = -2k^2.$$

$$\mathscr{I}_1 = \int_0^1 dv \log\frac{v^2-v(1+\alpha-\beta)+\alpha}{v(\beta-\alpha)+\alpha},$$

$$\mathscr{I}_2 = \tfrac{1}{4}\int_0^1 dv \log\frac{v^2-v(1-\gamma+4\alpha)+4\alpha}{v(\gamma-4\alpha)+4\alpha},$$

$$\mathscr{I}_3 = \int_0^1 dx \int_0^1 dz \frac{x}{\alpha(1-x)+\beta xz+\frac{1}{4}\gamma x(1-z)-\frac{1}{4}x[1+3z-x(1+z)^2]},$$

$$\mathscr{I}_4 = \int_0^1 dx \int_0^1 dz \frac{x}{\alpha(1-x)+\beta xz+\frac{1}{4}\gamma x(1-z)},$$

where

$$\alpha = \frac{\mu^2}{W^2}, \quad \beta = \frac{m^2}{W^2}, \quad \gamma = \frac{M^2}{W^2}.$$

In the computations given here α has been neglected in $\mathscr{I}_3$ and $\mathscr{I}_4$.

References

1) H. Stapp, Phys. Rev. **106** (1957) 135;
D. Amati and B. Vitale, Nuovo Cimento **5** (1957) 1533;
C. Ceolin and L. Taffara, Nuovo Cimento **6** (1957) 425
S. Barshay, Phys. Rev. **110** (1958) 743
2) M. Gell-Mann, Phys. Rev. **106** (1957) 1297
J. Schwinger, Ann. Phys. **2** (1957) 407
A. Pais, Phys. Rev. **110** (1958) 574
3) I. E. McCarthy and H. S. Green, Proc. Phys. Soc. A **67** (1954) 719
4) M. F. Kaplon, Cern Conference Report (Geneva, 1958)
5) A. Pais, Phys. Rev. **112** (1958) 624

2.J:4.E *Nuclear Physics* **12** (1959) 527—531; © *North-Holland Publishing Co., Amsterdam*
Not to be reproduced by photoprint or microfilm without written permission from the publisher

UN NOUVEL ISOTOPE DU GADOLINIUM TRÈS DÉFICIENT EN NEUTRONS

J. OLKOWSKY, M. LE PAPE, I. GRATOT et L. COHEN

Section des Réactions Nucléaires à Moyenne Énergie, C.E.N., Saclay, Gif-sur-Yvette (S & O)

Reçu le 6 avril 1959

Abstract: An isotope of gadolinium has been obtained from (α, xn) reactions on ^{144}Sm. The half-life is measured to be 24 ± 1 min. It decays by electron capture and β^+-emission. The branching ratio β^+/X_K is 35 %. Beta-energy, determined by absorption method, indicates that $E_{max} = 2.5$ MeV. This isotope shows a 780 keV γ-ray. Its mass is 144 or 145. ^{144}Eu does not present the 18 minute half-life given in tables [1,2]).

1. Introduction

Les isotopes très déficients en neutrons du gadolinium sont mal connus et leurs nombres de masse peu sûrs. Nous avons entrepris une étude de ces isotopes pour préciser certains résultats que nous avions obtenus lors de l'étude du mécanisme de la spallation du terbium par protons de 170 MeV [3]).

2. Méthodes Expérimentales

2.1. CIBLES ET IRRADIATIONS

Les cibles sont constituées par de l'oxyde de ^{144}Sm enrichi, la composition isotopique étant la suivante:

144	147	148	149	150	152	154
85.72	5.22	2.36	2	0.87	2.25	1.58

Ces cibles sont irradiées au cyclotron de Saclay, en faisceau sorti, l'énergie maximum des α étant 44 MeV.

2.2. CHIMIE

L'élimination de ^{17}F et ^{18}F dans les irradiations par α de l'oxygène, et l'élimination de ^{13}N, de ^{17}F et ^{18}F dans les irradiations par protons de l'oxygène, sont obtenues comme suit:

Les oxydes des terres rares sont dissous dans le mélange NO_3H-ClH à chaud. On ajoute FH comme entraîneur. Les fluorures de terres rares précipitent et on les redissout dans le mélange acide NO_3H-BO_3H_3. On précipite

les hydroxydes de terres rares par la soude. Le précipité est lavé et dissous dans ClH. On répète trois fois les opérations de précipitation, lavage et redissolution. La dernière solution chlorhydrique sert à préparer les sources.

2.3. ÉTUDE DES RAYONNEMENTS BÊTA ET GAMMA

Rayonnements β: Nous utilisons des compteurs β du type cloche à paroi mince (2 mg/cm^2). L'énergie β a été déterminée par absorption dans l'aluminium.

Rayonnements γ. Un cristal d'iodure de sodium de 1.5×1 pouce est monté sur un photomultiplicateur EMI 6097 F. Nous utilisons les mêmes méthodes expérimentales que dans le travail [3]).

3. Détermination des Caractéristiques de l'Isotope de Période 24 Minutes Trouvé

3.1. DÉTERMINATION DU NOMBRE ATOMIQUE

Les alpha de 44 MeV, dans la région des terres rares, produisent les réactions (α, xn), x variant de 1 à 4, les réactions $(\alpha, p\,xn)$ $(x = 1, 2)$ n'étant pas complètement exclues. Les isotopes que nous pouvions former étaient donc $^{144-147}$Gd et $^{145-146}$Eu d'origine et aussi ^{144}Eu par filiation du gadolinium de même masse.

En faisant varier l'énergie du faisceau (voir ci-dessous), nous avons pu vérifier que l'isotope de période 24 minutes était de masse 144 ou 145. Il restait donc quatre possibilités de situer l'isotope 24 minutes: ^{144}Gd et ^{145}Gd, ^{144}Eu (de filiation) et ^{145}Eu (de filiation ou d'origine). L'europium 145 a une période de 5 jours [4]) et son nombre de masse paraît sûr, car il a été obtenu par recul alpha de ^{149}Tb, ce dernier isotope ayant eu sa masse déterminée par spectrographie de masse [5]).

L'europium 144 étant indiqué dans la table [1]) avec une période de 18 minutes, il était nécessaire de vérifier que ce n'était pas l'isotope de 24 minutes trouvé, provenant de la filiation d'un gadolinium de période très courte. Nous avons reformé ^{144}Eu par la réaction ^{144}Sm(p, n)^{144}Eu, en utilisant le faisceau de protons de 11 MeV du cyclotron de Saclay.

N'observant aucun rayonnement de période égale à environ 20 minutes, nous avons monitoré cette expérience par la réaction ^{141}Pr(p, n)^{141}Nd, ce dernier isotope étant connu [6]). Il a une période de 2.5 heures.

Nous avons donc soigneusement mélangé les oxydes de Pr et ^{144}Sm à masses égales et bombardé ce mélange avec le faisceau de protons pendant 15 minutes.

L'activité due à ^{141}Nd est importante. Nous retrouvons les raies annoncées dans le travail [6]). Il n'y a aucun rayonnement de période 18 minutes.

En conclusion, ^{144}Eu n'a pas la période 18 minutes. Il n'y a toujours pas de

précision sur cet isotope dans la table [2]), aucune publication n'ayant été faite à son sujet. L'isotope de période 24 minutes est donc ^{144}Gd ou ^{145}Gd.

	144	145	146	147	148	149	150	151	152	153	154	155	156
Sm		A ≈400 j EC	B 5×10^7 ans α					A 100 ans β^-		A 47 h β^-		B 25 min β^-	B 9 h β^-
Eu	C 18 min β^+	B 5 j EC	C 38 h EC	B 24 j EC	A 50 j EC	D 120 j	A 15 h β^-		A 9.2 h EC β^- β^+		A ≈10 ans β^-	A 1.7 ans β^-	A 15 j β^-
Gd			52 j (B)	B ≈30 h EC	B ≈100 ans α	B 9 j EC	D $>10^7$ ans	A 150 j EC		A 225 j EC			

Remarquons d'ailleurs que, d'après le tableau 1, les isotopes du samarium, autres que le 144, contenus dans la cible, ne peuvent donner que des isotopes de période beaucoup plus longue que 24 minutes. Le samarium 155, de période 25 minutes, est complètement exclu des réactions utilisées.

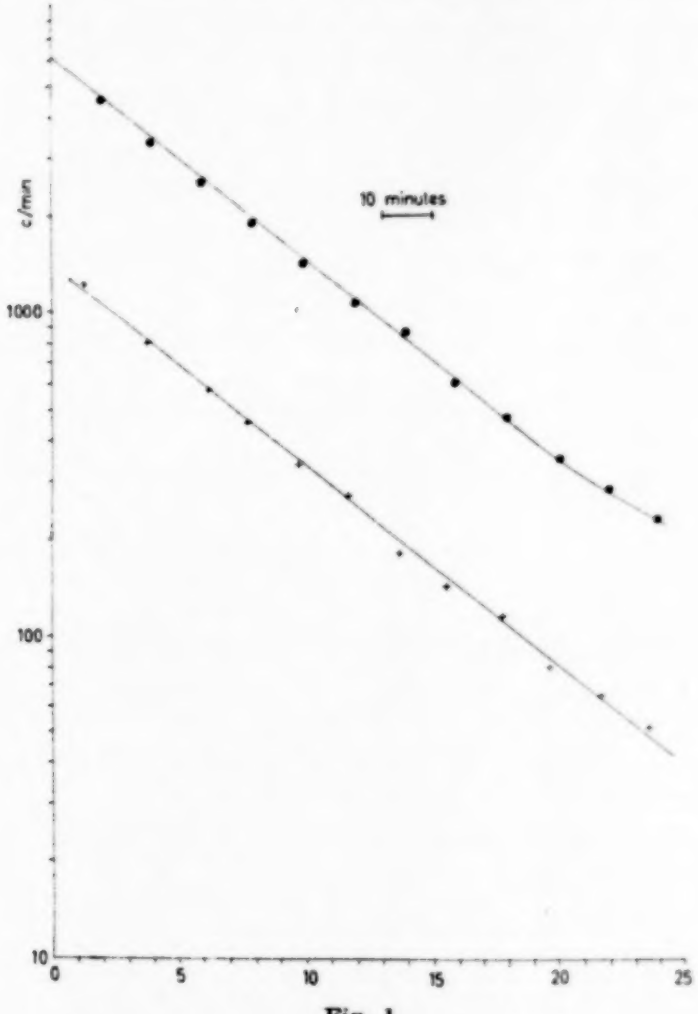

Fig. 1

Absorption des β dans l'aluminium
• — • = Sans écran la courbe tourne sur une période de quelques jours.
+ — + = Avec écran (481 mg/cm²) la période est pure.

3.2. DÉTERMINATION DU NOMBRE DE MASSE

Nous avons utilisé la connaissance des fonctions d'excitation dans la région des terres rares. Expérimentalement, nous utilisons des empilements de sachets avec écrans de platine pour changer l'énergie du faisceau. Au-dessous de 30 MeV, l'isotope de période 24 minutes ne se forme plus. Or, cette énergie correspond au maximum des réactions (α, 2n) et (α, pn). Le seuil de la réaction (α, 4n) et le maximum de la réaction (α, 3n) se situant vers 40 MeV, les résultats nous permettent de donner à l'isotope de 24 minutes les masses 144 ou 145.

3.3. SPECTRE GAMMA

Le spectre gamma présente les raies suivantes décroissant avec une période de 24 minutes (fig. 2). Leurs intensités relatives, corrigées de l'effi-

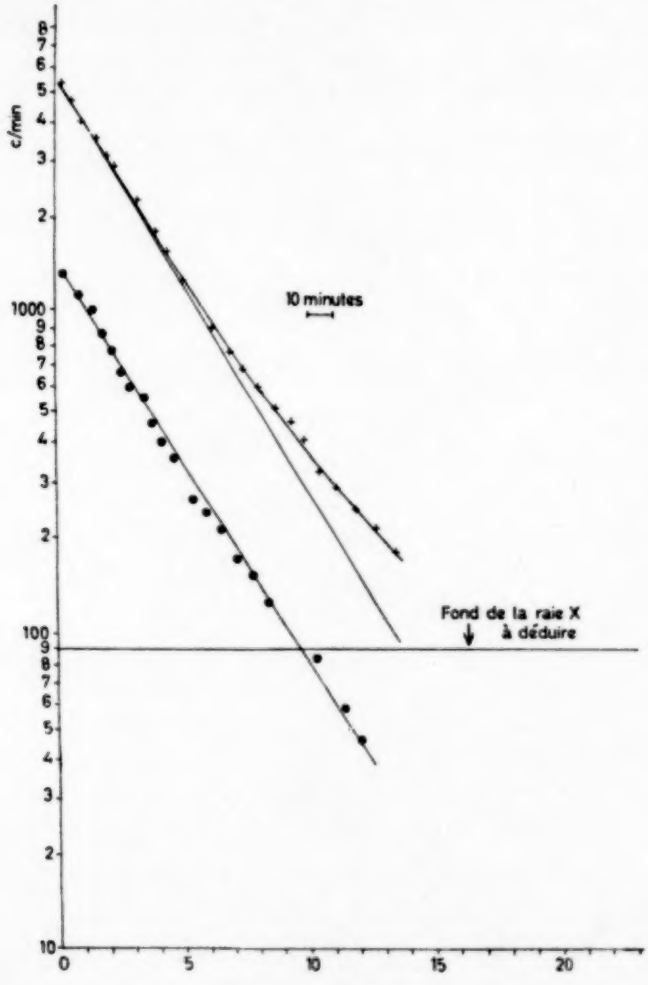

Fig. 2

Décroissance de raies γ
+—+ = Raie X, le fond déduit à une période de quelques jours
• — • = Raie 511 keV.

cacité de l'installation, sont les suivantes:

raie X_K	511 keV	780 keV
100	35	15

3.4. ÉNERGIE DES β (ABSORPTION DANS L'ALUMINIUM)

Le facteur $d_{\frac{1}{2}}$ (réduction de l'activité d'un facteur 2) a été déterminé à 270 ± 20 mg d'aluminium. En utilisant une courbe d'étalonnage que nous avons établie avec une série d'isotopes dont les énergies β sont connues — et en bon accord avec plusieurs auteurs [7]) — nous pouvons fixer l'énergie des β à 2.5 ± 0.15 MeV (fig. 1).

Nous avons entrepris une étude de l'europium 144 (à paraître).

Bibliographie

1) J. M. Hollander, I. Perlman et G. T. Seaborg, Revs. Mod. Phys. **25** (1953) 469
2) D. Strominger, J. M. Hollander et G. T. Seaborg, Revs. Mod. Phys. **30** (1958) 585
3) J. Olkowsky, M. Le Pape, I. Gratot et L. Cohen, J. Phys. Radium **20** (1959) 555
4) R. W. Hoff et J. O. Rasmussen et S. G. Thompson, Phys. Rev. **83** (1951) 1068
5) J. O. Rasmussen, S. G. Thompson et A. Ghiorso, Phys. Rev. **80** (1950) 475
6) H. L. Polak, W. Schoo, B. L. Schram, R. K. Girgis et R. Lieshout, Nuclear Physics **5** (1958) 271
7) Rudstam, Thèse Uppsala (1956)

1.D.1

Nuclear Physics **12** (1959) 532; © *North-Holland Publishing Co., Amsterdam*

Not to be reproduced by photoprint or microfilm without written permission from the publisher

NOTE ON „DOUBLE BINOMIAL COEFFICIENTS"

HERBERT IZBICKI

Österreichische Studiengesellschaft für Atomenergie, Wien

Received 11 May 1959

In a recent article [1]), K. W. Ford and E. J. Konopinski made use of the "double factorial"

$$(2n+1)!! = 1 \cdot 3 \cdot 5 \cdots (2n+1) \tag{1}$$

and the "double binomial coefficient"

$$\begin{Bmatrix} r \\ s \end{Bmatrix} = \frac{(r+1)!!}{(s+1)!!(r-s+1)!!}, \tag{2}$$

where r and s are (obviously even) integers. Clearly $\{{r \atop 0}\} = \{{r \atop r}\} = 1$, and $\{{r \atop s}\} = \{{r \atop r-s}\}$. It might be of interest to point out that these so-called "double binomial coefficients" can easily be expressed in terms of ordinary ones. Rewriting eq. (2) as

$$\begin{Bmatrix} 2r \\ 2s \end{Bmatrix} = \frac{(2r+1)!!}{(2s+1)!!(2r-2s+1)!!}, \tag{3}$$

eq. (1) as

$$(2n+1)!! = \frac{(2n+1)!}{2^n \cdot n!}, \tag{4}$$

and substituting (4) in (3), we readily obtain

$$\begin{Bmatrix} 2r \\ 2s \end{Bmatrix} = \frac{1}{\binom{r}{s}} \frac{(2r+1)!}{(2s+1)!(2r-2s+1)!}. \tag{5}$$

This gives three equivalent forms for $\{{2r \atop 2s}\}$:

$$\begin{Bmatrix} 2r \\ 2s \end{Bmatrix} = \frac{\binom{2r+2}{2s+1}}{\binom{r}{s}(2r+2)} = \frac{\binom{2r+1}{2s}}{\binom{r}{s}(2s+1)} = \frac{\binom{2r+1}{2s+1}}{\binom{r}{s}(2r-2s+1)}. \tag{6}$$

Reference

1) K. W. Ford and E. J. Konopinski, Nuclear Physics **9** (1958/59) 218

NORTH-HOLLAND BOOKS

ANALYTICAL and CANONICAL FORMALISM in PHYSICS

by ANDRÉ MERCIER

Head of the Department of Theoretical Physics University of Berne

6×9″ VIII + 222 pp. Guilders 20.00 (40s.)

CONTENTS

i. Lagrangian Formalism
ii. Lagrangian Density
iii. Canonical Formalism
iv. Canonical Form of Electrodynamics
v. Hamiltonian Densities
vi. Transformations
vii. Canonical Formalism with Vanishing Jacobian Determinant

Those who are not highly specialized in these matters but do want to get a fairly broad knowledge of the subject are not aware of the fact that the greater parts of this formalism, including many specific conclusions of physical concern, do not involve in the least quantum theory, i.e. "quantization" of the fields. To show this and to provide the reader with a fairly complete presentation of the *classical* (i.e. not yet quantized) theory of fields is one of the main aims of the book.

This formalism is presented with great generality. Some special topics have also been included when they are found to be of importance in connection with the problems raised; however, they are not elaborated with the same generality, but just formulated as far as is found necessary for the understanding of these connections; for instance we can name: tensorial formalism and spinorial formalism.

A special chapter has been devoted to transformations of several kinds including canonical transformations, reversibility and the like as well as their interrelations, so that the ground is prepared for an understanding of the CPT-Theorems.

A short chapter on Dirac's dynamics with vanishing Jacobian closes the book.

The work builds upon the well-known *Principles of Analytical Dynamics* by the same author (in French), where particular weight is laid upon the homogeneous formalism, but it can easily be read with profit without knowledge of the latter by any advanced students in physics, astronomy or mathematics as well as by research workers who want to get a thorough practice in the use of these methods.

Many examples and as many as 124 problems illustrate the formalism exposed.

Sole Agency for U.S.A.: Interscience Publishers Inc. - New York

NORTH-HOLLAND PUBLISHING COMPANY - AMSTERDAM

REPRINTS OF NUCLEAR PHYSICS

Available at the Publishers

NUCLEAR ENERGIES AND THE SHELL MODEL

by

NISSAN ZELDES

Department of Physics, The Hebrew University of Jerusalem, Israël

and

Department of Mathematical Physics, University of Birmingham, England

volume 7 (1958) no. 1,
84 pages, 20s., $ 2.80

PARTICLES AND SYMMETRIES

by

E. CORINALDESI

University College of North Staffordshire, Keele, England

volume 7 (1958) no. 4
68 pages, 17s., $ 2.25

ENERGY LEVELS OF LIGHT NUCLEI. VI

by

E. AJZENBERG-SELOVE

Department of Physics, Haverford College, Haverford, Pennsylvania

and

T. LAURITSEN

Kellog Radiation Laboratory, California
Institute of Technology, Pasadena, California

volume 11 (1959) no. 1
320 pages, 40s., $ 5.30

NORTH-HOLLAND PUBLISHING COMPANY

NIEUWE ZIJDS VOORBURGWAL 68-70 AMSTERDAM-C HOLLAND